uyty

ADDIS ABABA UNIVERSITY

COLLEGE OF NATURAL SCIENCES

SCHOOL OF EARTH SCIENCES

SATELLITE BASED RAINFALL ESTIMATION: EVALUATION AND CHARACTERIZATION WITH HOMOGENEOUS RAINFALL REGION CLASSIFICATION USING GIS AND REMOTE SENSING

(Case Study of Awash River Basin)

Thesis Submitted to the School of Graduate Studies in Partial fulfillment of the Requirements for the Degree of Master of Science in GIS and Remote Sensing

By: Zerihun Bikila

Advisor: Dr. K.V.Suryabhagavan

JUNE, 2014

SATELLITE BASED RAINFALL ESTIMATION: EVALUATION AND CHARACTERIZATION WITH HOMOGENEOUS RAINFALL REGION CLASSIFICATION USING GIS AND REMOTE SENSING

(A Case Study of Awash River Basin)

Dissertation submitted for Partial Fulfillment of the Requirements for the

Award of the Degree of

MASTER OF SCIENCE

In

Geographic Information System (GIS) and Remote Sensing, Addis Ababa University, Addis Ababa, Ethiopia

Under the guidance of

Dr. K.V. Suryabhagavan

School of Earth Sciences

Addis Ababa University, Addis Ababa, Ethiopia

By: ZERIHUN BIKILA

JUNE, 2014

ADDIS ABABA UNIVERSITY

COLLEGE OF NATURAL SCIENCES

SCHOOL OF EARTH SCIENCES

Satellite Based Rainfall Estimation: Evaluation and Characterization with Homogeneous Rainfall Region Classification Using Remote Sensing and GIS (Case Study of Awash River Basin)

A Thesis Submitted in Partial Fulfillment of the Requirements for the Degree of Master of Science in Remote Sensing and GIS, School of Earth Sciences.

By

Zerihun Bikila Ayana

APPROVED BY EXAMINING BOARD

Dr. TILAHUN MAMMO ----------

Chairman, School

Graduate Committee

Dr. K.V.SURYABHAGAVAN ----------

Advisor

Dr. GETACEHW BERHAN ----------

Examiner

Mr. DEGELO SENDABO (MSc.) ----------

Examiner

ACKNOWLEDGMENTS

First of all, I would like to thank “Almighty God” who made it possible for me, to begin and finish my study successfully and also for his protection and favor in my entire life.

I express my deep sense of gratitude and indebtedness to my advisor, Dr. K.V. Suryabhagavan, who helped me from the very beginning of the research to its completion. His benevolent guidance and constant encouragement helped me to complete the research work successfully.

National Meteorological Agency (NMA) deserves special thanks for all the support provided me during my study. Very special thanks are given to Dr. Diriba Koricha, Meteorological Forecast and Early Warning Directorate Director, Dr. Tufa Dinku, Columbia University, USA, who taught me the skills and concepts necessary to undertake this study. I must express my deepest sense of gratitude and acknowledgement for all my instructors and staff members of the Department of Earth Sciences, Addis Ababa University for sharing their experiences, materials and unreserved cooperation during my course work. I am also thankful to Ethiopian Meteorological society (EMSO) for their financial support provided me during my research work.

For various meteorological data and information I received, my heart full thanks go to the National Meteorological Agency, Mr. Zerihun Walelign and Ms. Yitaktu T/Tsion, Meteorological data and climatology Directorate, Taye Assafa, NMA, Meteorological Studies and research directorate (Librarian). I am also grateful to Ministry of Water, Irrigation and Energy and Awash River Basin Authority, for providing me necessary Awash River Basin data.

I would like to thank my friend Estifanos Fikadu and my brother Soressa Bikila who provided me invaluable advice and moral support that was necessary for the completion of this thesis. I also thank my class mates Asnake, Teshome, Kokeb, Bamlaku, Yalew, Birehanu, Abinet, H/Gebriel and Mohammed with whom I had fruitful discussions on many scientific and technical issues during the course of this thesis work.

I extend my thanks to my mother, father, brothers and sisters for all the loving and encouraging support. In particular, I would like to thank my brother Gaddisa Bikila for his unlimited moral support and encouragement during my stay in this study

I am very grateful to extend my thanks to my wife Tigist Tsegaye (Tigi), my family and my son Yonatan (Babba), who are source of my strength. I am highly indebted to them for their blessings, guidance, advice, encouragement and support.

I apologize many of my friends and organizatitions who helped me in various means, whom I did not mention by names. I equally appreciate and acknowledge all of them.

TABLE OF CONTENTS

LIST OF TABLES

LIST OF FIGURES

ACRONOMY

ARB	Awash River Basin
AVHRR	Advanced Very High Resolution Radiometer
ASCll	American Standard Code for Information Interchange
CCD	Cold Cloud Duration
CPC	Climate Prediction Center
EUMETSAT	European Organization for the Exploitation of Meteorological Satellites
METEOSAT	Meteorological Satellite
HRRs	Homogenous Rainfall Regions
ITCZ	Inter Tropical Convergence Zone
GIS	Geographic Information system
GOES	Geostationary Operational Environmental Satellite
GPS	Global Positioning System
MM	Millimeter
MW	Microwave
WCP	World Climate Program
WMO	World Meteorological Organization
NMA	National Meteorological Agency
NASA	National Aeronautics and Space Administration
PCA	Principal Component Analysis
RFE	Satellite Estimated Rainfall
SEDI	Satellite Enhanced Data interpolation
TAMSAT	Tropical Application of Meteorological Satellite
TRMM	Tropical Rainfall Measuring Mission
TIR	Thermal Infrared

ABSTRACT

The study mainly covers the delineation of Homogeneous Rainfall Regions (HRRs) and comparison of Tropical Application of Meteorological Satellite (*TAMSAT) rainfall estimate with rain gauge recorded rainfall data over Awash River basin (7.8^{o} - 12^{o}N and 38^{o} - 43.4^{o}E) using dekadal rainfall datasets during the period of 2008-2010 and long year mean data(1990 -2010) available at National Meteorological Agency (NMA). TAMSAT rainfall data is satellite derived rainfall estimates available over the region generated using different satellite rainfall estimation techniques from international centers of excellence. Several methods that include descriptive and continuous statistics such as scatter plots and histograms, measures of variability that include the standard deviation and coefficient of variation, correlation coefficient, mean error, Principal Component Analysis (PCA), scree plot of eigenvalue and geostatistical kriking were used in the evaluation. The delineation result showed that Awash River basin has four HRRs because of its slight different character of receiving rainfall. The analysis result reveal that all HRRs in the basin receive a bi-modal rainfall cycle but the rainfall cycle at HRR1 is slightly near to mono-modal type rainfall. The two rainy seasons at each HRRs of the basin are Kiremt (June to September) and Belg (February to May). The monthly mean rainfall amounts were peak at HRR2, HRR3 and HRR4 during the month of August with a value of 261.3 mm, 99.0 mm and 125.0 mm, respectively. But the monthly mean peak rainfall amount at HHR1 is during July with a rainfall amount of 229.8mm. The evaluation and comparison of satellite rainfall estimate with rain gauge data showed that the mean error value between satellite rainfall estimates and rain gauge value are higher (>-10mm dekade^{-1}) at HRR1 and HRR2 during second dekade of August where the distribution and amount of rainfall amount is high. However, the mean error value was minimum over the arid and generally low latitude areas of the region (HRR3). For the year of 2008 which is considered as relatively normal rainfall distribution year, the correlation coefficient result against the gauge record was found to be higher (r=0.73) compared to the selected years. The correlation coefficient result for the year considered as wet year (2010) is 0.52. During the relatively low rainfall distribution year (2009) the correlation coefficient result is 0.46. Generally, the result indicates the satellite estimated rainfall totally explained in better way the spatial and temporal pattern relationship of the rainfall climatology characteristics of each HRRs for dekadal, seasonal and annual cases considering the observed differences in the rainfall magnitude between the satellite rainfall estimates and gauge rainfall value.*

Keywords: Rainfall, TAMSAT, HRRs, Evaluation and Comparison

1. INTRODUCTION

1.1. Background

The Ethiopian economy is mainly dependent on rain-fed agriculture and subjected to vagaries of weather and climate system (Dereje, 2012); many investigations have shown that fluctuations of rainfall have always been the natural curse of agriculture and cause droughts (e.g. Workineh, 1987). Moreover, rainfall risk assessments, warning and response systems are not yet to be well functioning integrated with vulnerability and risk management. Conventionally, rainfall is measured using rain gauges, which provide the measurement of the amount of rain in the surrounding area. The distributions of rainfall stations are also very sparse and non-evenly distributed and most of which are located along the main roads. It is so that, further improvement of data availability from different sources and accuracy should be vital. The devastating effect of drought and flooding is now recurring event that cause the loss of life, properties and evacuations of settlements. Particularly, at higher rainfall values, problems may arise in early warning and preparedness system if such data are unavailable.

Flood early warning systems and drought monitoring are one of the most effective ways to minimize the loss of life and property. It is very important to have a reliable drought and flood forecasting system as a basis for establishing a reliable early warning system which can be transmitted down to the community in order to minimize the impact of flood and drought disasters. Precipitation is highly variable in both space and time and is an important input in rainfall runoff modeling and drought assessment and predicting. The amount of rainfall and its spatial distribution are important factors in meteorology, climatology, and hydrology (ICIMOD, 2013). Accurate rainfall estimations are essential for timely drought and flood forecasting and warning. In many regions, operational drought and flood forecasting has traditionally relied upon a dense network of rain gauges or ground-based rainfall measuring radars that report in real time. Flood forecasting in basins with sparse or non-existent rain gauges poses an additional challenge. In such areas, satellite rainfall estimates (RFE) could provide information on rainfall occurrence, amount, and distribution (Adler et al., 2003; Hong et al., 2007; Shrestha et al., 2008 a,b) and be used for hydrological modeling to predict floods.

The availability of global coverage of satellite data offers an effective and economical means of calculating areal rainfall estimates in sparsely gauged areas (Artan et al., 2007).

Several high resolution global satellite-based rainfall products are currently available from various operational agencies, as well from research and academic institutions (Ebert et al., 2007; Huffman et al., 2007; Kubota et al., 2009). For example, satellite algorithms like the Global Satellite Mapping Precipitation (GSMaP) (Ushio et al., 2009), CPC_RFE2.0 (Xie et al., 2002), TAMSAT (Grimes et al., 1999) and CMORPH (Joyce et al., 2004) are currently available at a spatial resolution of 0.1 degrees or higher and a temporal resolution of ten days or less. The availability of high resolution satellite-based products at a finer temporal (hourly, daily and dekadal) and spatial (0.1° or less) resolution provide an opportunity to apply rainfall estimates for timely flood forecasts in data sparse regions. However, satellite-based rainfall data have uncertainty and, when applied in rainfall runoff models for flood simulation, this uncertainty has an effect on the accuracy of the predictions. Thus the satellite rainfall estimates need to be validated against rain gauge measurements at a detail HRRs to gain an idea of their accuracy and expected error characteristics in various applications before they can be used in modeling and other applications. Following the successful validation of satellite rainfall estimates for regions in Africa, and similar estimates made over other parts of the world (Kidd, 2005; Laurent et al., 1998; Vila et al., 2003; Dinku et al., 2008).

In general, the satellite based rainfall estimation process can assist mainly to get rainfall data and disseminate to user agencies on a real-time basis via satellite link. Weather satellite particularly has been hand into efficient tools for both observing and communicating weather and rainfall data in timely fashion. In addition to this, some of the advantages over the conventional techniques are like: combining remote sensing, GIS and GPS in an institutionalized framework with multi-sectoral linkages, identifying the regions that have the highest amount of risks to help policy formulation towards disaster reduction, rapid mapping of disaster events and disseminating the information to end-users on a real-time basis.

This study is mainly intended to delineate homogeneous rainfall regions and to show the practical application of satellite based rainfall estimations using the METEOSAT -TIR image data and to validate the results and compare it with the actual rainfall over the delineated HRRs of Awash river basin. Therefore, of these different measuring devices, satellite is useful and advantageous in providing continuous, large area coverage and real-time estimation of rainfall for operational applications, and in particular helps to monitor and evaluate the basin rainfall characteristics. The use of meteorological satellite data

certainly could expand the spatial and temporal coverage of rainfall estimation and improve the consistence with the nature and development of precipitating systems within the basin in the objective of providing the rainfall information and meteorological service to end users.

1.2. Statement of the problem

Rainfall is the meteorological parameter affecting people in the most direct way. Obtaining real time and continuous data on the spatial and temporal distribution of rain is one of the major challenges for the meteorological services to support various socio-economic activities in different sectors. Accordingly, scarcity of rainfall data for un-gauged places and remote area within the basin is one of the major problem and gap to obtain rainfall information for various activities. The distribution of rain gauge network of stations for point measurements can be made but to derive continuous aerial amounts would still remained inadequate because of an unfeasibly dense network. In the country, it takes months to collect rainfall data from the stations which are not equipped with radios and telephone service.

Besides, the shortage of gauge stations, the management of the existing stations and dissemination system are conventional and this have its own problem on the need of rainfall data for immediate and future uses in development research program and other meteorological services. This is witnessed on that many users and research institutes are facing a problem to have timely data at least for those few of stations having a gauge records. In addition, the ground rainfall data collection and processing system have been used to make securitization and statistically proof for its effective application in operational and seasonal forecasting system. In such situation, satellite remote sensing of rainfall could help to solve such problem if the technology and methods of rainfall estimation is validated for its accuracy in different HRRs of complex topography like Awash River basin.

As a whole, this study address to investigate the delineation of Homogeneous Rainfall Regions (HRRs) for Awash river basin and to obtain estimated rainfall value from satellite source data and to evaluate and characterize the representation of the estimated rainfall value comparing with the corresponding gauge recorded value and rainfall climatology of the basin at temporal and spatial profile for each delineated HRRs to solve the data requirements in areas of the basin specially in the scarce and no rain gauge stations areas.

1.3 Objectives of the Research

1.3.1 General Objectives

The general objective of this study is to delineate Homogeneous Rainfall Regions (HRRs) for Awash River basin and to obtain estimated rainfall value from satellite source data and to evaluate and characterize the representation of the estimated rainfall value comparing with the corresponding gauge recorded value and rainfall climatology of the basin at temporal and spatial profile for each delineated HRRs.

1.3.2 Specific Objectives

- To delineation the similar climatic zones (HRR) within the study area based on long year climatologically mean rainfall data.
- To Validate and compare the satellite rainfall estimates with ground rain gauge data using statistical analysis for each HRRs in the basin at different temporal and spatial time scale.
- To evaluate and characterize the pattern relationship of satellite rainfall estimate value and gauge rainfall value under different dekades, months, seasons and annuals and rainfall peak time within the basins.
- To map “Satellite” and “Ground” rainfall amounts in spatial dimension using standard Kriging method for some selected months, seasons and years of 2008, 2009 and 2010.

1.4 Benefits and Beneficiaries from Expected Output

The expected output of the study will be two types.

Digital dekadal satellite estimated rainfall value and average over time and places in the basin, so as to put it in use when it is required in the future study. The other output is guiding reports and documents, with graphs and maps based on the performance of estimated rainfall particularly for inaccessible area in the basin.

As a general understanding, it introduced the efficiency and optimizations of data collection through remote sensing techniques where field measurements are not sufficient.

Therefore, there is no doubt that satellite based real time rainfall measurements contribute substantially for sectoral development and research objectives if its accuracy is evaluated with gauge data.

The benefits of the research here include:

Application of modern approaches for satellite based rainfall estimation which can assist for planning and decision making in research activities and sectoral development strategies. It is also serve in improving operational status of meteorological, Agricultural and hydrological applications in measuring and studying the spatial variability of rainfall.

Beneficiaries of the research project area:

Planners, decision makers, and all interested agencies and individuals above all involved in rainfall forecasting, flood monitoring, and risk assessment both in the basins and throughout the country. It can also increase short-term weather forecast system of NMA, and enhanced rainfall-monitoring network over the upstream parts of river catchments. Efficient communication system in up-to-date and fast rainfall information exchange system, among the stakeholders like researchers and academia institutes, NGOs and other users regarding rainfall situation over the basin as a whole.

1.5 Structure of the thesis

This thesis is divided in to seven chapters. The first chapter is an introduction part that includes the background, problem of statement, description of study area, previous research work, objectives of the study, and benefits and recipient of the result of this study will be elaborate. This is followed by the second chapter of the review literature that describes the concepts or theories and earlier studies on related to the topic under consideration. This chapter describes the basic concept and scientific literature on satellite based data source that is related to the different rainfall estimation approaches.

Chapter three is about nature of the data, materials, methodology, activities of data preparation, processing and creation of database are briefly discussed. In order to better understand the rainfall estimation process and how the estimated rainfall value is extracted from RFE image over ten daily periods (dekadal) base are discussed in this chapter.

The work of delineating homogeneous rainfall region, validating the estimated rainfall values as well as characterizing it with the coincident climatic condition of the study area is fully described in the fourth chapter. The combination of estimated and gauge records will be statistically verified and analyzed. The chapter mainly dealt on the applicability of the methodology and its results obtained from the analysis output. Chapter five gives conclusions, recommendations, limitation of the work and ideas for future investigations.

1.6. Description of the Study Area

1.6.1. Overview

As (MoWR, 1996), Ethiopia has 12 river basins with an area of $1.129*10^6$ km^2 with annual flow of $122Bm^3$ of water. Eight of these are river basins, one lake and three dry basins. Four of the river basins, Abbay, Baro-Akobo, Merebe and Tekeze are part of Nile River system, flowing generally in the western direction towards Sudan. Five basins namely, the Omo-Gibe, Awash, Rift Valley lakes, Denakil and Aysha can be categorized the rift valley system as all of them drain their water along in the great east African Rift valley system. The remaining three, Geneale-Dawa, Wabishebale and Ogaden are part of the eastern part of Ethiopia that generally flows in the southeastern direction towards the Somali and then to Indian Ocean. A review master plan studies related river basin surveys shows that the aggregate annual runoff from the nine river basins amounts to $122Bm^3$ excluding ground water. The three largest river basins (Abay, Baro-Akobo, and Omo-Gibe) contribute 76 percent of the total runoff from catchments area, comprising only 32 percent of the total area of the country

"A river catchments (also often: watershed or river basin) is an area that topographically appears to contribute all the water that passes through a given cross section of a stream. A river basin is the portion of land drained by a river and its tributaries. It encompasses the entire land surface dissected and drained by many streams and creeks that flow downhill into one another, and eventually into one river" (Admasu, 1989).

1.6.2 Location of the Study Area

Awash River basin is geographically bounded by latitude of 7.8^o - 12^oN and longitude of 38^o - 43.4^oE as it is indicated in (Figure 1.1). Part of the Great Rift Valley in Ethiopian river basin system covers a total area of 110,000 km^2 of which 64000 km^2 comprises the western catchment, which drains to the main river or its tributaries. The remaining 46,000 km^2, most of which comprises the so called eastern catchments, drains to arid area and does not contribute to the main river course (MOWR, 2010). The River Awash rises at an elevation of about 3,000 m in the central Ethiopian Highlands, west of Addis Ababa near Ginchi and flow to north eastwards along the Rift Valley into the Afar triangle where it terminates in Lake Abe at an elevation of about 250 m on the border with Djibouti. The main river length is about 1,200 km. Based on physical and socio-economic factors the Awash Basin is divided into Upland (all lands above 1500 m asl), Middle (area between

1500 m and 1000 m asl), Lower Valley (area between 1000 m and 500 m asl) and Eastern Catchment (area between 2500 m and 1000 m asl).

The Awash basin covers the central and northern part of the rift valley and is bounded to the west, east, southwest, south and southeast by the Abay, Ayisha, Omo-Gibe, the rift Lakes and Wabi-Shebele basins respectively (Abraha, 2006).

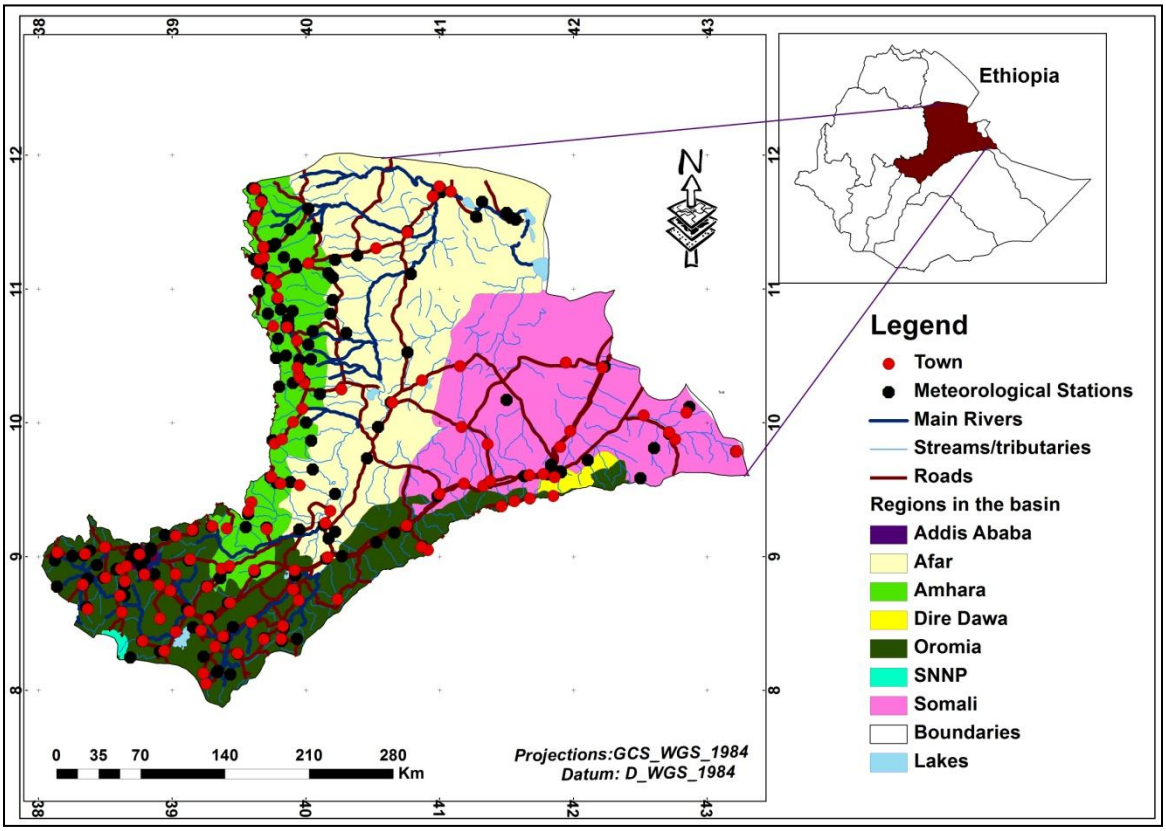

Figure 1.1: Location map of the study area

1.6.3 Demography

The population of the basin was derived from the 1994 population and housing census estimated at 9,295,530 out of which about 37.5% of the basin are in Oromiya, 18.7% in Amhara, 9.9% in Afar ,7.5% in Somalia, 22.7% in Addis Ababa and 2.7% in Dire Dawa. There are substantial differences in population densities with highland densities ranging between 100 and 250persons/km^2. The age profile of the population, based on the 1994 census, shows a very similar situation in Amhara, Oromiya and Afar regions as well as Addis Ababa and Dire Dawa City administrations (MoWR, 2010).

1.6.4 Physiography

The combined action of various tectonic, volcanic, and geomorphic processes have resulted in complex landmass of Ethiopia. The classic geological and geomorphic changes through geologic time-scale include tectonic and volcanic processes in the Precambrian Era that formed huge mountains followed by intense denudation-peneplanation during the Paleozoic Era. Later, slow sinking and progressive rising of part of the present east African Landmass resulted in transgression and regression of the sea respectively, forming Mesozoic sediments (Kronberg *et al*., 1975).

The prominent physiographic features in Ethiopia, however, have mainly been brought about by geologic and geomorphic processes of the Cenozoic Era, which are still active. Following uplift of Afro-Arabia, extensive flood basalt volcanism occurred which formed plateaus.

Subsequently, East African Rift System was formed, which incorporated relatively older Red Sea and Gulf of Aden Rift Systems to form Afar depression (Tadiwos, 1995). Main Ethiopian Rift (MER) is the northern branch of the continental East African Rift System that stretches from south Ethiopia to Afar area. Post-rifting volcanism and tectonics mainly continued on the rift floors while lacustrine, fluvial, piedmont, aeolian and other sediments deposited along margins and axes of the Rifts.

In the Awash Basin and its immediate vicinity, Main Ethiopian Rift (MER) and Afar depression, separate the north-western plateau from the south-eastern plateau, where wide escarpments have formed along their well-defined to rough margins (Figure 1.2). The nearly N-S trending western Afar structures merge with the N-S to NNE-SSW and NE-SW structures of northern and central MER to form the northwestern escarpment while the approximately E-W trending border structures of Afar and the NE-SW to NNE-SSW trending structures between Asebe Tafari area and Lake Langano mainly outline the southeastern escarpment (Kronberg *et al*., 1975).

The northern MER southern Afar transition region, the area north of Fentale volcano, is considered as an important physiographic and structural transition. Interestingly, the physiographic transition at about the latitude of junction is concurrent to the rift embayment in which Addis Ababa is situated (Tadiwos *et al*., 1998; Tadiwos and Hart, 1999). This feature is presumed to have been related to the ESE-WNW cross rift structure, E-W structures of southern Afar marginal graben and the Addis Ababa-Ambo Lineament,

the latter possibly reflecting the regional influence of the Gulf of Aden (Tadiwos, 1995; Kazmin *et al*.,1980).

Wonji Fault Belt (WFB) is a wide belt of intense faulting and volcanism, considered as the active extensional axis of the MER. The several segments comprising this recent belt are arranged en echelon and are built-up of several fault swarms (showing normal type of displacements in many places), volcanic centers, flows and cones. They run mainly along the eastern part in central MER and further proceed by being relatively closer to the western escarpment in Afar depression to be bounded apparently by the NW-SW trending Tendaho rift and other faults of central Afar (Tadiwos, 1995).

The Afar and MER rift floor fractures and fault systems, predominantly follow the structural trend of the Red Sea System (NNW-SSE to NW-SE) and the orientation of the East African Rift System / MER (NNE-SSW to NE-SW), while still others tend to be parallel to the Gulf of Aden trend (WNW-ESE/ WSW-ENE to E-W) (Kronberg et al.,1975).

To generalize, the main physiographic units (components) of the Awash basin, it comprises some of central, northeastern and south-eastern highlands (plateaus & escarpments) and the rift valley (MER and Afar depression). Another important feature is part of central-western highlands that forms part of upper Awash basin.

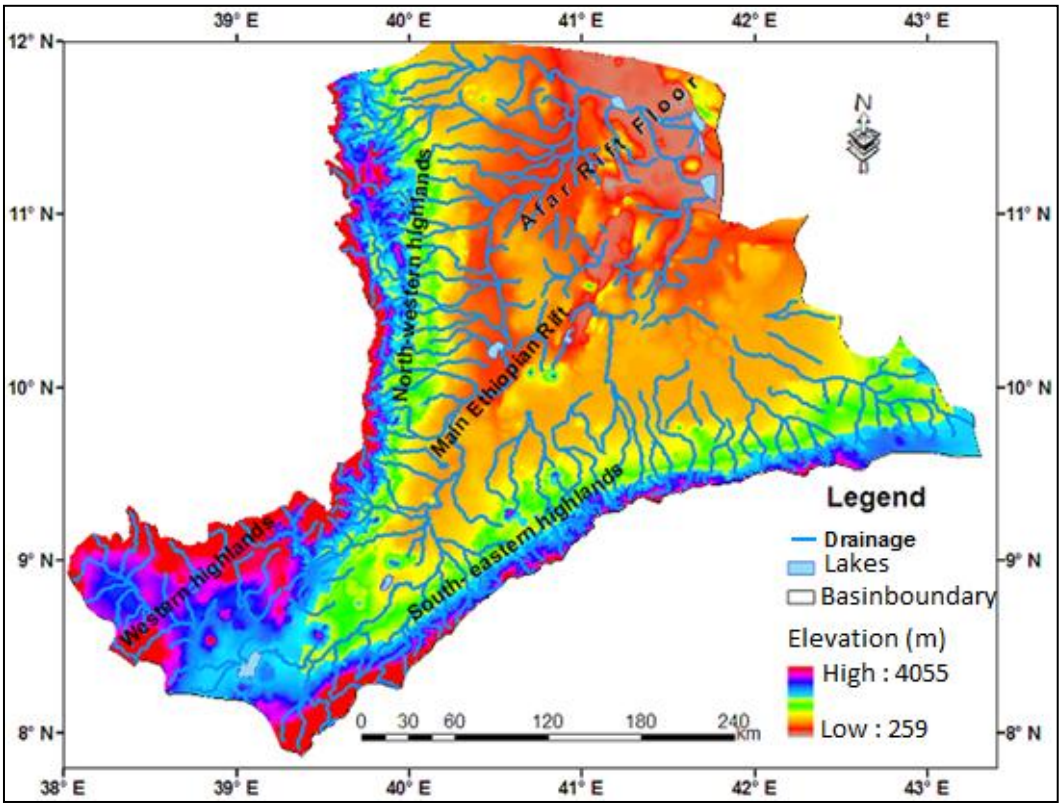

Figure 1. 1: Awash River basin physiographic and drainage map

1.6.5 Geology

On the plateau dominant rocks are the Tertiary volcanic: basalt tufts and agglomerates of the Trap series (Paleocene to Miocene age) and the younger, more silica-rich rhyolites, trachytes, tufts and ignimbrites of the Magdala group (Miocene to Pleistocene). On the floor of the Rift Valley, the volcanic rocks are mainly the basalts and ignimbrites of the Afar group (Pleiocene to Holocene) and Holocene lavas are present near the active volcanic centers like Fentale, Dafan and Afrera. During the Pleistocene pluvial period, very large lakes were formed on the floor of the Rift Valley and flat Plains of Wonji, Metehara and the lower Awash plains contain thick succession of lacustrine deposits comprises the deltaic alluvial plains in the Tendaho, Assaita, Dit Behri area and the terminal lakes area. Middle and lower valleys are part of the Great Rift Valley systems. The Rift Valley part of the Awash River basin is seismically active. The international border region of south-western Djibouti and northeastern Ethiopia, also named the Afar Depression or Afar Triangle or the Dankil desert, is a result of three separation of three tectonic plates (Arabian, Somali and African) Shared between Djibouti, Ethiopia and Eritrea, this region is an arid to semi-arid region (Sogreah, 1965).

1.6.6 Land Use/Land Cover

A generalized land use-land cover map of the Awash River basin and its immediate environs is presented in (Figure1.3). The data used for land use/land cover preparation were obtained from ministry of Agriculture, Woody Inventory and Strategic Planning Project(WBISPP) and it is simplified to less than 30 main classes, the map is in agreement with the broad climatic (agro-ecological zones) and physiographic components of the basin described earlier.

Cultivated lands are mainly croplands under rain-fed or irrigation. Rain-fed agriculture is the most commonly practiced traditional farming system in the basin. Generally, the area below1500m is considered as rough lower limit for the highlands and rain-fed agriculture. As a result, most of the upper basin, north-western and south-eastern highlands including some parts of the upper valley are intensively cultivated. Agriculture is the dominant sector of the economy accounting for about 45% of GDP, compared with services-20%, and manufacturing-under 10%. Agriculture provides a livelihood for 85% of the population. Approximately 65% of the total land area of 120million hectares is classified as agricultural land. Cereals, e.g. teff, maize, wheat, barley are the most important

agricultural output (80% of cropped area). The principal cash crops grown mainly in the Awash valley; fruit and vegetables (MoWR, 2010).

The type of vegetation and their spatial variation mainly describes land cover. Major mapping units (Figure 1.3) include grassland, shrub land, woodland and forests. The north-eastern and southeastern escarpments are predominately shrub lands. On the highlands, shrubs are associated with croplands. The pediment slopes along escarpment margins are mainly covered by shrubs and grasses.

Part of the rift valley has been mapped as bare lands: exposed volcanic rocks and sands/soils with sparse vegetation. While still to some extent the rift is semi-desert grassland with shrubs, riparian vegetation's occur along considerable stretches of mainstream Awash. On the other side, the Awash basin is endowed with several wetlands of various types (open water, perennial and seasonal swamps/marshes). Mentionable lakes on the north-western highlands are Hayk and Hardibe while Lakes Bishoftu, Hora, Beseka, Le Ado, Hertale, Yardi,Gemeri, Adobed, Afambo and Abe are some of the rift lakes in the basin. On the other hand, artificial lakes like Koka and Aba Samuel are reservoirs primarily constructed for hydro-power generation whereas Geffersa and Legedadi are reservoirs constructed to supply potable water to the metropolitan area of Addis Ababa after treatment.

Large perennial swamps in the basin include Gedebassa swamp bordering Yardi near Gewane, Borkena swamps within the structural graben on the north-western highlands, and lower plains swamps near the terminal lakes. Other permanent swamps and seasonal marshy areas are also found in the vicinity of other lakes and where topography permits their existence, predominately within structural basins.

Major urban centers of mappeable scale include the capital city of Ethiopia, Addis Ababa,and Dire Dawa. However, Holeta, Shewa Robit, Debre Sina, Ankober, Dese, Kombolcha,Debre Zeit, Mojo, Nazareth, Metahara, Awash, Gewane, Semera, Tinsae Birhan (Abomsa),Teferi and Meiso, are important towns of the basin amongst many. Having relatively significant populations, most of these towns are located on the highlands, while others in the valley are mainly found along the major state farms, rail road, and highways.

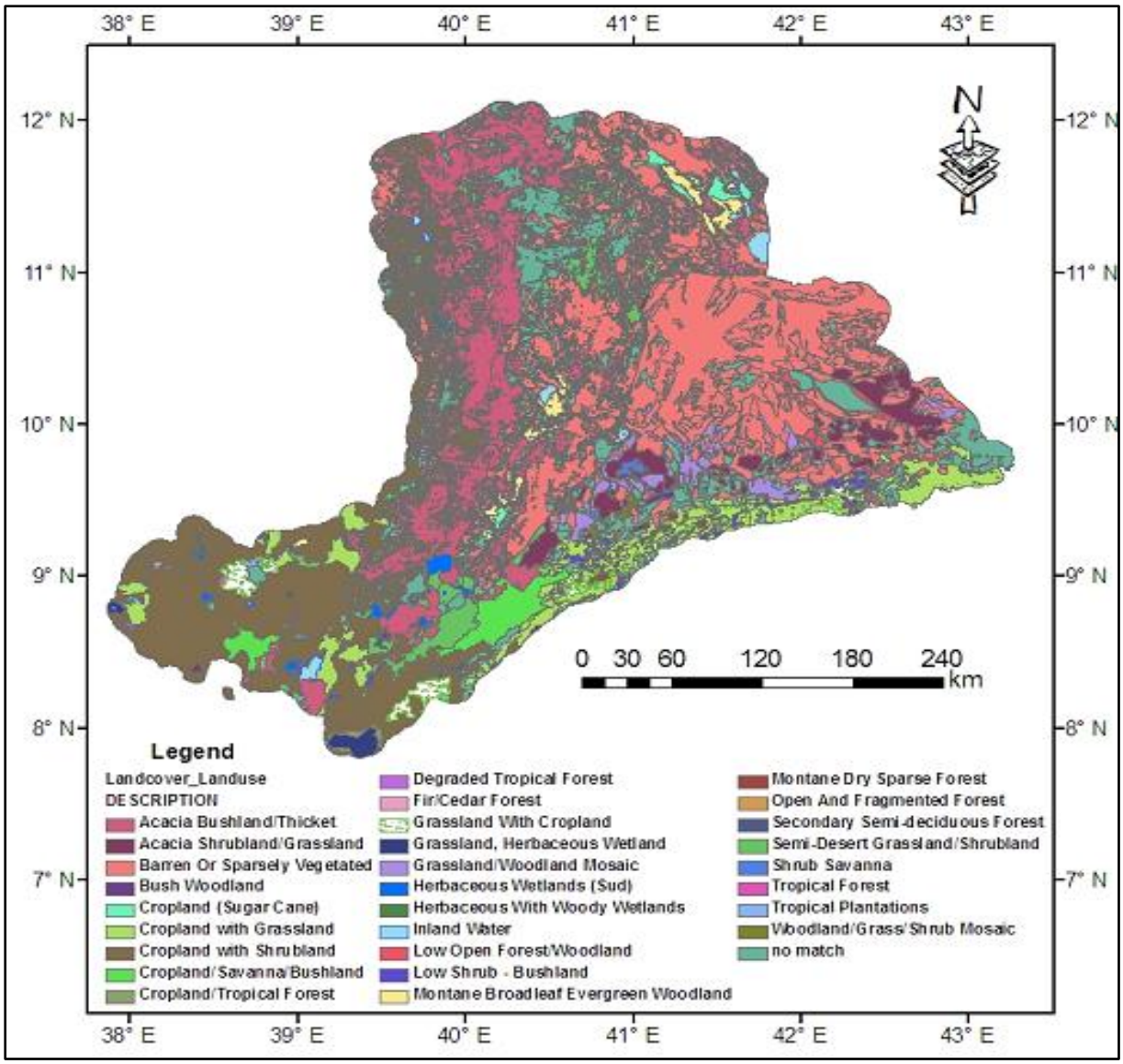

Figure 1.2: Land Use/Land Cover map of the Awash River basin

1.6.7 Soil

Soil map of Awash river basin is presented in (Figure in 1.4).The data used for soil map preparation were obtained from Food and Agricultural Organization (FAO).Among the soils in the basin approximately 30% of the area is occupied by Eutric Regosols in association with Lithosols, Eutric Fluvisols, Eutric Cambisols and Orthic Solanchaks.

Eutric Regosols are spread throughout the lower and the middle Awash valley. These soils are characterized by no-profile development loose soil material deposited on underlying hard rock, low water retention and have very limited agricultural potential. About 18% basin soils are orthic Solenchak in Chromi Fluvisols. Orthic Solenchaks are

spread throughout the northeastern part of basin in lower Awash valley. These soils are characterized by presence of soluble salts (EVDSA, 1989).

About 15% soils are Lithosols in association with Eutric Regosols and calcaric Flubisols and are scattered throughout the lower basin. About 12% area of the basin is occupied by Eutric Fluvisols in association with Chromic Fluvisols, Lithosols, Orthic Solanchak and Eutric Regosols are spread in middle valley and northeastern and north western parts of the basin. Eutric Fluvisols are recently deposited alluvium soils, fertile; medium textured and gave very good potential for agriculture. In upper Awash valley, peripheral western parts of the basin the soils are Eutric Cambisols, in association with lithosols, vetric cambisols and Luvic Phaeozems, coverage area is about 16% and agriculturally limited to moderate agricultural potential. 9% in the upper valley is occupied by Pellic Vertisols and Mollic Andisols, high clay content, swelling and cracking properties, impeded drainage and intensely rain-fed cultivation. These soils have good potential for cotton and Sugar cane.

With regard to basin, land suitability for irrigation is estimated about 35% area is suitable and out of this 10% is moderately and 25% is marginally suitable. The rest 65% is temporarily and permanently (35% of the 65%) not suitable for irrigation agriculture (EVDSA, 1989)

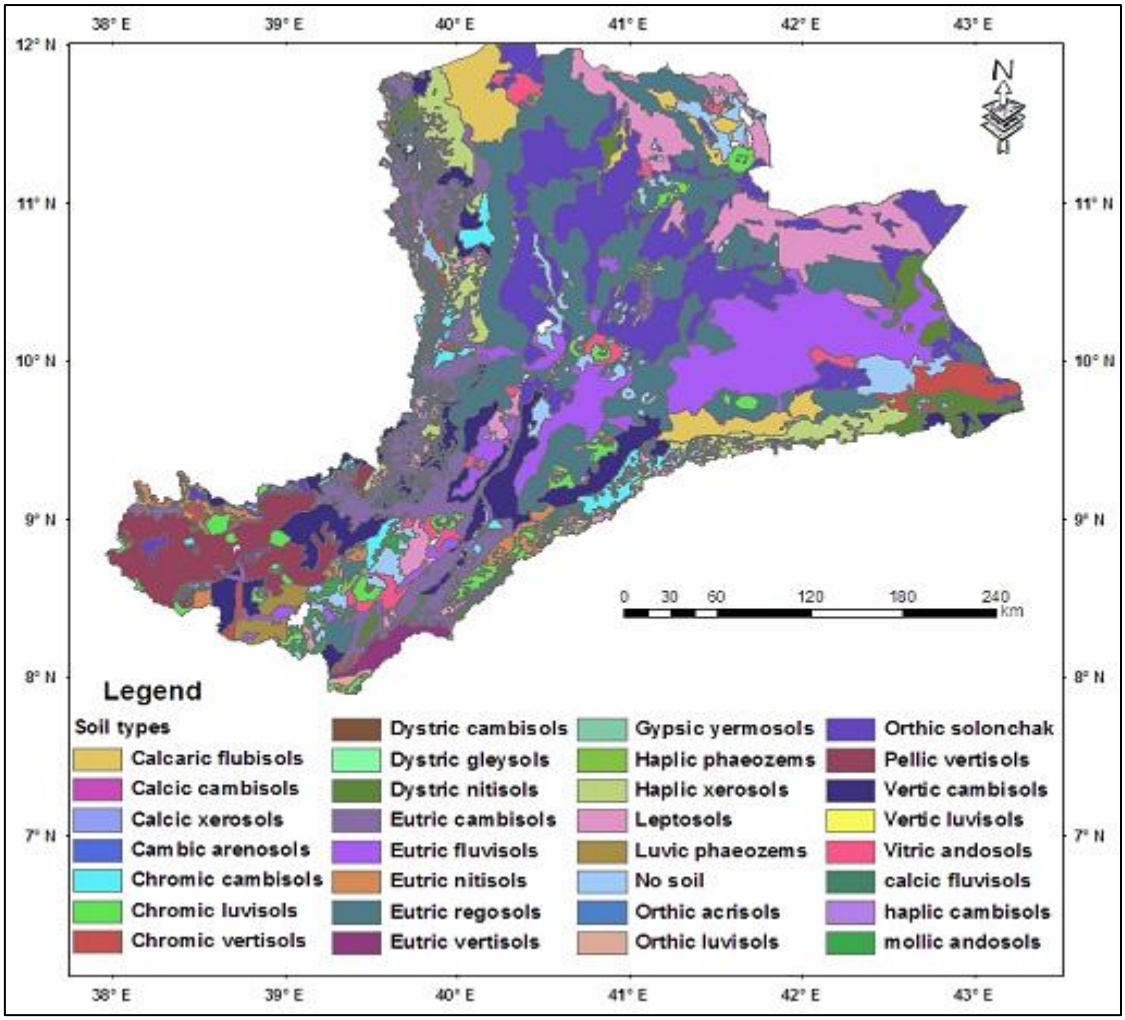

Figure 1. 3: Soil Map (FAO, 2002)

1.6.8 Climatic Features

The climate of the Awash Basin comes under the influence of the Inter-Tropical Convergence Zone (ITCZ) (MoWR, 2010). This zone of low-pressure marks the convergence of dry tropical easterlies and the moist equatorial westerly. The seasonal rainfall distribution within the basin results from the annual migration of the ITCZ. In March, the ITCZ advances across the Basin from the south, bringing the small or spring rains.

In June and July it reaches its most northerly location beyond the Basin that then experiences the heavy or summer rains. It then returns southwards during August to October, restoring the drier easterly air streams, that prevail until the cycle repeats itself in March.

The annual rainfall distribution resulting from this cycle is exhibited most clearly in the two distinct rainy periods, which are characteristic of the northern plains of the basin.

Moving southwards the more prolonged exposure to the moist air-stream is evident in the tendency for the two dominant rainy periods to merge into a contiguous distribution. On the high plateau to the west of Addis Ababa, the rainfall distribution shows a continuous increase from the spring rains to the summer peak rainfall. The distribution of rainfall over the highland areas is modified by orographic effects and is significantly correlated with altitude (Figure 1.5).

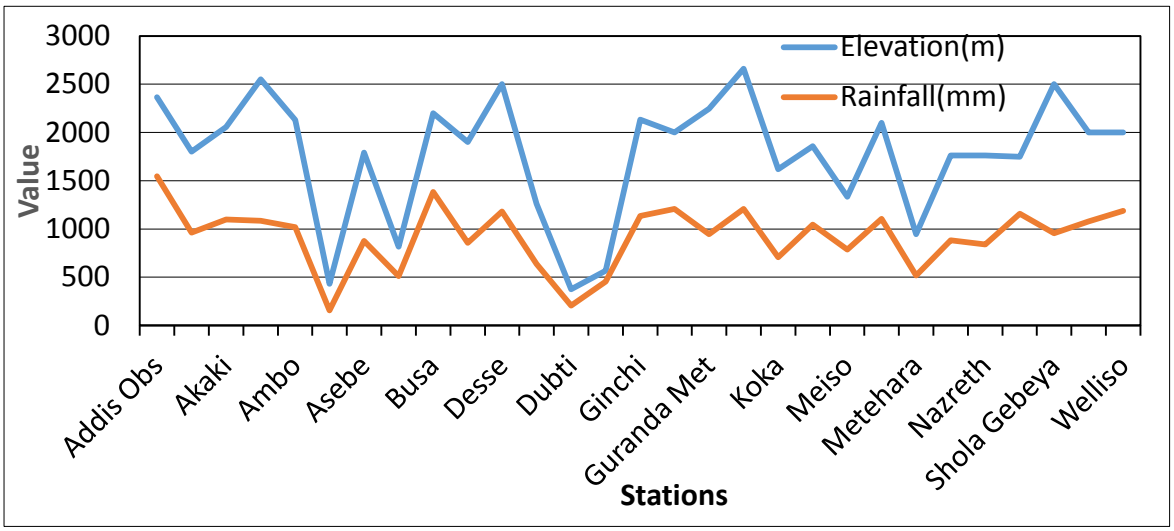

Figure 1.4: Mean Annual Rainfall vs Elevation plot for selected stations in the basin

The mean annual rainfall map indicated in (Figure 1.6) shows that the spatial rainfall distribution over the basin. The mean annual rainfall in the highlands of central and northwestern escarpments of the basin reaches more than 1020mm while the mean annual rainfall over eastern areas of the basin is less than 526mm. The mean annual rainfall over the entire western catchment is 850 mm.

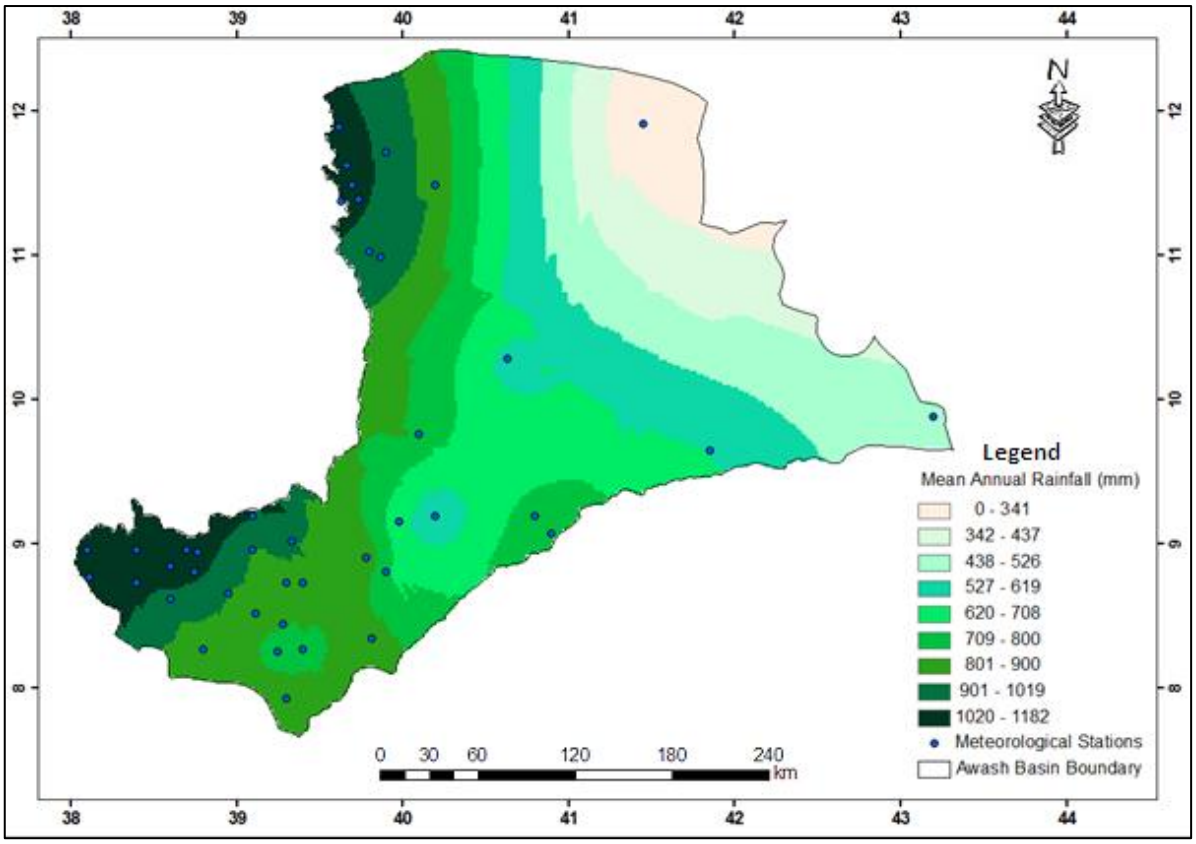

Figure 1.5: Mean annual rainfall map

The mean seasonal temperature varies from west to east and south to north of the basin. The north and north east of the basin receives more temperature during kiremt season (June, July, August and September) over stations like: Dubti, Assaita and Gewane. The western catchment of the basin receives low temperature during kiremt season. Western parts of the basin receives more temperature during Belg season (February, March, April and May) and the mean seasonal temperature value over most stations of western catchment is between 15-20^{o}C during kiremt season. Seasonal temperature distribution for selected stations in the basin is given in (Figure 1.7).

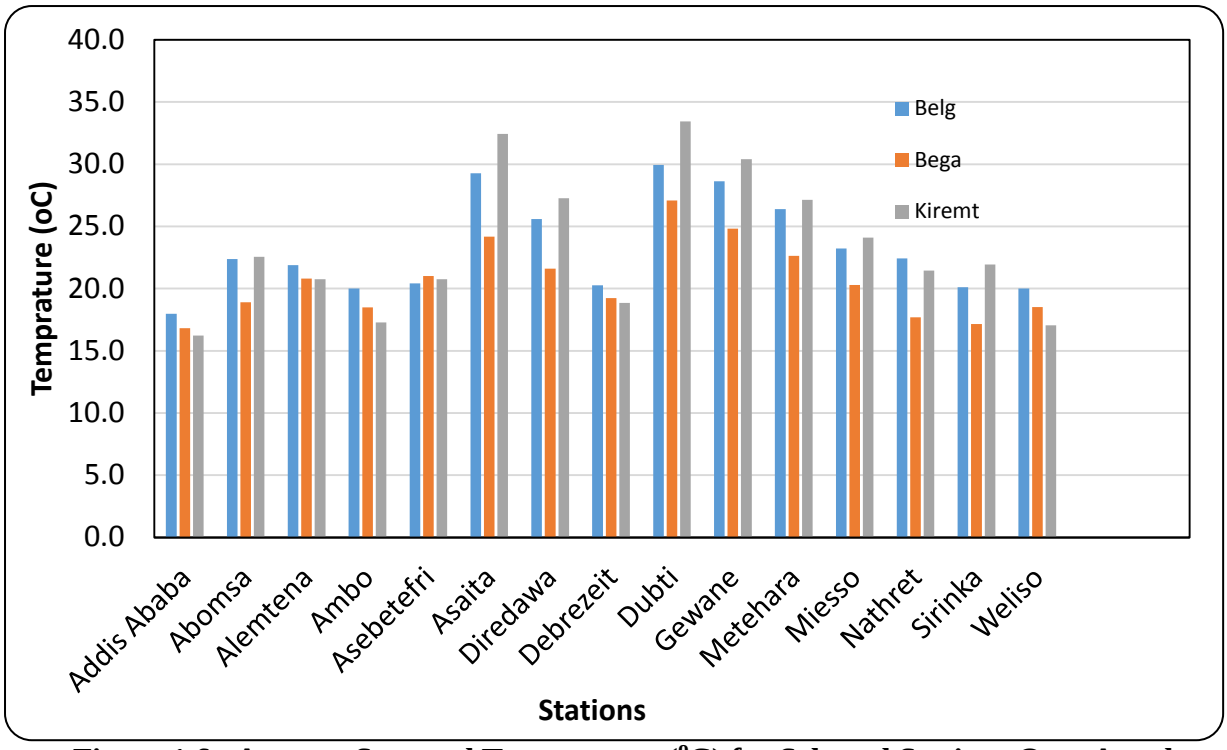

Figure 1.6: Average Seasonal Temperature (^{o}C) for Selected Stations Over Awash River Basin

1.7 Previous Research Works

Several studies have been conducted on delineation of HRRs and evaluation of satellite based rainfall estimation over the country including Awash River basin. Gissila *et al*., (2004) made study for the spatial variability in rainfall by grouping the rain-gauge station into four geographical cluster zones based on the seasonality and cross-correlation rainfall analysis for all Ethiopia. This study also followed the TAMSAT method and argued the satellite estimates were representative for the cluster zones defined both spatially and temporally. The study suggested that the estimate of rainfall using the linear regression method may provide the base of an operational seasonal forecasting system for Ethiopia.

Among the works, that addresses the general description of Awash River basin Integrated Development Master plan (MoWR, 2010) is also a very good document cited that indicate the rainfall characteristics in relation to the basin physical and socio-economical features. This document was the leading materials that provide both the geographical and the rainfall information about the basin.

Dinku (1994) has been studied making comparison of the gauge data with the estimated satellite rainfall for March to October for all the country. In his study, the TAMSAT was the method applied based on five years dekadal average for the western and north eastern

part of the country. The result of the study shows that the accuracy of satellite rainfall estimate is different for different parts of the country.

In general, published researches and scientific exercises within the study area are very coarse and they lack detail and sub-detail information since they are not specific to the basin. Those studies have shown some good result, but there is still some works to be done for detail homogeneous rainfall region areas of Awash River basin regarding the validation and evaluation of satellite based rainfall estimation since its contribution to Ethiopian economy is very high.

2. LITERATURE REVIEW

2.1. Rainfall and Rain-gauge

2.1.1 Rainfall

Rainfall is one of important climatic control factor in the hydrological cycle. It is the main source of water that is most vital for human life. The spatial and temporal depth of rainfall is necessary for all activities, scientifically, in the earth and atmospheric system. Thus, rainfall studies are essential in order to understand the supply and demand of water. Rainfall varies in its frequency, duration, intensity and spatial distribution and hence requires accurate observations. Tropical rainfall is mainly convective and thus it is more localized and its spatial and temporal distribution as well as the intensity of rainfall is highly variable.

Rain consists of liquid water drops mostly larger than 0.5mm in diameter. Rainfall usually refers to amount of liquid precipitation. In most countries rain is reported in three intensities these are: light for rates of rainfall up to 2.5mm/hr, moderate from to 6.0 mm/hr, and heavy over 7.6mm/hr (WMO, 1988).

2.1.2 Rain-gauge

A rain gauge is simply an instrument that is designed to measure the amount of rain that reaches the ground surface during a storm. Rain gauges are considered the most traditional method for measuring rainfall. They have been used historically to provide rainfall quantities and rates at a single point in space. The basic idea of most rain gauges is to collect rainwater into a cylindrical vessel of a fixed diameter. Rainfall measurements are usually provided in units of water depth (inches or millimeters). The volume of collected water is divided by the area of the cylinder opening and converted into a depth or rain (AMS Glossary, 2000).

There are different types of rain gauges that can be classified in to two main Categories: non-recording gauges, and recording gauges.

Non-recording gauge are basic storage devices that measure the cumulative amount of rain. A common type of these gauges is called the 8-inch Standard Rain Gauge (SRG) which has been used by many weather offices in the world. The standard gauge is simply a large cylinder with a funnel and a plastic measuring tube inside the cylinder.

A recording gauge is designed to automatically record the amount of rainfall reaching the surface as a function of time during the lifespan of a storm. The most common types of recording gauges are: Tipping-bucket rain gauge, Weighing rain gauge, Optical rain gauge and Disdrometer (AMS Glossary, 2000). Rain-gauge has the following advantages and disadvantages:

I. Advantages

Rain gauge is cheap and easy to maintain and read, also the rain gauge data are available for many years and hence it is possible to do climatological analysis using long period gauge data. Comparison between gauge data from different region is possible.

II. Disadvantages:

Although gauges are read once every day to get real time information they should be located in places where there is easy access for an observer, but there are remote areas of interest that are difficult to be accessed every day. Therefore, gauge networks can not cover all area of interest to make a real time observation. Source of errors in the reading gauge can also easily be occurred due to some cases like: airflow (wind direction and speed), unrepresentative orientation and exposure of the gauge, protection problem; by local community over the site, human Observation and transmission, error and miscode, evaporation from within the cylinder and gauge leaks and overflow.

Sometimes there might be time delay in getting the gauge data due to communication problem between the observer and the main center.

2.2. Satellite Remote Sensing

2.2.1. Remote Sensing

Because of considerable development of space technology airborne or satellite techniques are now common and most widely applied technology to obtain data on earth phenomena from distance. In simple language, remote sensing meant acquisition of data from a distance without physical contact of the objects. In fact, aerial photographs date back quite a way, satellite based remote sensing is a very new

technology dating from the launching from the first weather and earth observant satellites in 1960s (OECDE,1988).

Remote sensing, defined as "the transport of information from an object with a distance to a receiver (observer) by means of radiation transmitted through the atmosphere" (http.www.gis.com/whatisrs/dowithgis.html) offers the possibility of observing rainfall in real or near real time over relatively large areas and of complimenting the conventional precipitation measurements. The basis for all remote sensing is the electro-magnetic spectrum (EMS) viewed in (Figure 2.1).

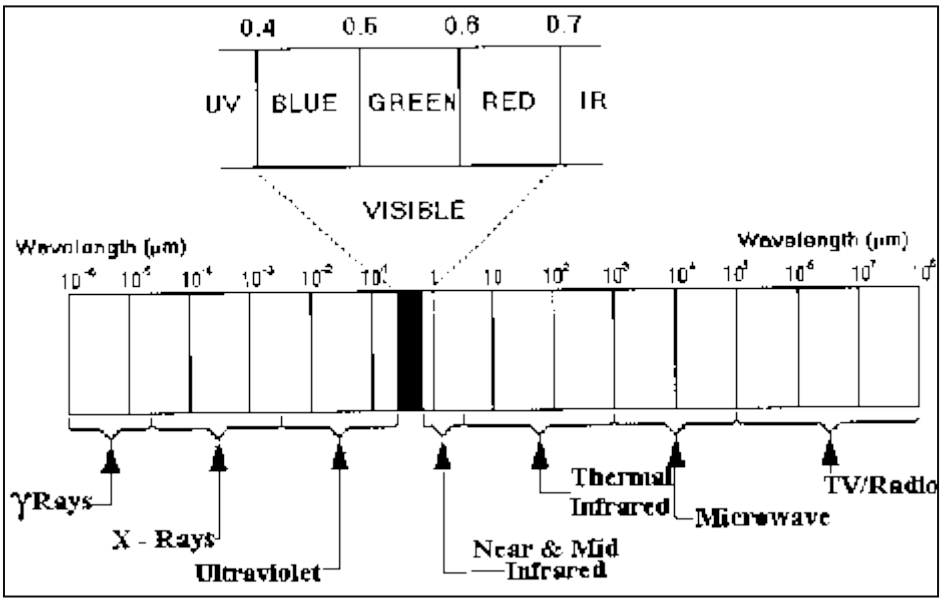

Figure 2.1: The Electromagnetic Spectrum

(Source: http://www.geo.mtu.edu/rs/back/spectrum/)

Remote sensing takes the advantage of unique interactions of radiation from the specific regions and the earth. There are four basic component of a radiation based remote sensing system, given as follows:

I. Radiation source (e.g. the sun, radar laser)

II. Transmission path (atmosphere vegetation canopy, shallow soil surface)

III. Target (e.g. river soil.) and

IV. Sensor (multi-spectral-scanner, thermal sensor, microwave sensor).

Remote sensing is based on interpreting measurable variations in spectral, temporal and spatial characteristics of the earth. Spectral characteristics (or signature) of the target are the unique spectral reflectance for specific earth features (Engman and Gurney, 1991). The process of data acquisition in remote sensing is the fruit of a complex set of operation using the serious of sophisticated methods. These consists satellite and data reception or processing stations. Remote sensing also classified into three types in respect to the wave length region as shown in (Figure 2.1).

These are:

I. Visible and reflective infrared remote sensing (0.4-0.7μm).

II. Thermal infrared remote sensing (Greater than 3μm).

III. Microwave remote sensing (1mm-1m).

2.2.2. Satellite

(a) Overview

A Satellite is a spacecraft that orbits the earth and returns images of the earth and the atmosphere back to the receiving station on the ground. Satellites are used to estimate rainfall using radiation signals reflected or emitted from the ground and atmosphere and observed by it. Satellite based rainfall estimation is also one part of this technique, and it is a method of deriving qualitative(image) and quantitative(value) using visible and infrared techniques through indirect relationships between solar radiance reflected by clouds, that is, the clouds brightens temperature and rainfall. The detail will be discussed in the coming sections in this study.

There are two basic and important approaches in using satellite for rainfall estimation purposes. These are:

(a) Cloud index and

(b) Life-history method.

The first type based on the cloud classification and does not require serious consecutive observations of the same cloud system. The second type is makes use of data from the geostationary satellites which produce images usually every half an hour. It has been applied mostly for convective cloud system.

(b) Satellites are divided into two functional Sub-Systems.

I. Surface-Based Sub-system

This system comprises stations of various kinds making observations at or from the surface of the earth and oceans including observation made aboard aircraft and by instruments carried aloft by balloons or rockets. The main component of this system is a network of surface and upper air by members for their own use and as a contribution to international meteorological information exchange system. Some of these are for example: Ozone stations, World Climate Program (WCP), etc.

II. Space-based sub system

This system comprises Satellite of two types, polar orbiting and geostationary satellite. Both satellites provide qualitative information such as visible and infrared cloud images over wide areas.

(c) Satellite Data Receiving System.

The ground segment of the space-based sub-systems of the satellite has two functions.

I. To provide for reception of signals from satellite containing qualitative and quantitative information, including observations from data collection platforms and others similar systems.
II. To process, format, display and distribute the information received either directly from satellites themselves or digital forms received at required standards.

There are also two type of transmissions utilized for dissemination of satellite data. These are:

Special digital transmission (High Resolution-HR) and conventional analogue transmission method

(d) Advantage and Disadvantage of Satellite-Based rainfall Estimation

I. Advantage

Relatively time consuming, and easily for large volume of data acquisition and extraction system, easy to operate and maintain.
It is Tried and Proven, but mainly in tropical zone.

In connective rainfall, accurate monthly totals can be obtained

II. Disadvantage

At night, no visible data are available therefore rainfall estimation are achieved using infrared and, perhaps, microwave data.

The techniques for rainfall estimations are based upon assignment of temperature and/or brightness thresholds to rainfall amounts vary in performance with month and seasons.

If the satellite sensors fail, there is no possibility of repair until another satellite is launched.

Radar is also a very good devise used to estimate rainfall over a given area by observing the back-scatter of electromagnetic radiation from liquid water drops. Radar has an advantage over rain-gauge for providing a spatially continuous image. Here, we don't discuss about radar because it is not the scope of this study.

2.3. Rainfall and Satellite–Based Measurements

2.3.1. Meteorological Satellite - METEOSAT

As many references cited, understanding the importance of observing weather from space Verner Sumoi and colleagues at the University of Wisconsin developed the first successful meteorological satellite that was launched on 13 October 1959. This satellite used a Suomi radiometer and returned coarse maps of reflected solar radiation from the earth surface and infrared radiation emitted by the earth (Tuker, 1997). On 01April 1960 a first satellite completely dedicated to meteorological purpose was launched and TIROS 1 (Television and Infrared Observational Satellite) was the 22nd successfully launched satellite. TIROS 1, had a lifetime of 79-day, was the first satellite that returned an image of the earth with its weather systems as a whole. Since then several technological improvements were made in the TIROS series and eventually the present standard TIROS N-series is reached.

Geostationary Operational Environmental Satellite 1 (GOES 1) was the first operational geostationary satellite that was launched in 1975. In the late 70s Japan's Geostationary Meteorological Satellite 1 (GMS 1) and European Space Agency's METEOSAT 1 were launched. The METEOSAT 1 in addition to the visible and

infrared had a third channel of water vapor. Since 1978 one or more passive microwave sensors have been available on polar orbiting satellites, such as the Special Sensor Microwave/Imager (SSM/I) on the Defense Meteorological Satellite Program (DMSP).

The earth's artificial satellite can be classified according to their functions; but the interest of this study lies with the meteorological satellite such as METEOSAT, NOAA, etc. Indeed, it was for weather observation that these satellites were used. The first was polar orbited satellite up to until 1966 and geostationary satellite afterwards.

(a) Polar Orbiting Satellites

Polar orbiting satellites are launched into sun-synchronous orbits at an altitude of about 800km.The sun-synchronous orbit of the polar orbiting satellite enable them to observe the signal at each location with the sun always be in the same place in the sky (Houghton and Taylor, 1973). For example, if the satellite crosses a certain place at mid-day when it goes to the northern pole then as it goes to the southern pole it re-crosses the place at mid-night. The satellites have a period of about 100 minutes i.e. they take about 100 minutes to complete an orbit and scan the earth's surface in about 24 hours. The METEOR of the former Soviet Union and the US TIROS are polar orbiting satellites and of which the TIROS (NOAA Series) are the most widely used. India also launched two polar orbiters: Bhaskara-1 and Bhaskara-2 in 1979 and 1981, respectively. Polar orbiting satellites are essential to provide global and hemispherical image of the weather (Houghton and Taylor, 1973). However, images from polar orbiting satellite are obtained only once or twice per day, and hence for continuous monitoring of the weather it becomes difficult to rely only on polar orbiting satellites.

On the other hand, because of their low orbits the spatial resolution obtained from polar orbiting is higher than the geostationary one's (i.e. polar orbiters observe a lot of detail information than the geostationary satellites).

(b) Geostationary Satellites

Geostationary satellites were first launched in the 1970's. Each satellite has a lifetime of approximately 5 years. Satellites have been launched and maintained by NOAA (GOES E+W) and the space agencies of Europe (METEOSAT), Japan (GMS), India (INDSAT), Russia (Elektro) and China (FY-2). The Russian Elektro satellite has not

yet produced reliable operational imagery and the Chinese FY-2 satellite failed shortly after its launch. This leaves an unfortunate gap in the global coverage in this important part of the world. However, the latest Indian geostationary satellite, INSAT-2B positioned at 93.5^0 E does provide useful coverage in Asia.

Currently, METEOSAT-5 is also stationed over the Indian Ocean. The other regions poorly served by geostationary satellites are the Polar Regions, where image distortions occur due to the satellite's position above the equator. The global geostationary satellite coverage is illustrated in (Figure 2.2).

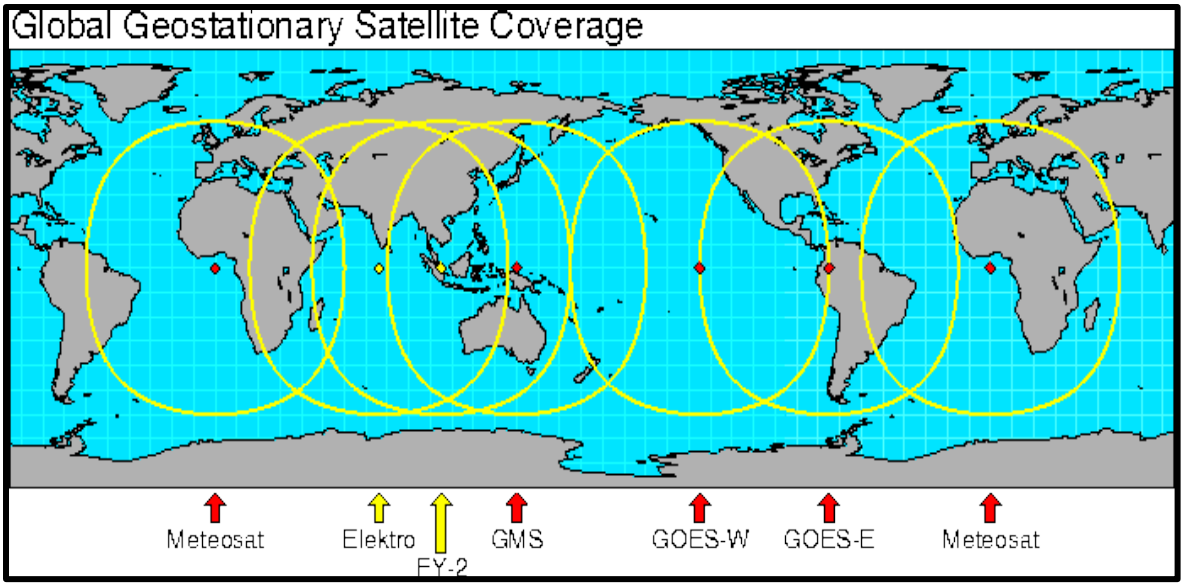

Figure 2.2: Areas viewed by geostationary meteorological satellites

(Source: http://www.rap.ucar.edu/)

Geostationary satellite orbits eastwards around the equator at an altitude of approximately 36000km (Dugdale, 1994). An orbit at this altitude has a period of 24 hours, which means the satellite remains fixed relative to the Earth's surface, hence the name geostationary satellite. The scanning system allows about 42% of the Earth's surface to be viewed from a single satellite, so that a network of five satellites gives global coverage. The geostationary satellite can monitor developments in the field of view continuously and in almost real-time. This allows the user to follow quickly developing weather systems or diurnal variations in the weather. This is of great value to forecasters. However, the large distance of the satellite from the Earth's surface means the resolution is lower than with polar orbiting satellites. NASA launched the first Geostationary Operational Environmental Satellite (GOES) in 1975. Currently GOES numbers 8 and 10 are in orbit,

launched in 1997. One satellites is positioned at 75^{o}W (east coast of the US) and the other is positioned at 135^{o}W (west coast of the US). The satellites are named GOES-E and GOES-W respectively. The GOES satellites are equipped with radiometers with five spectral channels.

Table 2.1: The GOES radiometer channels

(Source: EUMETSAT, 1997)

Channel	Wavelengths
1	0.55-0.75 µm
2	3.80-4.00 µm
3	6.50-7.00 µm
4	10.20-11.20 µm
5	11.50-12.50 µm

With the advent of geostationary weather satellites in the 1960 and 1970, positioned above the equator at 5-6 positions around the globe to provide complete coverage, various techniques have been developed to estimate rainfall from visible and infrared (IR) radiation upwelling from the Earth into space. The higher the cloud albedo, the more droplets and/or ice crystals it contains and the deeper it tends to be, so the more likely rainfall is on the ground. And also the lower the IR brightness temperature, the higher the cloud top and the more likely the rainfall. A combination of both channels works best. Imagine a fair day with cirrus clouds, for instance. The IR channel may flag this as wet, because of the cold cloud tops; however cirrus is optically thin, so in the visible channel it is dry. The visible/IR rain retrieval algorithms work best at low latitudes, because at higher latitudes the view is more slanted, confusion arises with high-albedo surfaces of snow or ice, and deep-convective precipitation is less common. Another problem is incomplete pixel filling for small cumulonimbus clouds

At night no visible imagery is available. One can then use an empirical relationship between cloud-top temperature (deduced from the outgoing radiation in the 10.7-micron waveband), the simultaneous precipitation rate inferred from surface radar reflectivity, and the humidity profile (derived from radiosonde data). The rainfall rate (R, mm/h) depends on the cloud-top temperature (Temperature Degrees Kelvin) thus $R = 1.1183 \times 10^{11} x \exp(-3.6382 \times 10^{-2} xT^{0.5})$. Adjustments are then made according

to the perceptible water and surface relative humidity. The rate of change of cloud-top temperature can be used as well. It indicates the speed of cloud growth, and hence the areas of heavy rainfall.

In practice, the procedure allows useful estimates over 6 hour's periods. However, it overestimates rainfalls over 24-hours in the case of slowly moving thunderstorms with a broad anvil, by exaggerating the area of rainfall. On the other hand it underestimates rainfall from warm-top stratus, especially near coastlines and in mountainous terrain. In short, quantitative precipitation estimates from geostationary satellites can yield cumulative rainfall and thus flood warnings, for instance, because of the continuous coverage, but large discrepancies with rain-gauge data occur.

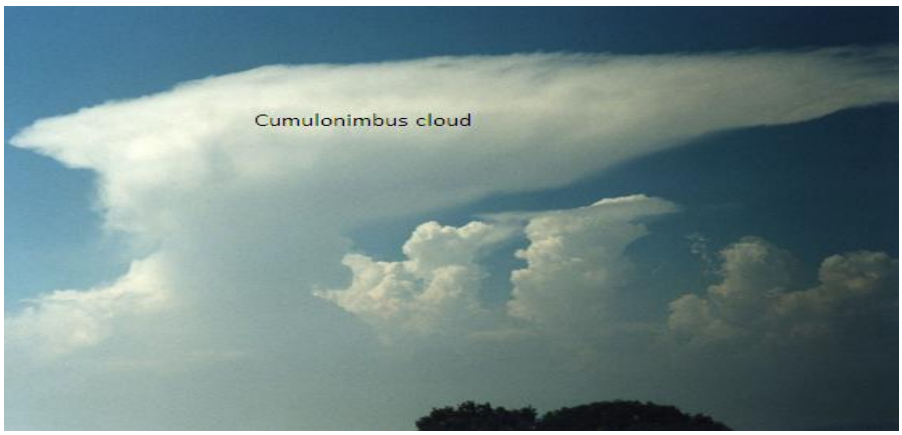

Figure 2.3: Rain Bearing (Cumulonimbus) Cloud

(Source: http://www.skybrary.aero/index.php/cumulonimbus)

Cloud towers like the one in (Figure 2.3) are visible from space bubbling up and decaying, particularly in the tropics. Satellites are able to measure the temperature of the cloud tops. The temperature of the atmosphere decreases regularly with height in the lowest 15 km of the atmosphere. The temperature at the tops of the tallest clouds can be as low as -80^{o}C and this contrast sharply with the warm ground. We can produce images showing the areas where the cloud-top temperature is below certain threshold temperatures.

Generally, when the cloud top temperature falls below approximately -40^{o}C, there is some rainfall occurring below. Such Clouds are Cold Clouds. The life cycle of this Cold cloud is also shown in (Figure 2.4).The time spent by an area with cloud top temperatures below the thresholds is known as cold cloud duration.

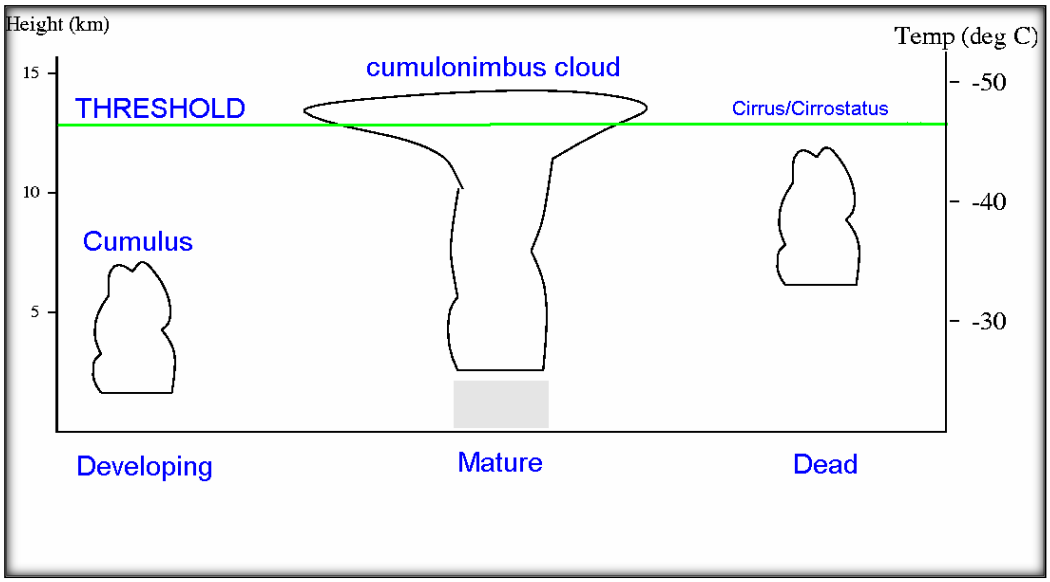

Figure 2.4: The life cycle of Cloud (Grimes et al., 1999)

In the life cycle of the cloud system, the developing stage produces rainfall before the top of the height of the cloud has exceeded the threshold. And then the rain bearing clouds have died down after the convective cloud weakened. The reflectance from the top of cloud at given temperature is a sensitive part to observe by the satellite mechanisms. There are various type of Satellite designed to perform specific tasks. However, there now follows a description of the major geostationary satellites. The scanning and transmission systems of each satellite are broadly similar, so only the METEOSAT system is discussed in detail.

2.3.2. Characteristics of METEOSAT Satellite

(a) METEOSAT

European Space Agency launched METEOSAT. The first METEOSAT was launched in 1977 after the success of the American TIROS satellites. Initially 8 European countries financed the project. Today there are thirteen countries working together under the EUMETSAT organization with the aim to "establish, maintain and operate a European system of operational meteorological satellites".

The headquarters of EUMETSAT is in Darmstadt, Germany. The latest, METEOSAT-7 was launched on the 2 September 1997 and became operational on the 3 June 1998 (EUMETSAT, 1997a).

A previous satellite, METEOSAT 5 was moved to a position above the Indian Ocean (around 63^{o}E) to support a 2 year experiment in that region. This is described in more detail in EUMETSAT's website. METEOSAT 6 was relocated to the stand-by position at 100 W after METEOSAT took over as the operational satellite

The METEOSAT satellite which is viewed in (Figure 2.2), it orbits at an altitude of 36000km above the point 0^{o}N and 0^{o}E in the Gulf of Guinea. This point vertically below the satellite is called the sub-point. The satellite rotates around an axis which passes lengthwise through the center of the satellite and is perpendicular to the plane of its orbit, completing 100 revolutions per minute.

A spin Scan Radiometer is the meteorological instrument on METEOSAT that enables it to return images of the earth and atmosphere in the Visible (0.4-1.1μm) and thermal Infra-red (10.5-12.5μm) and Water vapor (5.5-7.1μm). East-west optical scanning is achieved by the rotation of the satellite at the rate of 100rpm, while a scan mirror that moves in 192mrad steps does the north-south optical scanning. Thus, full-disk hemispherical image is obtained from the east west and north-south optical scanning. This takes a further 5 minutes, so a full image is produced every 30 minutes (EUMETSAT, 1997).

(b) Characteristics of METEOSAT

Thermal Infra-Red (TIR) Imagery

METEOSAT transmits TIR images every 30 minutes. It is from these CCD images are derived. You need to know the calibration data required to convert each TIR image in a cold cloud counter. You can add these to obtain CCD Images at any desired temporal step above 30 minutes but production is usually restricted to one day and ten day cold cloud duration images, requiring at least 24 and 240 TIR images, respectively.

The METEOSAT radiometer is equipped with a visible channel and two infra-red channels. Their wavelengths are shown in (Table 2.2).

Table 2.2: The METEOSAT radiometer channels

(Source: http://eoedu.belspo.be/en/satellites/MeteoSat.htm)

Channel	Wavelengths
1. Visible (VIS)	0.45 - 1.0 μm
2. Thermal Infrared (TIR)	10.5 - 12.5 μm
3. Water vapor (WV)	5.7-7.1 μm

The visible channel scans 5000 lines in each image, with each line consisting of 5000 pixels. The infrared scans 2500 lines and pixels. The sub-point resolution in the visible and infrared channels is 2.5km and 5km respectively. The resolution decreases somewhat towards the edges of the image (4.5km over Europe in the visible) due to the viewing angle of the radiometer (Source: http://www.tamsat.red.uk.edu/).

Currently EUMETSAT are working on the second generation of METEOSAT satellites. The new satellites will be spin-stabilized like the current generation, but with many design improvements including a new radiometer, which will produce images every fifteen minutes, in twelve spectral channels.

2.4. Rainfall Estimation Techniques

Different methods are available for estimating area rainfall using images of visible (wavelength between 0.4 and 0.7μm) and infrared (wavelength between 10.5 and 12.5μm) electromagnetic radiation from geostationary satellites.

The visible channel measures the short wave radiation backscattered by the atmosphere and the earth. This channel gives the albedo of the reflecting body and high brightness implies a highly reflecting cloud. The high cloud brightness in turn is related to the cloud optical thickness and liquid water content. However, this relation is valid only for cloud thickness less than 700m beyond which the relation saturates and there is little change in the cloud albedo.

The infrared channel measures thermal radiation emitted by cloud and this is related to the temperature of the emitting cloud by the Planck's radiation law. On this approach the height of the cloud is inferred from the temperature of the cloud top that is obtained from satellite infrared observation. Thus, cold cloud is assumed to be deep and rain giving.

Therefore, high brightness in the visible channel and low temperature in the infrared channel imply large cloud thickness and high cloud top respectively. These in turn imply greater probability of rain. Therefore, the brightness and or temperature of precipitating cloud are an indirect measure of convective rainfall intensity (Turk *et al*., 1997).

There are different type of methods are found to estimate rainfall from the satellite source. Microwave, CPC, OSTROM and TAMSAT are some of the common methods used by American climate prediction center and reading university in UK. Estimation of rainfall from satellite over Africa is useful in order to augment the rainfall data obtained from relatively sparse rain-gauge network in the region. Moreover, the real time satellite estimation also solves the delay of information on rainfall that might be caused by in effective means of communication from out station to the central office. For this study only TAMSAT rainfall estimation techniques are considered.

2.4.1. TAMSAT Rainfall Estimation System (TRES)

The TAMSAT methodology has been described in detail elsewhere e.g. (Milford et al., 1994, Thorne et al., 2001, GRIMES and DIOP, 2003) but here will give summary as background information for the study. This method of rainfall estimation utilizes the 10.8μm infra-red channel from the METEOSAT geostationary satellite and has data spanning more than 30 years. From this channel, the brightness temperature can be calculated. This methodology attempts to define a linear relationship between the numbers of hours for which a satellite pixel temperature is colder than a specified threshold temperature.

The TAMSAT rainfall estimation technique can be traced back to the work of (Arkin and Meisner, 1987) who used the idea of Cold Cloud Duration (CCD) to show that rainfall in the tropical Atlantic could be related to the fractional coverage of cloud with satellite-measured temperatures below 235K (-38°C). The TAMSAT algorithm was initially developed for rainfall estimation over North Africa for agricultural purposes and predicting famine and floods.

The TAMSAT technique does not merge satellite data with current gauge observations, but uses historical data that is perceived to be invariant over long time periods to generate climatological calibrations. The TAMSAT methodology (Grimes et al., 1999) in its simplicity uses only geostationary IR data on board METEOSAT satellites and exclusively covers Africa (Thorne et al. 2001). The calibrations are carried out separately

for each calendar month within empirically determined climatic zones. The methodology is perceived to the one of the simplest methods employed for remotely sensed rainfall which has better performance in rainfall estimation compared to more complicated methods such as those defined by Adler and Negri, (1988), Dinku et al., (2007), Chadwick and Grimes, (2012). The detailed basic assumptions inherent in the TAMSAT rainfall estimation method include as discussed by Grimes et al., (1999);

Rainfall predominantly comes from convective clouds.

Clouds only rain when their tops have reached a certain minimum height (threshold height)

Cloud top height can be identified by its temperature on the thermal infra red (TIR) image referred to as T_t

Over a given location, the quantity of rainfall can be calculated from the length of time the cloud top has been above the threshold referred to as the cold cloud duration (CCD).

$$Rs = a_0 + a_1 \mathbf{D} + \mathbf{e}$$

Where R_s is the rainfall over the pixel, D the cold cloud duration over the pixel and e the error with zero mean, E{e} = 0, and homogeneous variance {var} = σ^2. In practice T_t, a_0 and a_1 are calculated for each month for a number of empirically determined calibration zones. These zones are defined to be climatologically homogeneous areas with sufficient rain gauges to give a statistically reliable calibration. A further assumption is that the relationship between rainfall quantity and the cold cloud duration is linear provided there is adequate averaging of the data either in space or in time, then:

$$\hat{R}_s = \hat{a}_0 + \hat{a}_1 \mathbf{D}$$

Where, 'hat' indicates estimated parameters (Grimes et al., 1999). These above assumptions are explained schematically in the below figure;

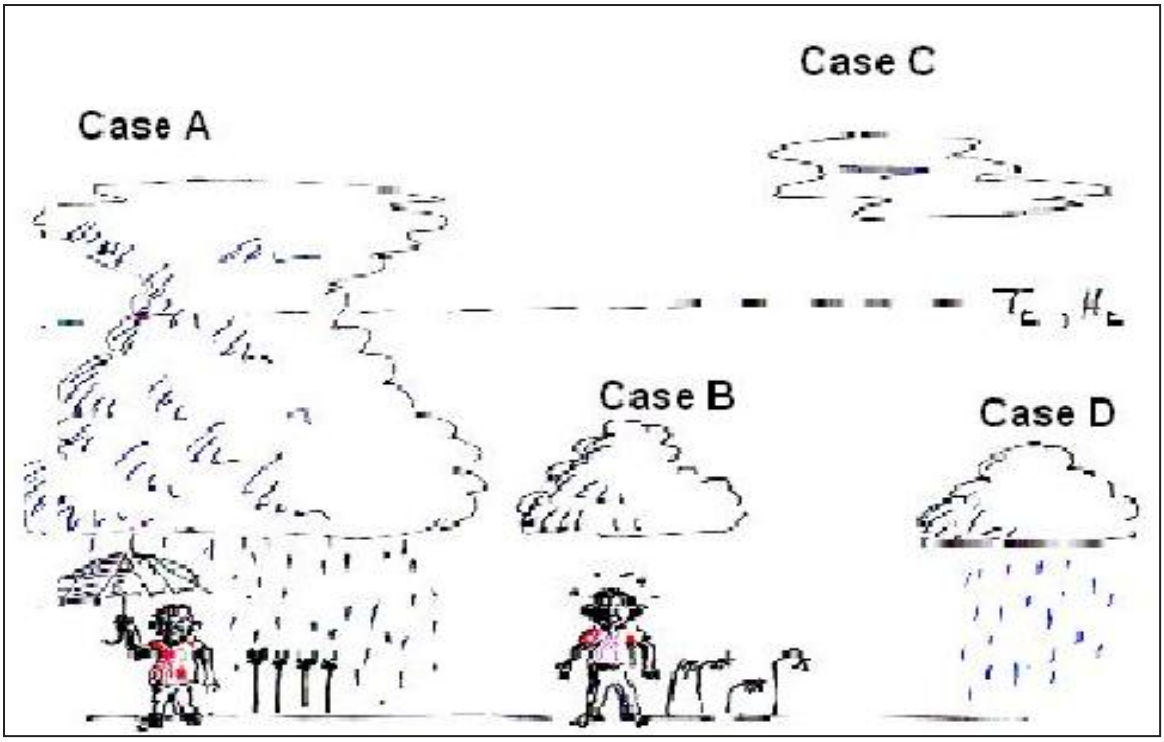

Figure 2.5: Schematic diagram of clouds with tops colder than threshold temperature Tt: (dashed line) are assumed to be raining, while clouds with tops warmer than Tt are assumed not to be raining (Source: Grimes et al., 1999).

From the discussions above, some limitations of the TAMSAT algorithm are evident as is shown by the schematic (Figure 2.5). These errors combined are associated with identification of cloudy scenes and identification of precipitation from cloudy scenes and non precipitating cloudy scenes. The problem of discriminating a cloud clear and cloud precipitating is represented in the above scheme, where small clouds generating precipitation without reaching the threshold temperature are missed or regarded as non precipitating clouds. Similarly high level non-precipitating cloud, when present, may sometimes be indistinguishable from convective cold cloud tops in TIR images, leading to overestimation of the rainy area.

3. Homogeneous Rainfall Regions

For the discussions of this section, it should be important to know the climatology of the rainfall characterized over the basin. Rainfall is one of the main components in defining the basin characteristics. In Ethiopia there are four major rainfall regimes and they are named as rainfall region A, B, C and D (Figure 2.6)

Area under Region A are characterized by bimodal-I having three distinct seasons Kiremet, Bega and Belg, Region B is a mono-modal type which have one long rainy

season throughout the year. In this region two distinct seasons are observed one being wet and the other dry season is encountered. Region C is the second bimodal-II type with dry season in between the first wet season is from March to May and the second is from September to November the rainfall peak month are April and October. The last rainfall region is region D, the rainfall in this region diffused that means it has no distinct pattern and meager and erratic rainfall. It covers the area near and around Dalol depression and extends to the Red Sea cost (NMA, 1996).

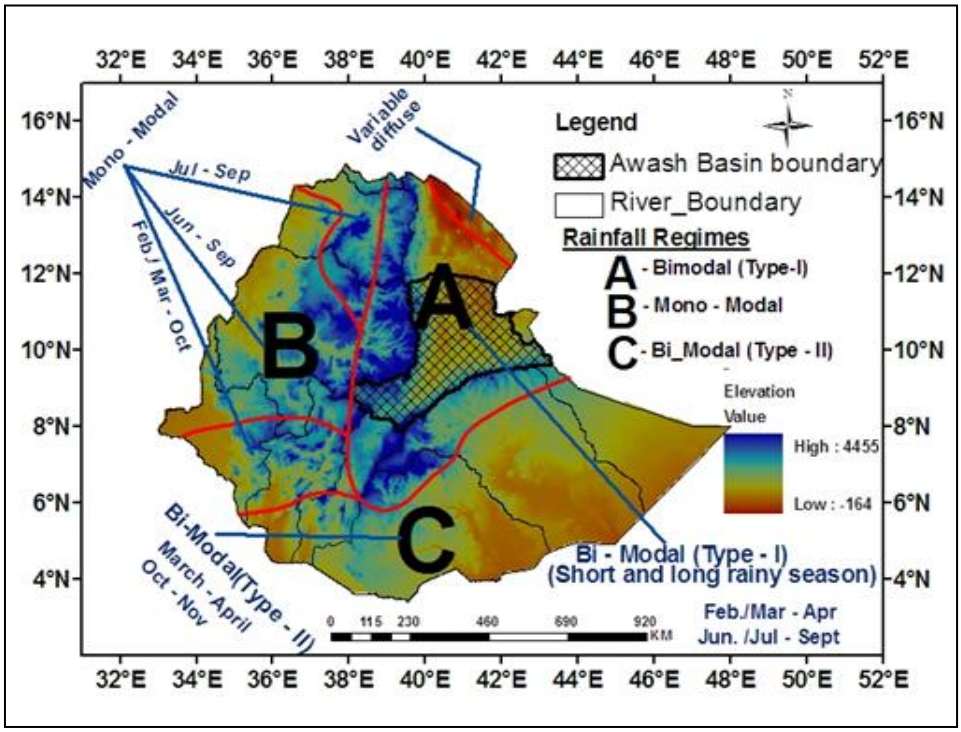

Figure 2.6: Rainfall Regimes of Ethiopia (Modified from: NMA, 1996*)*

As it is indicated in figure above, the rainfall of the basin is characterized under rainfall regime A (bimodal type I). Meteorologically, the seasons in this regime are classified into three main groups:

I. Belg Season (small rainy season) -- February to May

II. Kiremet Season (main rainy season) -- June to September

III. Bega (Dry season) -- October to January

3. MATERIALS AND METHODS

3.1. Data Type and Source

3.1.1. Data Types

In conducting this study some primary data sources from field observation and secondary data including gauging and satellite rainfall data, satellite image, other resources including published and unpublished materials, books, journals, articles, reports, and electronic web sites, which are written on the subject matter of this study were collected.

Dekadal (ten-daily) rainfall data from Gauge stations and RFE image derived from METEOSAT thermal infrared imagery (TIR) CCD data at Dekadal basis are the basic secondary datasets used throughout the study.

(a) Rain Gauge Station Data – is the gauge recorded rainfall data. This dataset consists of Dekadal rainfall from more than 50 stations over the Awash River basin. For the purpose of this study the rainfall data for the year of 2008, 2009 and 2010 are selected to compare Dekadal, monthly, seasonal and annual climatology of gauge with that of RFE obtained from the satellite data. Among the three selected years, the rainfall distribution during the year of 2008 is normal, 2009 is slightly below the average and 2010 is wet year. The selections of the years are based on the past synoptic features of the observed gauge rainfall analysis.

(b) Satellite Data- For this study, the TAMSAT dataset which normally at 0.0375° x 0.0375° grid boxes spatial resolution and 10-day temporal resolution was used. These images are processed and converted into RFE value using Geographic Information System (GIS) tool. Thus, for each selected year, 36 Dekadal RFE imageries and a total of 108 imageries for the three selected years were used. This later adjusted for the analysis based on geographical bounded location of the Awash River basin with respect to delineated HRRs.

(c) A dekade is defined as roughly one third of a month. These are:

Dekad-1: The first 1-10 days in the month.

Dekad-2: 11-20 days of a month

Dekad-3: 21-days to end of the Months.

For this study, the dekadal rainfall data obtained from both gauge and satellite were combined into monthly, seasonal and yearly totals.

c) Geographic Dataset - were collected and stored in the digital database of GIS environment, in which used to prepare the description of the study area and relevant geo-processing works. In this study, raster and vector datasets are used for the preparation of study area features like boundary, physiography, soil map and Land-use land-cover status of study area.

d) Field Observations - Field trip were arranged and carried out to different parts of the basin.

The data collected from the field includes:-

Observation and identification of meteorological stations with associated basin characteristics. Reference points are also taken for some meteorological stations in the basin during field visits.

Observation and description of the basin that have demarcated with good and poor rainfall distributions, including the identification of the watershed system and its association with topographical and rainfall (distribution and amount)

The field investigation tasks were constituted an important understanding to the researcher in the way how rainfall is associated with the nature of basin characteristics (over all basin physical characteristics, social and economic practices)

3.1.2 Data Sources

Dekadal rainfall of gauge stations were obtained from National Meteorological Agency (NMA) and satellite estimated rainfall data were downloaded from website of TAMSAT Research Group, Department of Meteorology, university of Reading, UK.

Vector and raster datasets including official documents and reports, and relevant information that are used for the preparation of study area like: study area boundary, climate of study area, physiography, soil map and Land-use land-cover status of study area are obtained from different sources like: National meteorological Agency, Ministry of Water, Energy and Irrigation, Ethiopian Mapping Agency, Ministry of Agriculture, Addis ababa university GIS and remote sensing laboratory.

3.2 Methodology

For the purpose of discussing the rainfall estimation processes, verification and analysis, appropriate software and large database was assigned to accommodate the serious of RFE images and gauge data at EXCEL format. The methods considered in interpolating and extraction of rainfall values from the satellite images, and comparing with the gauge observation includes the following:

I. Delineation of similar rainfall characteristics (HRRs) zones in the basins. Thus, dividing the Awash River basin into zones of homogeneous rainfall characteristics is the first step activities. Rainfall distribution is characterized by great spatial variations. There are different climatologically regions having different characteristics within the basin. Thus, for the construction of HRRs, different independent techniques were used to divide the rainfall stations into zones. Some of the techniques were presented below:

(a) Principal Component Analysis (PCA)

To identify appropriate HRRs, Principal Component Analysis (PCA) was carried out using Systat 2013 and ArcGIS 10.1 software. PCA is a multivariate data reduction technique used to analyze multiple observed variables that yields a relatively small number of components, which account for most of the variance in a set of observed variables (Stevens, 1992) PCA determines and assigns weights mathematically to capture relative importance of multiple indicators and maximize the variance of the linear composites. A principal component is rated meaningful if it yields an Eigenvalue ≥ 1, whereby the variables retained in the analysis should have a component loading ≥ 0.4, hence accounting for at least 16% of the variance within the component (kaiser, 1959). Conducting the PCA involved a trial and error process to determine, from a set of 10 variables, a combination which yielded the best accuracy performance. From initial PCA results the component matrix was checked and variables with component loadings lower than 0.4 were removed, in accordance with Field (2009). Positive loadings indicate a positive correlation of the variable with relative drought resilience and vice versa.

In the first stage, the applied method (PCA) estimates the relation between variables, the relation between stations and the relation between variables and stations (Maheras, 1985) aiming at the PC's extraction that produced the most and more significant information

II. TAMSAT methodology of rainfall estimation technique is selected and used to explain the process of rainfall estimation and further for comparing and characterization with the rain gauge data of the same period and regions. TAMSAT is developed by the Reading university in UK, for tropical Africa (Grimes, 1999) is employed based upon the basic assumptions that in tropics most of the rains comes of the convective clouds and also assumes simple linear relationship between the "CCD" and "Rainfall(RF)" which is given as:

$$RR = a*CCD + b, \quad \text{if } CCD > 0,$$

$$RR = 0, \quad \text{if } CCD = 0$$

Where 'a' and 'b' are constants determined by regression comparison of CCD values in hour with top temperature below defined threshold temperature (THT) to that of the rainfall from rain gauge data. Since the data format of TAMSAT data is in NetCDF file format it can be converted to human readable data format by using ArcGIS NetCDF file converting tool and the value were extracted for the study area boundary and the value is exported to excel format for further processing to achieve the objectives of this study.

III. Rainfall Verification Methodology

Many methods of spatial verification are available for comparing rain gauge measurements with remotely-sensed rainfall measurements. In this study, the statistical measures used to compare the satellite estimations with the ground truth data (rain gauge) were taken from the results of the 3rd Algorithm Inter comparison Project of the Global Precipitation Climatology Project (Ebert, 1996: Ebert et al., 2007). The spatial verification methods described here include visual verification and continuous statistics. The verification methodology selected in this study was based on dekadal, monthly, seasonal, and annual accumulation rain gauge data and satellite-estimated data.

(a) Continuous/Descriptive Verification Statistics: - Continuous verification statistics measure the accuracy of a continuous variable such as rain amount or intensity. These are the most commonly used statistics in validating satellite-based estimates; many people are familiar with them and find them easy to estimate. The mean error (ME) measures the average difference between the estimated and observed values averaged

over the data set (ICIMOD, 2013). The correlation coefficient(r) measures the degree of closeness of the RFE and Gauge values (Vila et al. 2003; Vila and Lima 2006).

Some of statistical formulas used were presented below:

$$AM = \frac{\sum Xi}{N}$$ Where,Xi =RFE and Gauge Value
N = Number of sample ……..equation 1

With the respective estimated and actual gauge data of rainfall mean values of dekadal, monthly and seasonal were characterized and compared in the selected years for HRR within the basin. The results from the above operation is illustrated by graphs, table and mapping.

$$Sd = \sqrt{\frac{\sum (Xi-\bar{X})^2}{N}}$$ Where, Xi = RFE & Guage Value
$\bar{X}$ = RFE & Guage Value Mean
N = Number of Sample ……..equation 2

The standard deviation is used for measuring the dispersion of the existing rainfall values around the mean (Dereje, 2012).

$$Cv = \frac{Sd}{\bar{X}}$$ Where, Sd = standard devation
$\bar{X}$ = RFE or guage value mean .....equation 3

Is computed as a percentage of the mean to indicate the variability between RFE and gauge measurements

Correlation Coefficient

$$\text{Correlation coefficient (r)} = \frac{\sum_{i=1}^{N}(Si-\overline{S})(Gi-\overline{G})}{\sqrt{\sum_{i=1}^{N}(Si-\overline{S})^2}\sqrt{\sum_{i=1}^{N}(Gi-\overline{G})^2}}$$ .....equation 4

where, Si is the satellite-estimated value at grid cell or point i, Gi is the observed ground rain gauge value at grid cell or point i, N is the number of observed samples, and $\overline{G}$ and $\overline{S}$ are the average values.

The correlation evaluation were used to measure the degree of closeness of the relationship between for RFE and Gauge values for the respective HRR

- Mean Error

$$\text{Mean error} = \frac{1}{N}\sum_{i=1}^{N}(Gi - Si) \quad \text{.....equation 5}$$

where, Si is the satellite-estimated value at grid cell or point i, Gi is the observed ground rain gauge value at grid cell or point i, N is the number of observed samples

The positive bias indicated that the RFE value exceeds the observed value on the average, while the negative bias corresponds to under estimating the observed value on the average

The bias indicates the average direction of the deviation from the observed rainfall dataset. But it cannot reflect the magnitude of the error.

c) Geostatistical Kriging methods and mapping were applied and characterized how Satellite based rainfall measurements are related with ground gauging depending on their relative locations.

"Geostatistical Analyst builds a bridge between statistics and GIS" (Grimes, 1999). One of the essential features of Geostatistics considered in this study is a Kriging methods used to generate a continuous surface map for gauge data from a point station, and to predict the exact value of their distribution to (unknown) unmeasured location in the study area. Later, the map would be evaluated and compared with The RFE image obtained for the same period.

Ordinary Kriging is one of the simplest interpolation techniques, is built on the assumption things that are close to one another are more alike than those farther away, and this is quantified as spatial autocorrelation. The method have the empirical semiviaograms model which can explore the relationships across the data set, and the Cross Validation dialog box function gives an idea of view how the predicted value at unknown location is distributed very well. The relation with farther locations can be also determined by search neighborhoods method (i.e. searching for the value of the closest cell and to assign a value to output cell). The searching will be performed using the variable search radius used for calculating the value of interpolated cell which is specified based on the number of measured points within the maximum radius. These help to relate farther measured location to be used in each prediction and computational speed.

Kriging can accommodate estimation for both point and aerial targets. In Geostatistical parlance estimation areas are known as "blocks", hence you will see Kriging estimation of areal average amounts described as block (ordinary) Kriging (Basistha et al. 2007). The reason is that the satellite provides information on a pixel basis, so by using block Kriging we provide estimates of rainfall on the same geographical support.

The general mathematical formula of interpolation using Kriging method formed as a weighted sum of the data:

$$P_i = \sum_{i=1}^{N} W_u R_i \quad \text{.....equation 6}$$

Where, **Pi =** is the prediction location

Ri = is the mean annual Rainfall in millimeter at the location (Station)

Wu = is weights to be assigned for the measured value at the location (Station)

In this study, Arc map is enabled to display the image format and used to delineate active rainfall areas by reclassification using spatial analyst function, in such case, the values of the rainfall is assigned based on the color table and legend defined on the map during RFE image processing system. Each color defined on the legend map is represented the extracted rainfall value at an average over HRRs.

All selected average value of dekadal, monthly, seasonal and annual RFE value were exported to GIS environment for mapping to compare with the map showing the gauge value interpolated using GIS, geostatistical ordinary kriging method.

d) Visual Analysis

Visual verification method compares maps of satellite estimates and observations. Rain gauge data) and estimated satellite data were remapped to the same projection with the same color scale to show the spatial distribution and amount of rainfall. This method is not quantitative but subjective (ICIMOD, 2013).

3.3 Software

There are various data processing software developed, which assist for rainfall extraction from remotely sensed imageries and station rainfall. Among such software, ArcGIS10.1 and its Geostatistical tools were widely used for data storing, processing, analyzing and interpretation purpose. As a general, a software like: Systat 2013, Surfer 8 and ILWIS 3.3 are used in this study

3.4. Data Processing Method

3.4.1. Input Dataset Format

In order to identify the basic objectives of the analysis and to create a database that helps to solve the problem of the study, the data processing activities is drawn in two type of procedure. These are:

I. Identifying and arranging the layers and the attributes required for each feature dataset. Processing of the data on each of the dataset has done based on that the layers are required further during the rainfall analysis. This involved in digitizing of study area boundary, delineation of HRR, and associated physiographic features

I. And conversion of the METEOSAT TIR – CCD images into RFE value for each dekades of 2008, 2009 and 2010 by using ArcGIS environment with appropriate format and coordinate system for further processing.

Table 3.1 Data format Generated from Different Sources for the Analysis

No.	Type of Dataset	Format	Descriptions of feature
1	Point	Vector	Dekadal Rainfall Value of meteorological gauging stations
2	Line	Vector	Contour lines, Drainage system
3	Polygon	Vector	Study area boundary, HRR, Soil, land-use/Land-cover
4	Point	vector	Dekadal satellite estimated rainfall Value after extraction

3.4.2 Extent of Data Records

The total number of meteorological station data that were collected in the Awash River basin was 86 in numbers. However, over 36 gauge station, the records of the available data required in the analysis are not found adequate due to missing data in different dekade. Therefore, only 50 meteorological gauge stations are selected and used in the processing procedure. Those selected stations have almost sufficient rainfall records for

the year 2008, 2009 and 2010 and were very useful considerably for processing and interpretation purposes. The station distribution network in the western, northwestern and central highland catchment area of the basin is relatively densely situated than the eastern and northeastern catchment areas of the basin.

In the northeastern, eastern and southeastern parts of the basin, the gauge station distributions have not been found evenly distributed.

However, according to WMO (1994) conventional requirement of station distribution standards, the resolution requirements for point measurement (gauging station) based on elevation categories are given as follow:

I. In mountainous area above 2000 meters the maximum resolution required is less than 20 km^2.
II. In area 1500-2000 meter, is required a resolution of 20 - 40 km^2
III. In the area below 1500 meter, above 40 km^2 resolution is required according to expansions of the area.

It is also cited that the use of satellite- based techniques to measure areal rainfall in the tropical Africa recommended when the rain gauge spacing resolution is less than about 40km (WMO, 1988a). Therefore, the spacing or distribution of the selected gauging station in most highlands areas of Awash River basin is denser than the lowland areas of the basin and it is enough for the analysis to achieve the objective of the study.

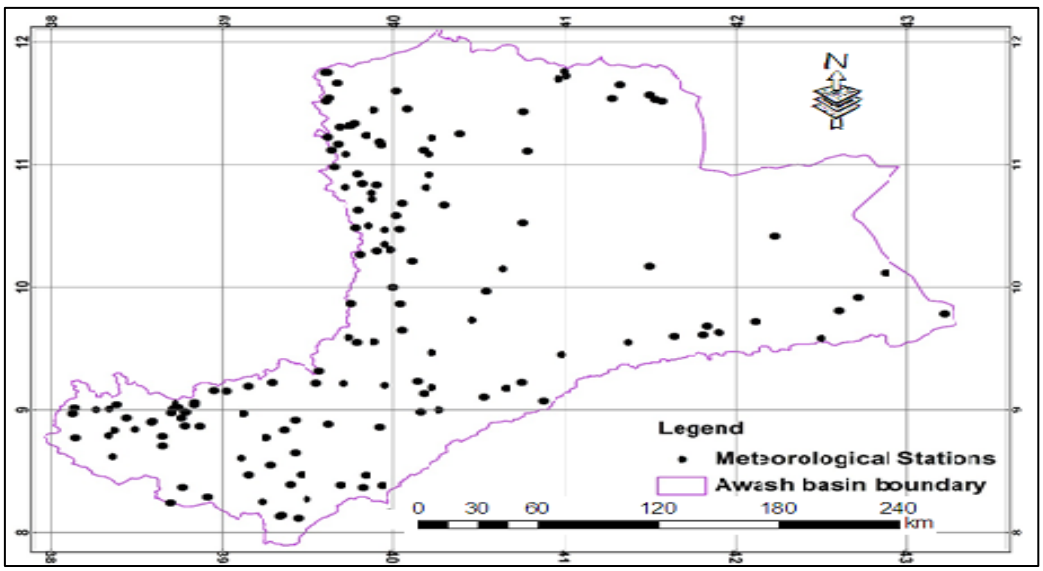

Figure 3.1: Rainfall stations distribution map

(Meteorological Station data source: NMA)

3.4.3. Processing of Gauge Rainfall Data

Since the gauge observation and satellite data are not at the same location, it is often necessary to adjust their representation in the same period and spatial extent for interpretations and comparison.

Evaluating the geographic distribution of stations and the statistical quantities were significant during the gauge data processing task. These patterns are also used as the basis of analysis in the comparison of RFE and gauge records. The gauge dataset consists of dekadal total rainfall from 50 stations over the study area. Before proceeding for analysis, the collected data were cheeked in two ways: qualitatively and by performing diagnostic statistics and graphical computations on the measured gauge records. These are:

I. Visual analysis of tabular data and Graphs
II. Inspection of gauged data value with the classification of rainfall regime in Ethiopia, and with the study area as well.
III. Inter -station correlation analysis.
IV. Determination of rainfall with Altitude
V. Mapping station locations

The rainfall measurements taken at the station are processed at Dekadal, monthly, seasonal and annual base are used to interpolate in Kriging over the HRRs within the basin.

Twenty years data from 1990 to 2010 is also computed to show the mean monthly, seasonal and annual rainfall over the target of HRRs.

3.4.4. Building RFE image from METEOSAT -TIR raw data

RFE image is derived using the methodology by detecting cold cloud in each thermal infrared image and then converting these detections into rainfall estimate. The methods, by default, create CCD based rainfall estimates for ten-daily periods for each pixel. The CCD images further can be used to produce RFE value which are taken typically for a given dekade and pixel.

It is explained that the TMSAT rainfall estimates method is pre-calibrated for tropical Africa, it is therefore, all the criteria and parameters assigned were also used in the Awash River basin for which this study is carried out and it cannot require calibrating again. Therefore, the METEOSAT-TIR raw data in NetCDF file format is exported to

ArcGIS to produce RFE image. The RFE image is converted to raster for further extraction of RFE value

3.4.5. Value Extraction Process RFE image

(a) RFE image

The steps of producing estimates of RFE image is basically started from the process of determination of rain from the CCD data which is already discussed earlier in the literature and its approach in TAMSAT methodology. In the process of producing the RFE image, there are various methods of versioned algorisms depending on the data format used.

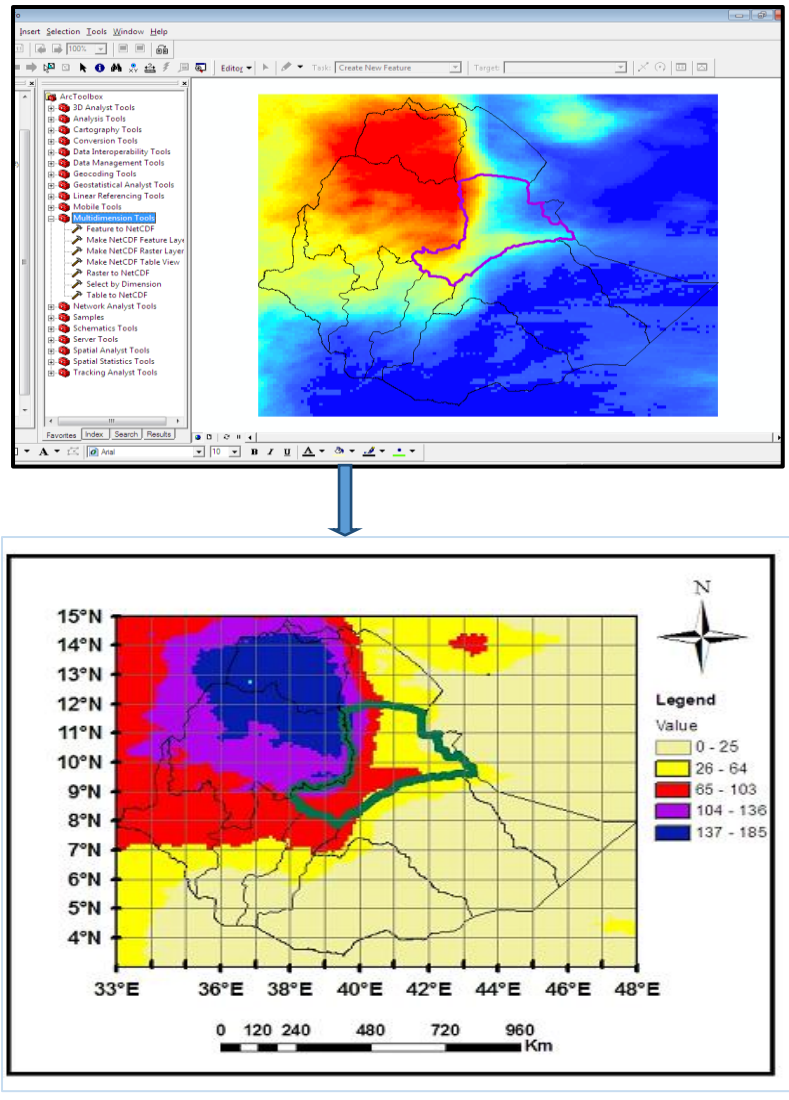

METEOSAT-TIR CCD image at for August 2nd dekade of 2010

Adjusted RFE image for the METEOSAT-TIR CCD image for 2nd dekad of August 2010 by converting NetCDF file format to raster layer and further processing using Arc GIS software.

Figure 3.2: The Raw METEOSAT-TIR CCD image and Processed RFE Value

(b) RFE Value

The RFE images used for the purpose of this study are the output of the process that prepared earlier from CCD image in TAMSAT approach and it is presented on the website in NetCDF file format. For further processing of the RFE value it is required to change this file format to the readable file format by human eye. This is done by using ArcGIS as it is presented in Figure 4.2. In this process, the estimated rainfall values were extracted based on averaged pixel value for each HRR within the basin and this value is extracted for each dekade of the three selected years. However, the quantitative value of rainfall at required geographic unit of HRR within Awash basin was the next process determined by creating it in automated statistical extraction process.

The extracted dekadal RFE values are calculated at each pixel value of HRRs within the basin and these data are exported to EXCEL format and further processed at monthly, seasonal and annual basis.

3.5. Schematic Flow Chart

According to the steps put on the flow chart below, the first step is to decide and display the type of data that need to use in the analysis. Therefore, the input data in this study is gauge rainfall from existing meteorological stations and satellite TIR image which put on view with a raster dataset. The second step is delineation of homogeneous rainfall from long year data. In the third step, the new information RFE and GIS data are derived from the input datasets. Based on the analytical and automated software processing system, the values of rainfall at HRR region for the periods have been calculated and presented as layers.

Fourthly, the input datasets are further analyzed using statistical and spatial interpretation methods according to the values of attributes within each dataset that have describe the accuracy and difference of estimation. The final results have been presented specifying the scientifically examined application of the satellite-based rainfall estimation technique and the observed characteristics of the value of datasets. This is found to be a very good supplement for the need of rainfall information with the required spatial extent within the basin.

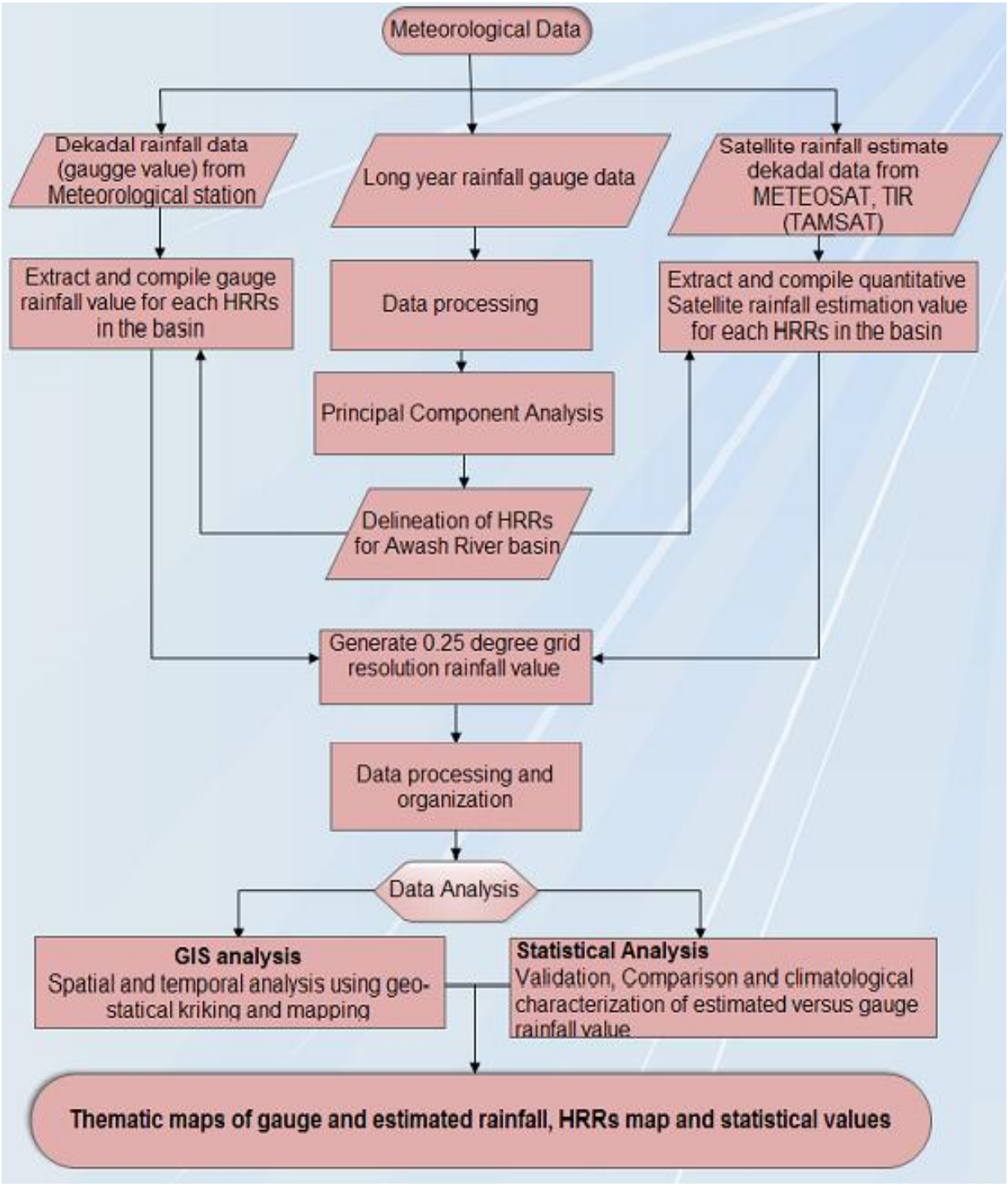

Figure 3.3: Schematic Flow Chart

4. RESULTS AND DISCUSSION

4.1 Delineation of Homogeneous rainfall Regions for Awash River Basin

In this topic, an attempt is made to analyze the spatial structure of the rainfall climate of the basin, which was represented by few stations in previous studies for delineation of rainfall regions.

The aim of this topic is firstly, to describe characteristics of rainfall mean in the basin by using the method of Principal Component Analysis (PCA) and secondly, mapping and interpolation method were applied in order to determine and delineate the homogeneous rainfall regions of the stations in Awash River basin by using Geographical Information System (GIS) techniques together with the first four Principal component loadings.

In the first stage, the applied method (PCA) estimates the relation between variables, the relation between stations and the relation between variables and stations (Maheras, 1985) aiming at the PC's extraction that produced the most and more significant information. The results of the analysis (eigenvalues, variances and PC loadings) are presented in (Figure 4.1 and Table 4.1).

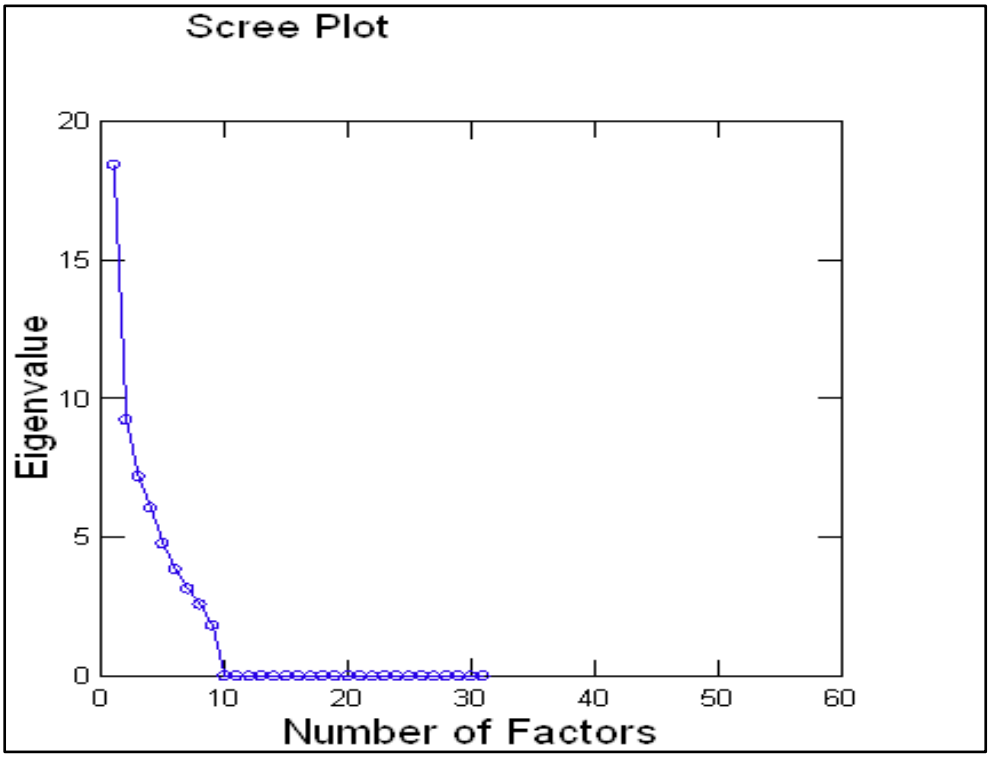

Figure 4.1: Scree Plot Results of Principal component Analysis

Table 4.1: Results of Principal Component Analysis

Loading	PC1	PC2	PC3	PC4	PC5	PC6	PC7	PC8	PC9	PC10
Percent of variance	25.1	21.0	18.9	17.3	4.7	4.4	3.6	1.8	1.2	1.0
Cumulative (%)	25.1	46.1	65.0	82.3	88.0	92.4	96.0	97.8	99.0	100.0

According to Kaiser's criterion (Kaiser, 1959) the cut-off value (elbow) for the eigenvalues of scree plot in (Figure 4.1) was at the eigenvalue number 0. All eigenvalue above the value 1(one) in (Figure 4.1) is important but the first four PC are selected for further analysis in this study because the PC are sorted in decreasing order of variance, so the most important PC is always listed first. These first four components accounted for 82.3% of the total variance of the rainfall whose 25.1%, 21.0%, 18.9% and 17.3% was extracted for the first, second, third and for the fourth principal component respectively. The first four principal component analyses is selected depending on the statistical results presented in (Figure 4.1 and Table 4.1) where Awash River basin is divided into four sectors that constitute four homogeneous groups. This will contribute to a better understanding of the spatial and seasonal variability of the rainfall climate in Awash River basin and it is also important for the understanding of validation of RFE value on spatial and temporal basis that can be discussed in the next sections.

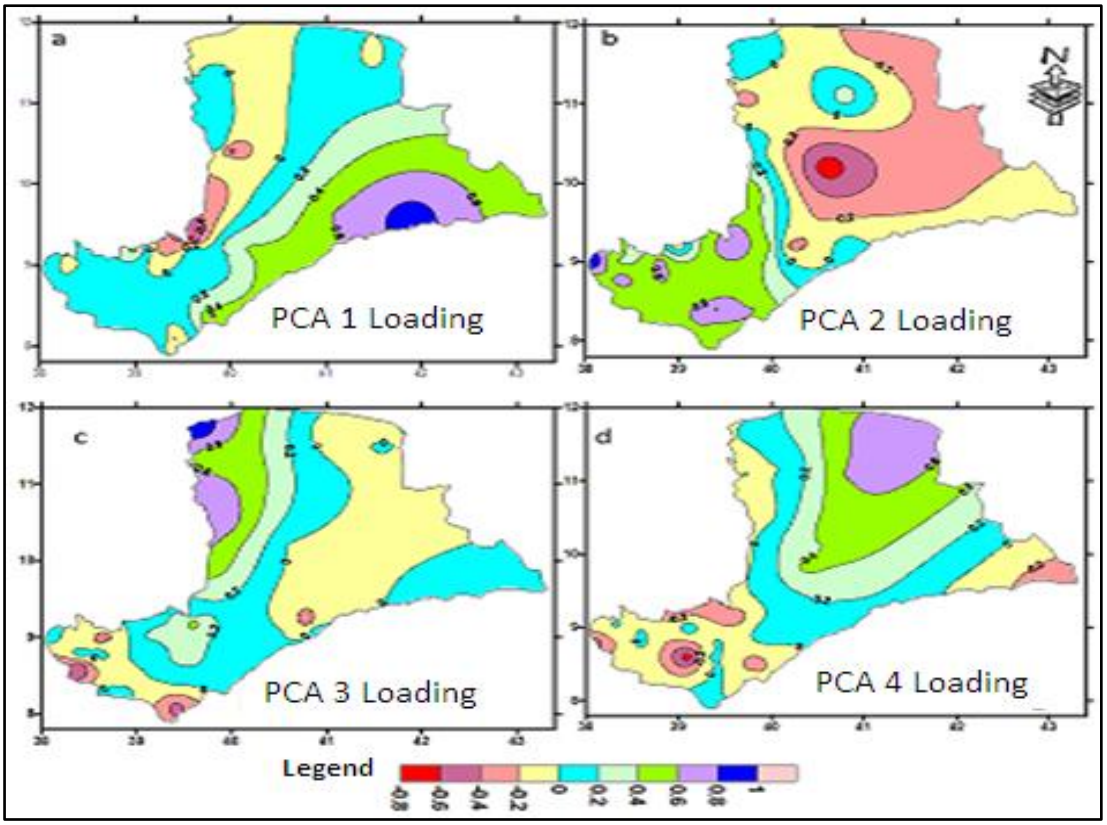

Figure 4.2: Principal Component Analysis Loadings

The map that is shown in (Figure 4.2,a) comprise the station with positive value scores under PCA 1 and this include some areas of central Rift Valley and eastern highland escarpment of the basin. This region show positive scores under PCA 1 because of its slight different character of receiving rainfall from the rest of PCA scores (PCA 2, PCA 3 and PCA 4). The areas that show a positive scores in PCA 1 receives a bimodal type of rainfall with one peak is during kiremt season of August with rainfall amount of 125 mm and the other is during the April month of Belg season with a rainfall amount of 84.4mm as it is shown in (Figure 4.7). This area is delineated as HRR4 as it is shown in (Figure 4.3) for further discussions of this study. The map that is shown in (Figure 4.2,b)is also include the station with positive value scores under PCA 2 and this area represents the central highland areas of the basin and it is also extends to some areas of central Rift Valley. This area receives a maximum mean rainfall during the August month of kiremt season with amount of 227.2mm of rainfall. For the areas delineated under PCA 2 the bi-modality is not shown clearly as the rest of the PCA`s but the area receives rainfall during Belg season with the monthly mean rainfall amount of 66.2mm during April and 66.3mm

during May as it is shown in (Figure 4.6). PCA 2 is delineated as HHR 1 as it is shown in (Figure 4.3).

The PCA loading that is shown in figure 4.2, c separates the monthly mean rainfall distribution of the basin from the rest of the regions as they are indicated by their PCA scores. The positive scores characterized under PCA 3 separates the rainfall distribution situations of north western escarpments of the basin. This region receives a better rainfall during Kiremt and belg season when compared with the rest of PCA scores. The mean monthly rainfall amount of kiremt season of August in the areas that is separated as PCA 3 reaches 261.3 mm and the mean monthly rainfall amount of Belg season during April reaches 93.6mm as it is shown in (Figure 4.4). The PCA 3 score that is shown in (Figure 4.2, c) is delineated as HRR2 as it is indicated in (Figure 4.3). The positive PCA scores that are indicated on (Figure 4.2, d) separates the rainfall situations of Rift Valley areas of the basin. The areas separated under PCA 4 receives low amount of rainfall when it compared with the rest of the areas separated by the rest of PCAs. The mean maximum rainfall amount of the basin separated as PCA 4 is only about 99.0 mm during kiremt season of August. This region is also receives small amount of rainfall during Belg season of March and the maximum mean monthly rainfall amount during this month is about 52.3mm as it is indicated in (Figure 4.5). The PCA score that is shown in (Figure 4.2, d) is delineated as HRR3as it is indicated in (Figure 4.3).

As it is shown in principal component analysis loading (Figures 4.3) mapping and interpolation method were applied in order to determine the homogeneous Rainfall groups of the stations in Awash River basin by using Geographical Information System (GIS) techniques together with the first four PCAs scores. The result is illustrated in (Figure 4.3), where Awash River basin is divided into four sectors that constitute four homogeneous rainfall regions:

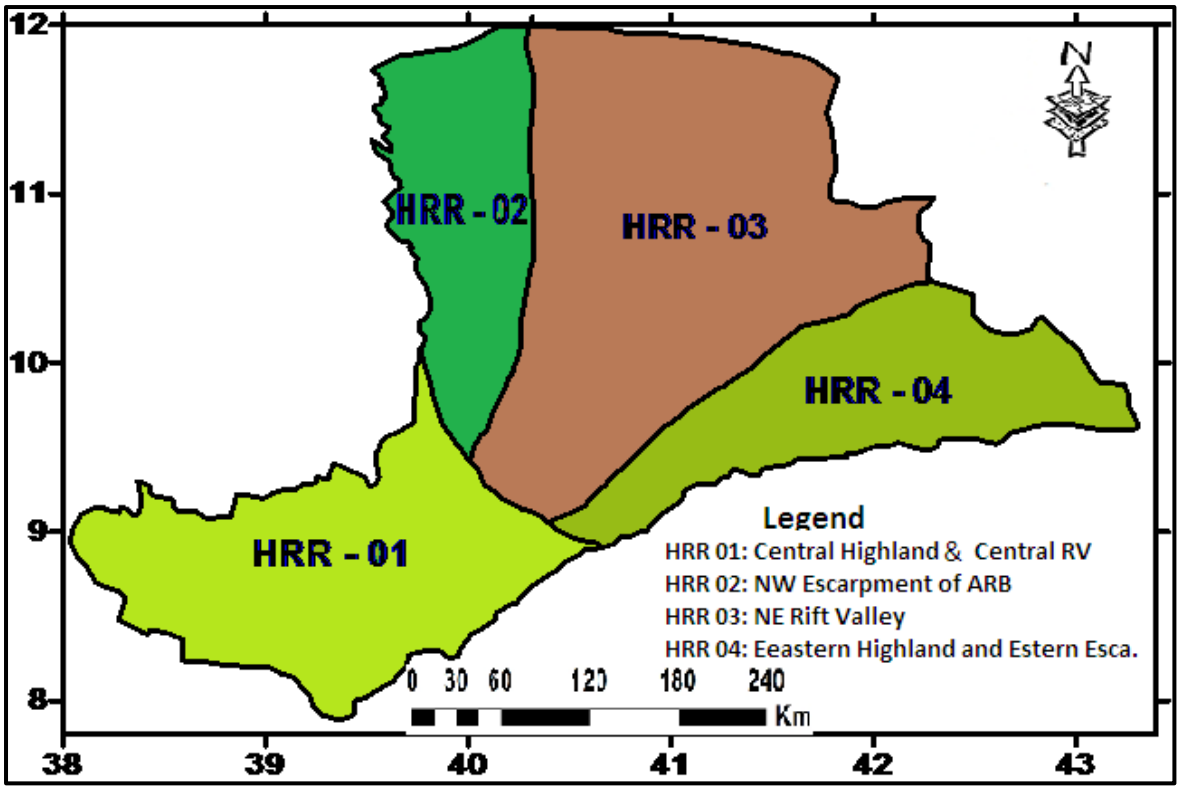

Figure 4.3: Homogeneous Rainfall Classified Regions of Awash River Basin

The map shown in (Figure 4.3) indicates that homogeneous rainfall regions in Awash River basin and it is obtained by standardizing station data, evaluating PCA approach and knowledge of local climate and topography of the area. More emphasis was given to PCA data analysis. Each number represents homogeneous rainfall region of the basin and they are described in detail in the next section.

4.1.1. Homogeneous Rainfall Regions 02 and 03

Northwestern escarpments and the adjoining lowlands of northeastern Rift Valley of Awash River basin are categorized into HRR2 and 03 respectively(Figure 4.3). Most of the kiremt (Jun-Sep) and belg (February-May) rainfall amounts and distributions over these regions are produced under the influence of tropical or mid latitude frontal systems. The Red Sea Convergence Zone (RSCZ), which develops over the Red Sea region, is often associated to the formation of spring and autumn rains over these parts of Ethiopia (Tucker and Pedgley, 1977). Moreover, Tucker and Pedgley (1977) suggested the presence of the Afar Convergence Zone (ACZ) between northwesterly over the southern Red Sea and south-westerlies over the Gulf of Aden that eventually produces convection rain over both sides of ACZ.

The northeastern Rift Valley areas of the basin (HRR3) is generally categorized as semi-arid, which is dominated by hot weather and severe heat waves in kiremt (Figure 1.7). It receives the major and small rains during the Kiremt (Jun – Sep) and belg (Feb – May). Seasons with rainfall maxima occurring in kiremt season of August month for both HRR2 and 03 and belg season of March for HRR3 and April for HRR2 (Figure 4.4 and 4.6). The monthly mean rainfall of HRR2 during August and April is 261.3mm and 93.6 mm respectively (Figure 4.4). HRR2 receives a better bimodal type rainfall when it compared with the rest of regions in the basin. In HRR3 the monthly rainfall mean reaches 99.0mm during August and 52.3mm during March (Figure 4.5). HRR3 is one of the driest regions in Awash River basin (less than 413.1mm/year of rainfall as shown in (Table 4.2). Region 02, the northwestern escarpments of the basin, also has the major and small rainy seasons during kiremt and belg season, respectively, but it is different from region 03 both in amount and length of rainy seasons (Table 4.2 and Figure 4.5). In Gissila et al. (2004) and Diro et al. (2011) regionalization, the two regions were represented as one rainfall region. However, previous studies made by Kassahun (1986), Camberlin and Philippon (2002) and Segele et al. (2009) documented that there is a substantial difference in rainfall amounts and rainy season over these parts of the basin.

According to this study, HRR2 receives over two fold of monthly rainfall totals with a value of 261.3 mm in August (Figure 4.4) compared to HRR3 with monthly rainfall totals of 99mm in August (Figure 4.5). Annual rainfall amounts and seasonal rainfall patterns for HRR2 are far more stable and higher as compared to HRR3 (Table 4.2). During kiremt season when the rain-producing systems approach the regions from western direction, the systems are forced to precipitate along the windward side of northwestern mountain chains and the passages of moist air toward the northeastern Ethiopia becomes very low.

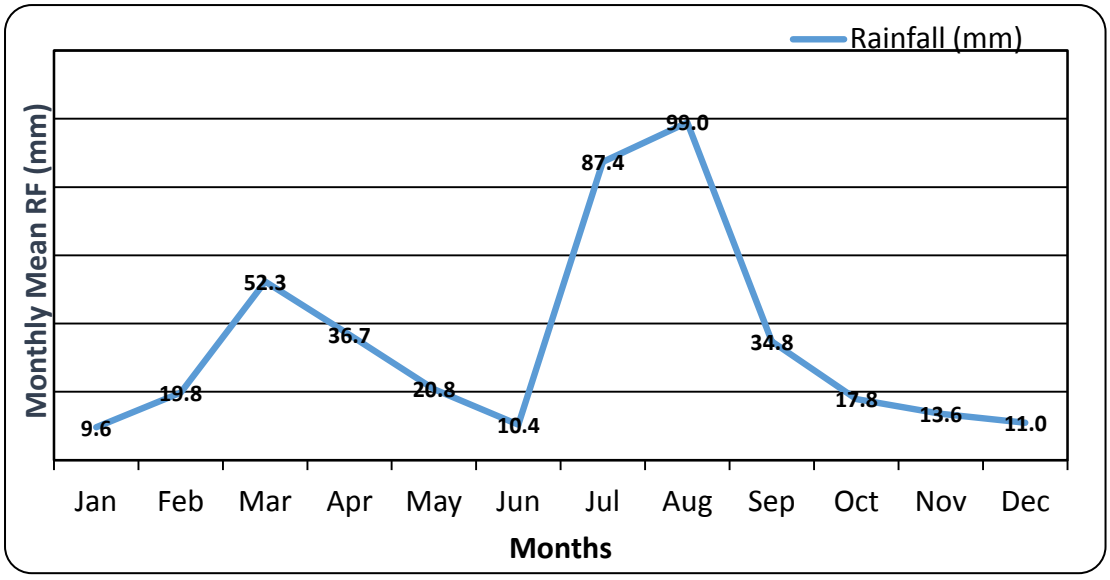

Figure 4.4: Monthly Mean Rainfall for Homogeneous Rainfall Region 02

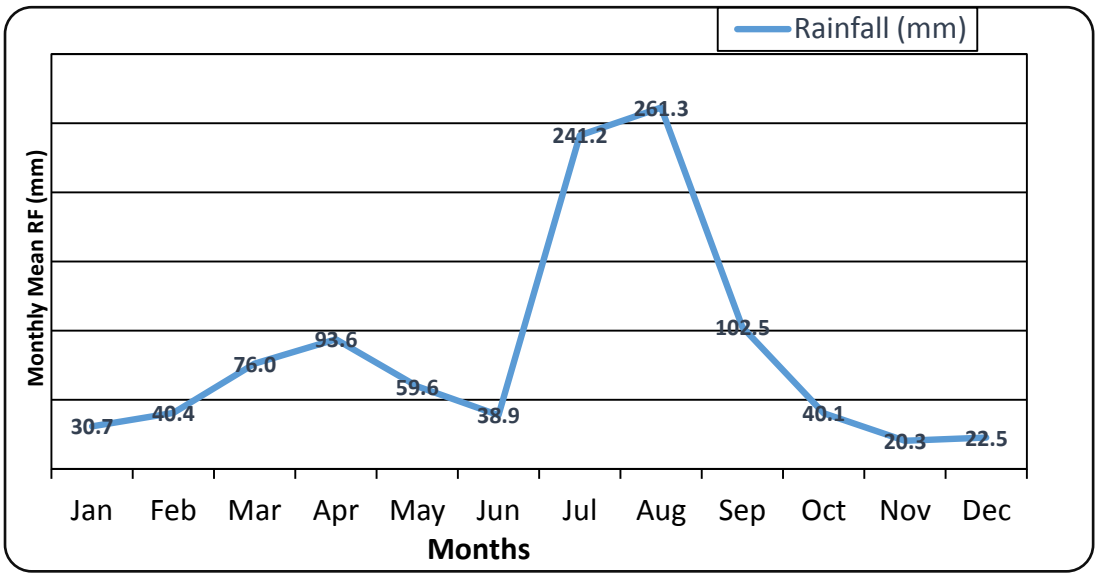

Figure 4.5: Monthly Mean Rainfalls for Homogeneous Rainfall Region 03

4.1.2 Homogeneous Rainfall Region 01

HRR1 covers all areas of central highlands located in western parts of the Awash basin catchment to main Ethiopian rift valley areas of the basin (Figure 4.3). Rainfall amounts are usually high during the rainy season from June to July and also this region receives rainfall during February to May (Figure 4.6). Kiremt is the major rainy season in this region with a maximum rainfall during July. The average rainfall amount during the month of July is 229.8mm (Figure 4.6). Belg is also the other rainy season

in HRR1 with a maximum mean rainfall during May. The mean monthly rainfall amount during belg season of May is 66.3mm (Figure 4.6). When this region is compared with HRR2 it receives nearly similar rainfall amount in kiremt season. But the rainfall amount is slightly lower than HRR2 during both seasons (kiremt and belg). The region experiences dry climate between November and February. The northward progressions of the southwest monsoon systems create favorable conditions for stable rainy season over this region. Unlike the adjoining Rift Valley and its northern regions, where the rain is scanty, this always benefits from the northward advancement and southward retreat of ITCZ (Segele and Lamb, 2005). Besides, the region varies from the nearby high grounds, the semi-arid central Rift Valley region because it receives rainfall mainly from westward and northward swinging of southwest monsoon storms. Conway (2000) argued that rainfall over the central Ethiopian Rift Valley shows little association with rainfall over the Central highlands. The dissimilarity between rainfalls patterns of Awash River basin are therefore agreed with this finding. Previous studies made by Gissila et al. (2004) also demarcated central Ethiopia as a separate homogeneous rainfall regime.

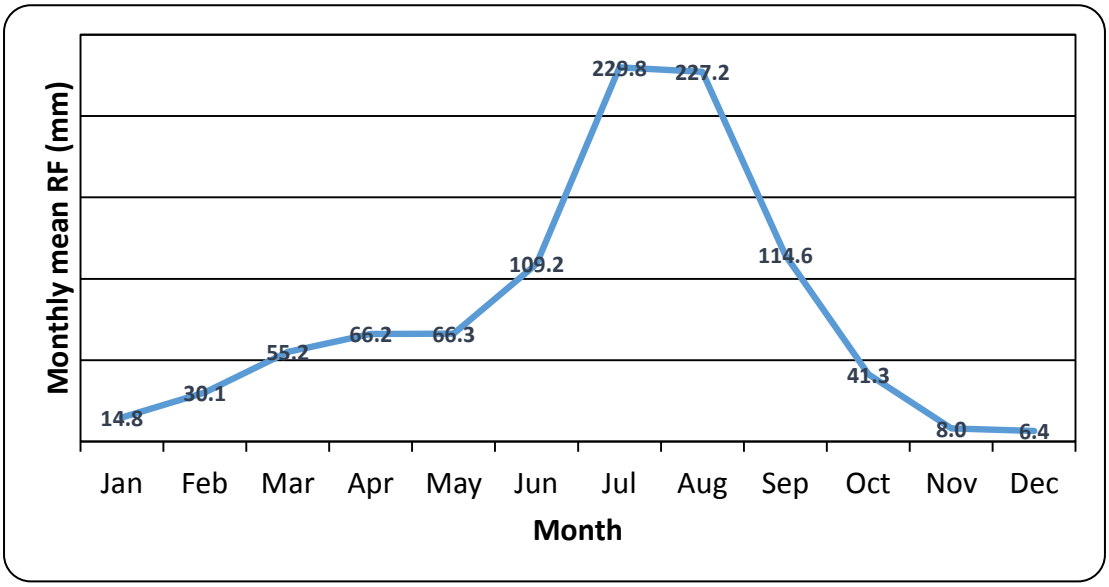

Figure 4.6: Monthly Mean Rainfall for Homogeneous Rainfall Region 01

4.1.3 Homogeneous Rainfall Region 04

The eastern Rift Valley escarpment and eastern highland areas in the basin experience a similar rainfall cycle and it is represented as HRR4 (Figure 4.3). This region represents some of central Rift Valley and the northern fringe of the eastern mountains as well as eastern highlands. The region experiences a bimodal rainfall cycle (Figure 4.7), with relatively shorter and weaker rainy seasons than the HRR1 and HRR2. Moreover, the mean monthly rainfall amount is lower in HRR4 than the central highlands (HRR1) and northwestern catchment of the basin (HHR 02) with rainfall maxima in April for belg season and August for kiremt season. The mean monthly rainfall amount of kiremt season in August is 125.0mm and the mean monthly rainfall amount of Belg season in April is 84.4mm (Figure 4.7). This region is known for its vulnerability to extreme rainfall conditions. For instance, the incidence of prolonged 2002 drought (Funk et al., 2005) explained as a regional phenomenon. In this region locally induced weather disturbances sometime produce intensive rains and dissipate quickly as a result of limited inflow of moisture due to its topographic suitability. Over this region, rain starts in March and gradually increases in April. There is a dry break in June before the major rainy season starts (Figure 4.7).

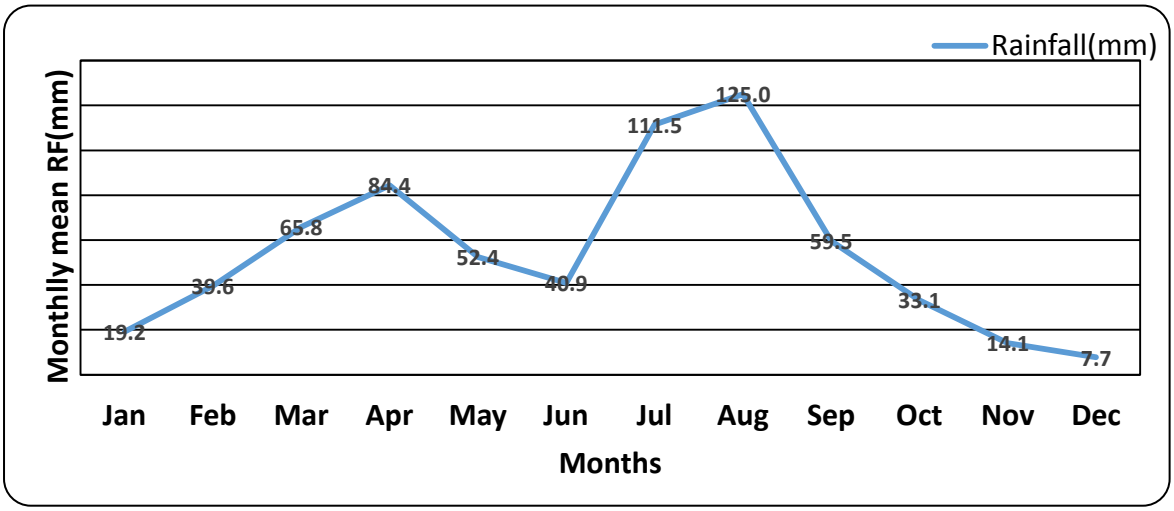

Figure 4.7: Monthly Mean Rainfall for Homogeneous Rainfall Region 04

This analysis was used to confirm the similarity of the rainfall over the delineated regions and further would help to assess the qualitative and quantitative RFE values derived from METEOSAT-TIR, CCD data. It is therefore, the rainfall values are extracted based on the spatial average of these regions containing the rain gauges observation for the same period.

4.2 Evaluation and interpretation of Estimated Rainfall

4.2.1 Performance of Value Extracted from RFE

The performance of extracted RFE Values for each region should be evaluated by using statistical and mapping technique with respect to gauge rainfall value. It is also important that some evaluation of the estimates be made and it is extremely desirable that this evaluation should be quantitative rather than just anecdotal. There are three reasons:

I. There is aneed to identify any area or time periods for which the estimation algorithm is inappropriate.
II. There is also a need to identify areas where the under and overestimated situations of rainfall should be modified.
III. There is a need to demonstrate the accuracy and reliability of the estimation process to interested end users of such information

The evaluation and comparison of the performance of satellite rainfall estimates with an independent set of data which can be regarded as ground truth is very important. In this part of discussion, the evaluation process is basically depending on comparison of the mean gauge value in HRRs with the mean satellite estimate for the same regions containing the gauges. It is possible to calculate the error associated with a gauge as an estimator of pixel rainfall by the mathematical technique of Kriging. However this is a somewhat complicated process and requires a reasonable density of rain gauges to give useful results, which means it may not always be feasible

Climatologically, statistics offer a convenient and practical approach to compare estimation for time series of rainfall fields. In order to assess the accuracy of the satellite estimates, it is necessary to compare them with rain gauge data. In this case, in fact, the satellite estimates represent the areal average while the gauge values the rainfall at point anywhere in the vicinity of the pixel. Of course, in any literature and research output these difficulties are often arises, but does not found the method

established the relationship between area and point rainfall. Instead, statistical parameters and Geostatistical kriging approaches are applied to quantify errors in order to determine the performance of the estimates (Dutarter *et al*, 1993).

4.2.2 Validation and Accuracy

4.2.2.1 Mean Error (ME)

(a) Dekadal Profile

Under this topic, the performance of overestimate and underestimate for RFE values were determined using quantitative evaluation of the mean error based on the equation (5). In computation of the mean error, all 50 rain gauge stations and RFE value are used. The derivation of mean error was made by calculating the difference of the values of RFE with the corresponding rainfall at an average rainfall value for all HRR and for all dekadal, monthly seasonal rainfall in the respective year of 2008, 2009 and 210. In determining the mean error indicator, graphical method was used discriminating just between over and under estimation conditions of the estimated rainfall values.

In the mean error analysis, the bias indicators explain only the performance of the satellite during the estimation process that is whether the value is overestimated or not. The bar graphs displayed in (Figure 4.8) were prepared to show the level of the bias for the estimated rainfall value. The positive mean error are indicators in which the estimated values are exceed the gauge value on the average and is said to be overestimated, with a negative mean error corresponds to under estimating the observed value on the average. When interpreting the result of such analysis, the smaller the value of the bias and closer to "0" is the better the performance of the estimation and closer to measured Gauge value. Several conclusions were drawn from the inspection of consecutive (Figure 4.8) for the validation of the selected periods.

Figure 4.8: Mean error indicators for 2nd dekade of August 2008, 2009 and 210

In Figure 4.8, second dekade of August which is the main rainy season over all HRRs of the basin is selected for validation of estimated rainfall in terms of its mean error. The figure emphasized that most of estimated rainfall from the satellite is under estimated over all areas of the region**.** In particular, the mean error over HRR1 and HRR2 is relatively high during the whole three years with a mean error value of about 23 mm dekad^{-1} over HRR1 during the year of 210 and 20 mm decade^{-1} over HHR2 during the year of 2009. However, estimated satellite rainfall values are relatively closer to the observed gauge value for whole the year of 2008 and 2009 over HRR3 and HRR4. In the other side, there is no estimated satellite values are observed overestimate for each region during the three selected years.

(b) Monthly Profile

The month considered for validating the estimated rainfall performance was April which is the second rainy season within the study area particularly northwestern parts of the basin in HRR2 receive better rainfall during this month. The rest of the regions in the basin also receive good amount of rainfall during Belg season of April. This month is also having better rainfall and experienced in the range of maximum records in all selected year during Belg season. This month is selected to show the evaluation of estimated rainfall value as the same method discussed earlier.

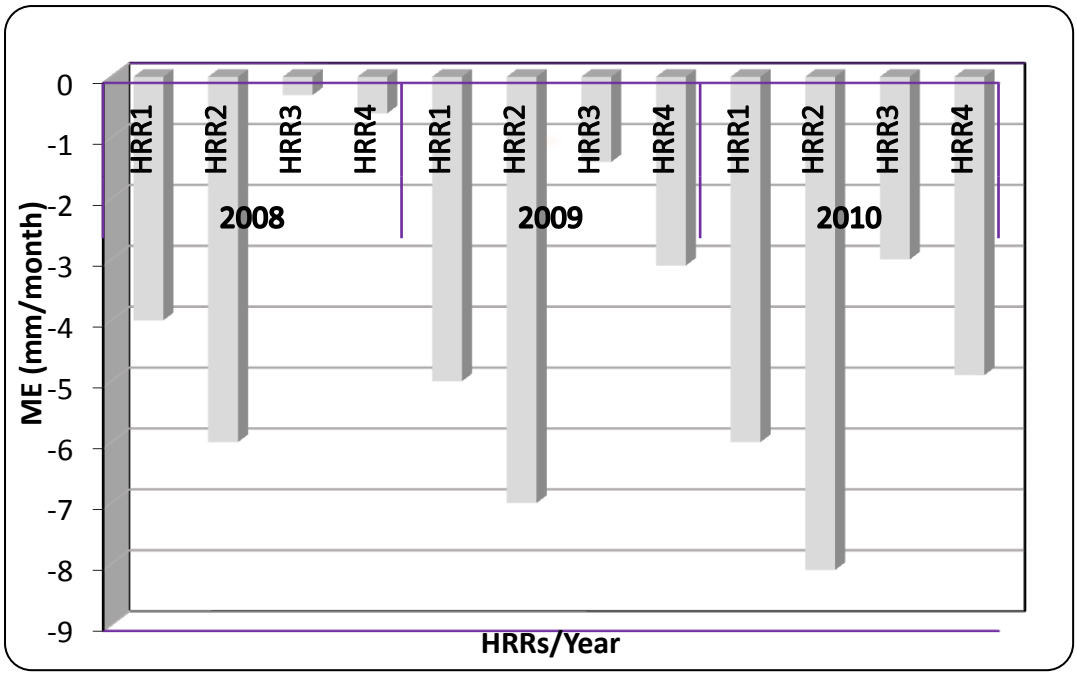

Figure 4.9: Mean error indicators for the Month of April 2008, 2009 and 210

The rainfall estimates in year of 2010 and 2009 of April at HRR2 were much underestimated but the rainfall estimates in 2008 at HHR3 and HRR4 are relatively good. The mean error indicated in (Figure 4.9) is variable from year to year and from HRR to HRR. This may be resulted from the rainfall amount and distribution condition, topography, formation of cloud type at each region in variable topography, calibration problem of CCD with historical data that is collected at a time of relatively low distribution of rain gauge over the region and the selection of threshold temperature for a complex topography of the area. The overall performance of the evaluation, whether it has positive and negative effect, most of the mean error indicator is in the range of 0 - 8mm month^{-1}. So that, it indicate that the rainfall estimated is nearly agreed with the observed gauge values during the selected month.

(C) Seasonal Profile

Among the three seasons over the area, Kiremet season is a selected for evaluation of the estimated rainfall over the assigned HRRs. As it has been displayed in (Figure 4.10), the rainfall estimated for HRR2 and HRR1 of 2010 were relatively much underestimated but the mean error situation for the year 2008, 2009 and 2010 over HRR1 and HRR2 is still relatively show in agreement with gauge data but still the mean is highly variable for each

HRR and the selected years with different rainfall conditions. This may be true for the reasons explained in the above monthly validation profile section. In such case the seasonal profile also observed that the rainfall value is underestimated a mean error value between 0 to 120 mm season^{-1} over different HRRs in the basin for the three selected years.

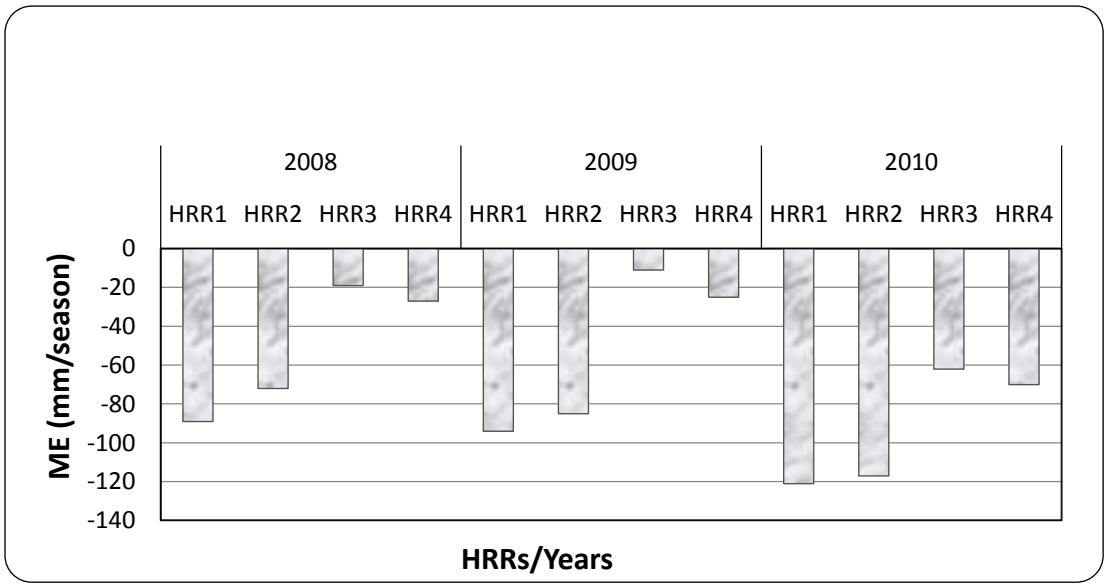

Figure 4.10: Mean error Indicator for Kiremet season 2008, 2009 and 2010

4.2.2.2 Validation using Correlation

The other method of validation of Satellite estimated rainfall data was done based on correlation analysis (Vila et al. 2003; Vila and Lima 2006). The result showed that such statistical method is useful tool for evaluation of the performance for estimated rainfall values. In this study, correlation analysis of estimated rainfall against gauge values have been made only for those purposely selected year of relatively normal rainfall (2008), dry (2009) and wet (2010) and this analysis result is shown in(Figure 4 .11- 13).

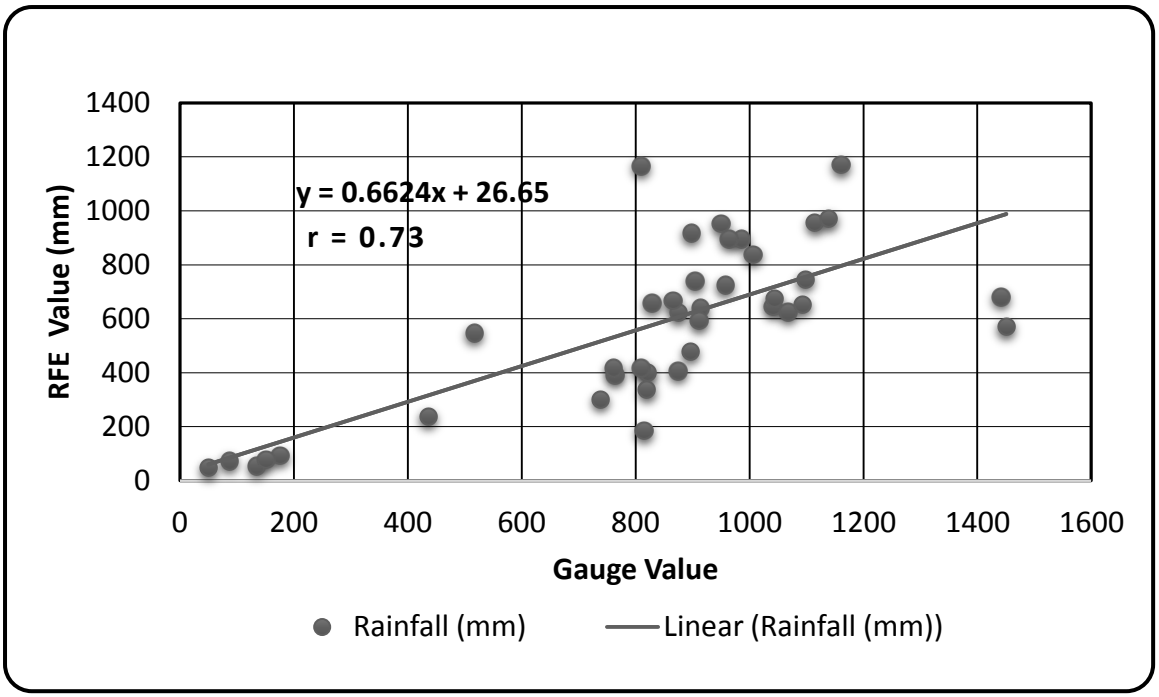

Figure 4.11: Correlation analysis of RFE Value against Gauge for the year of 2008

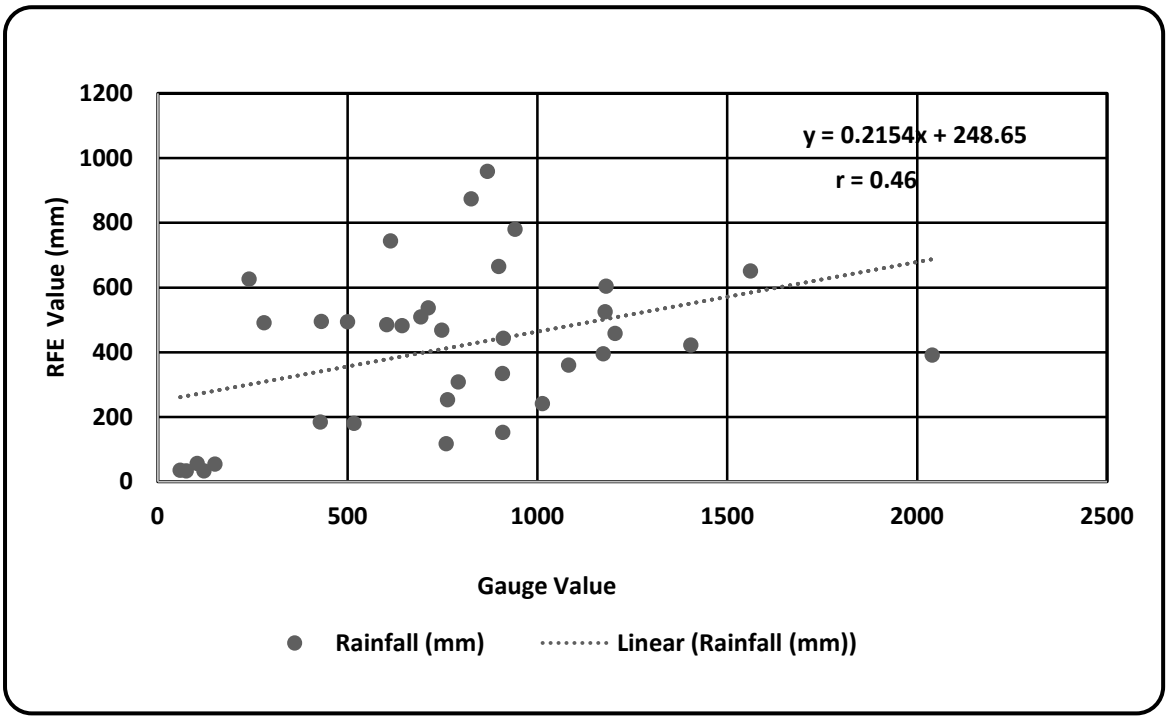

Figure 4.12: Correlation analysis of RFE Value against Gauge for the year of 2009

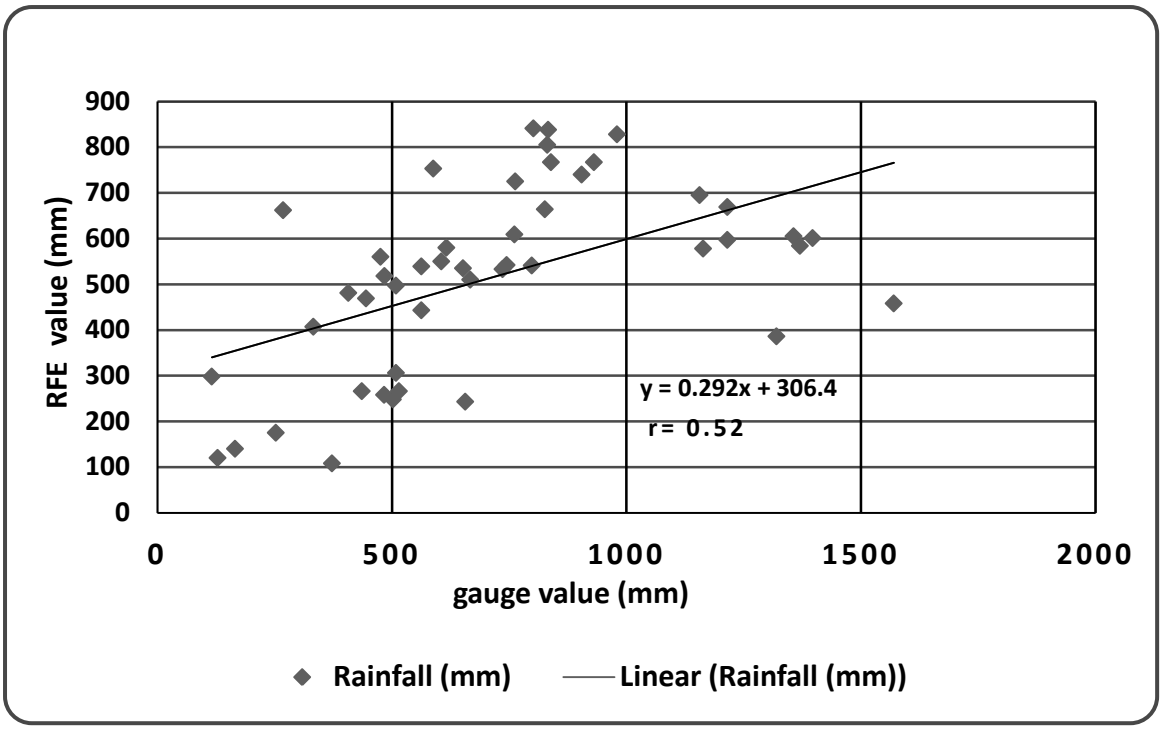

Figure 4.13: Correlation analysis of RFE Value against Gauge for the year of 2010

As it is shown in correlation analysis plots, if we look at the regression line and the associated data points, the data points which are confined closely to the regression line are the better relationship showing between the estimated and the gauge. The result of correlation indicate that for the normal rainfall year (2008) is the highest (r = 0.73) while it is r = 0.46 for the relatively dry year of 2009 and r = 0.52 for wet year (2010). In terms of their relation, all the three correlation plots show a good performance and representation. However, the correlation values are lower for the year of 2009 and 2010 and this situation is also observed in bias indictor section above.

4.3 Spatial Characterization of RFE and Gauge value

4.3.1 Rainfall Surface Map

4.3.1.1 Monthly total Rainfall Surface Map of RFE and Gauge Value

The other method applied for validating the estimated rainfall was based on the surface map showing the rainfall distribution and the value on the map for both RFE and Gauge recorded. In order to distinguish and evaluate the difference and similarity of estimated rainfall and gauge rainfall distribution on the surface map, the month of

April and August for the year of 2008, 2009 and 2010 were selected. As it is shown in (Figure 4.14), the spatial distribution of total monthly estimated rainfall value for April 2008 over all regions of the basin is less than 50mm while the total monthly rainfall value recorded by gauge measurement reached about 100mm over some HRR of the basins. Similarly, as it is indicated in (Figure 4. 15), during April 2009 and 2010 some areas of HRR1, HRR2 and HRR4 receives about 150mm monthly total rainfall amount as it is recorded by gauge in some rainfall stations but the satellite monthly total rainfall estimate is less than 100mm over all region of the basin. Generally, the satellite rainfall estimated value during April 2008, 2009 and 2010 is underestimate the rainfall value spatially and in total monthly rainfall amount but for the values less than 50mm it is almost in agreement over most areas of HRR3 and some places of HRR2 and HRR4.

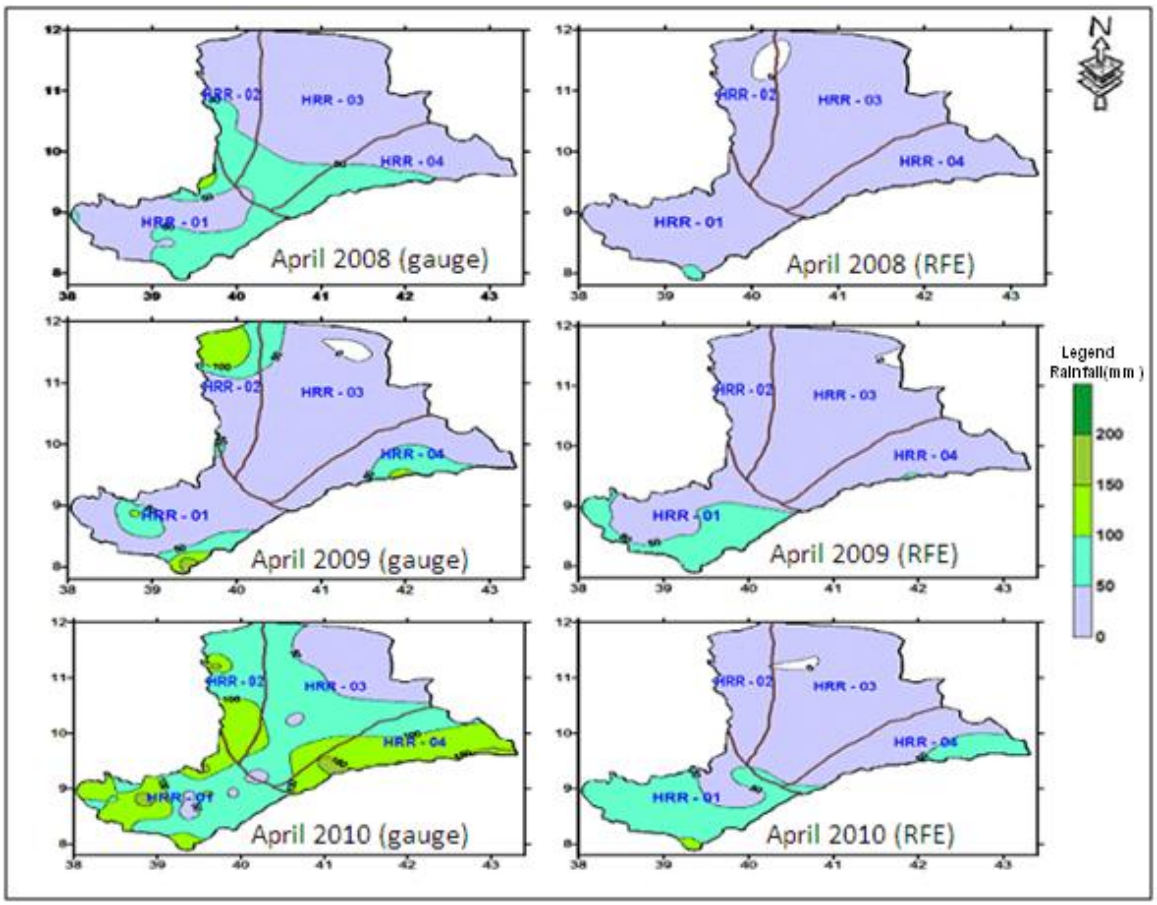

Figure 4.14: RFE and Gauge rainfall map for April 2008, 2009 and 2010

In Figure 4.15, the monthly total rainfall of RFE value and gauge value were presented for August 2008, 2009 and 2010. During August month, most of the HRR in the basin receive high amount rainfall. As it is indicated in (Figure 4.15) during August 2008, 2009 and 2010 some areas of HRR1, HRR2, HRR3 and HRR4 receives about 300mm and

above monthly total rainfall amount as it is recorded by gauge but the satellite monthly total rainfall estimate is less than 300 mm over all region of the basin. The spatial rainfall distributions of RFE and gauge value are almost in agreement over HRR1 for the three selected years. Additionally, the total monthly rainfall distribution of August 2008 and 2010 over HRR4 for both RFE and gauge value are slightly in agreement. As a general, the total monthly rainfall amount and spatial distribution of RFE value during the month of August 2008, 2009 and 2010 are underestimated over most areas of HRRs of the basin when it compared with gauge value.

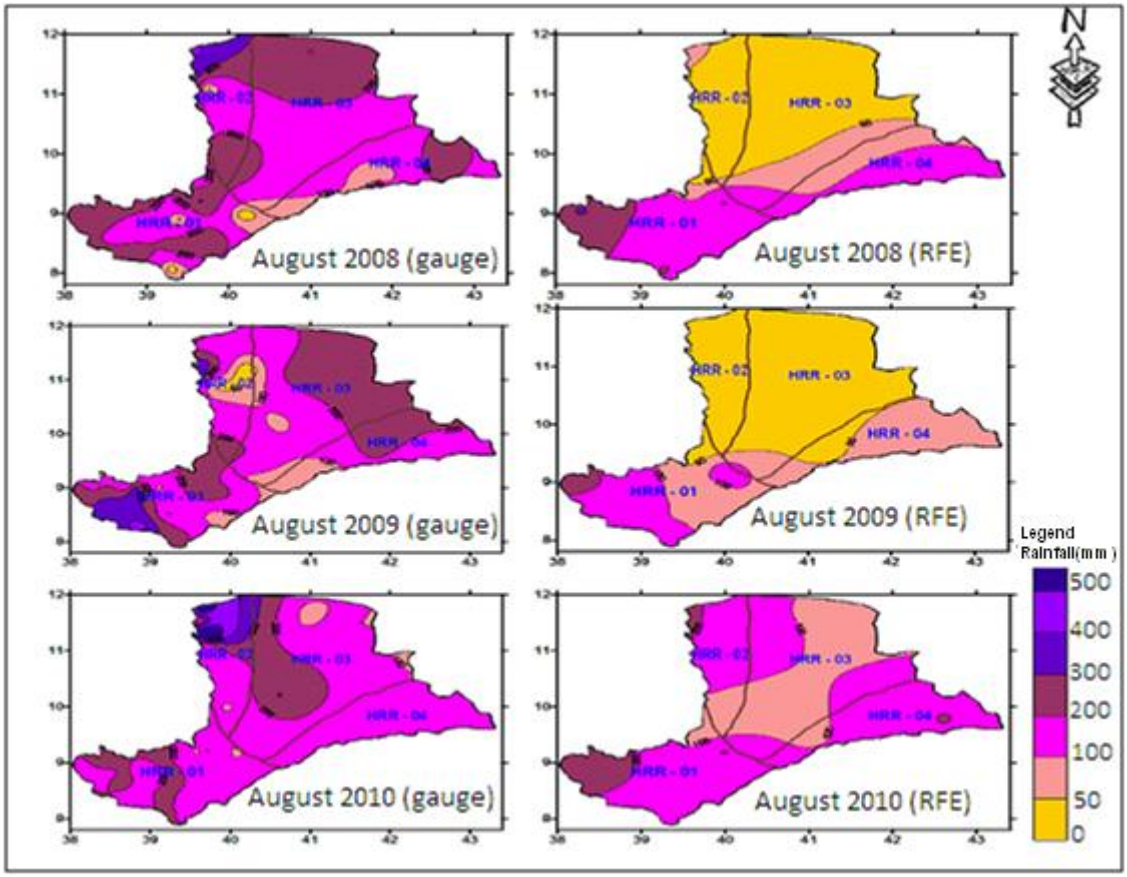

Figure 4.15: RFE and Gauge rainfall map for August 2008, 2009 and 2010

4.3.1.2. Seasonal total Rainfall Surface Map of RFE and Gauge value

To evaluate the seasonal spatial distribution of rainfall amount of RFE value with respect to gauge value over different HRRs of the basin, the two rainy seasons (Belg and Kiremt) are selected. As it is shown in (Figure 4.16), the RFE and gauge value filled contour map for Belg 2008, 2009 and 2010 are slightly similar over some HRRs but still the RFE value underestimate the total seasonal rainfall amount. Similarly, the distribution of rainfall in each selected season of the year for gauge and RFE value is in agreement with each other.

The gauge value of the seasonal rainfall distribution is better during belg 2010 than the rest of the years. This situation is also observed for RFE value of 2010.

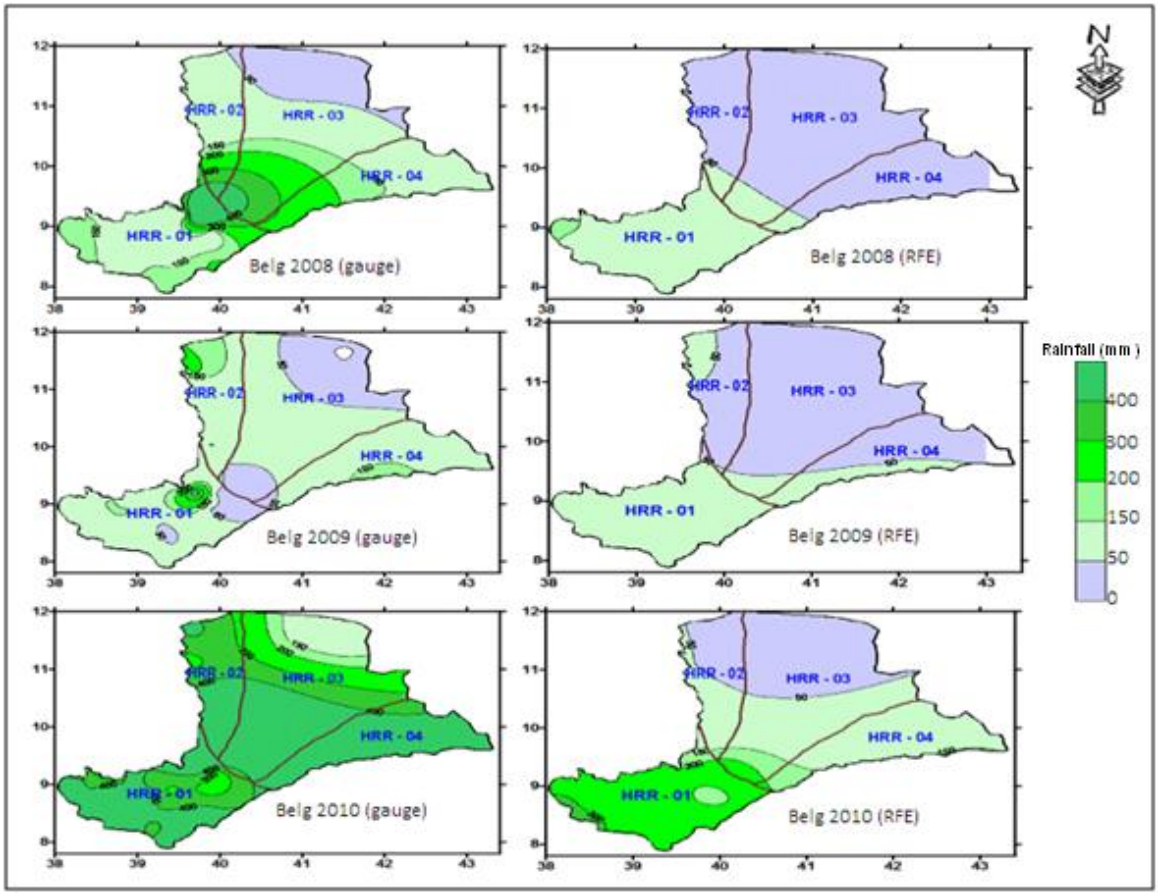

Figure 4.16: Seasonal RFE and Gauge rainfall map for Belg 2008, 2009 and 2010

Kiremt season (June, July, August and September) is the main rainy season for all HRRs of the basin. Among the months of kiremt season August receives better rainfall amount in terms of amount and distribution. Due to this reason, it is selected for spatial total rainfall distribution comparison purpose of RFE value with gauge value for the three selected years. As it shown in (Figure 4.17) the rainfall seasonality are explained better for kiremt 2008, 2009 and 2010 over HRR areas of the basin. In particular, in the western catchment of the basin (HHR 03) RFE and Gauge values are in agreement. But still underestimate situation are occurred over most places of the rest of HRRs because of the bias and other local conditions like topography and meteorological conditions.

As a whole, the situation of RFE value on the spatial and temporal variability of the basin is more or less explained with those of the limitations of bias and processing procedure, the estimated rainfall also showed the dry, normal and wet pattern of the seasons for each year of the selected seasonal distribution of rainfall maps.

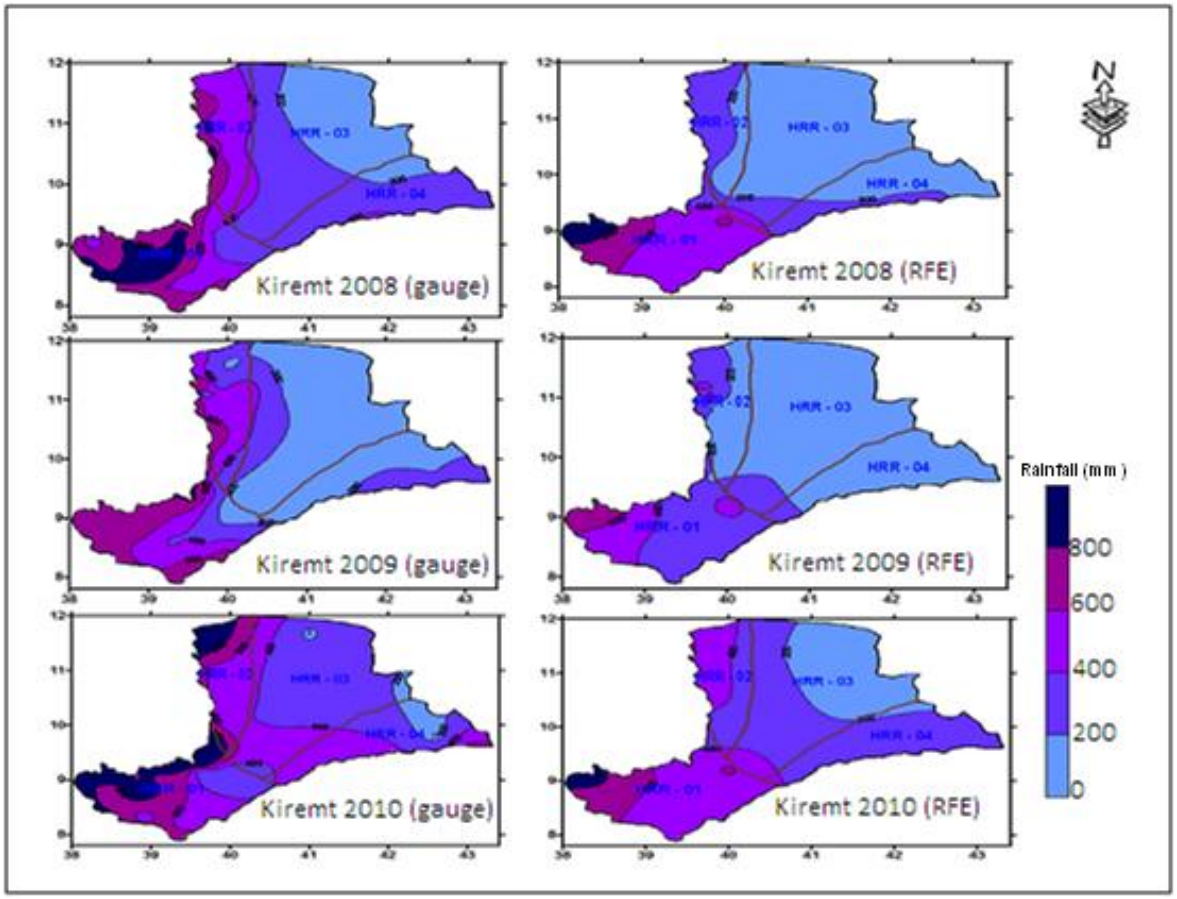

Figure 4.17: Seasonal RFE and Gauge rainfall map for Kiremt 2008, 2009 and 2010

4.3.1.3. Annual total Rainfall Surface Map of RFE and Gauge value

For the evaluation of annual total rainfall amount performance of RFE and gauge value of the year of 2008, 2009 and 2010 the analysis was done separately. According to the analysis shown in (Figure 4.18) the distribution of RFE value is slightly in agreement with gauge value over most of the HRRs in the basin. Over most areas of HRR1 and HRR2 the total annual rainfall reaches above 1400 mm as it is shown for gauge value analysis in (Figure 4.18). But the maximum total annual rainfall of HRR1 and HRR2 is not exceeded 1200 mm as it is shown on the analysis of RFE value in (Figure 4.18). For the total annual rainfall value less than 200 mm over some areas of HRR3, the analysis of RFE and gauge value shows the in agreement of both values. Generally, the analysis of total annual rainfall for the three selected years shows the underestimation RFE values.

The total annual rainfall value computed from the estimated value is also represented the dry, normal and wet situations of the year 2009, 2008 and 2010 respectively. As shown in (Figure 4.18) the estimated rainfall was highest by amount and distributions for the year of 2010 which is similar to the gauge values. Generally, the analysis of total annual rainfall for the three selected years shows the underestimation RFE values.

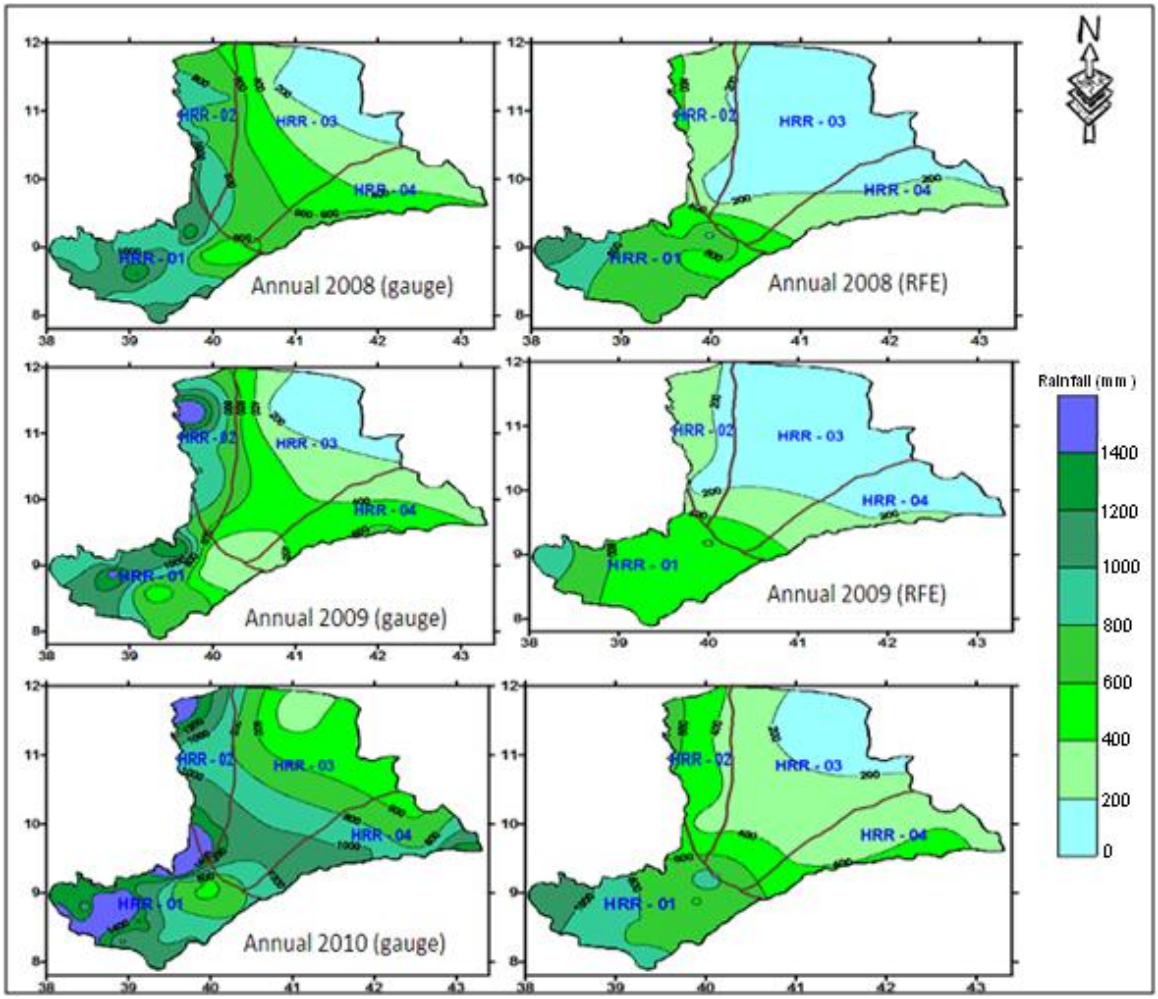

Figure 4.18: RFE and Gauge value Surface Rainfall Map for Annual 2008, 2009 and 2010

4.4. Temporal Characterization of RFE and Gauge value Rainfall

Approach of rainfall characterization over time and geographical unit is useful in carrying out a comparative assessment and understanding of the satellite based estimated rainfall as a signal for climatic condition of the study area. The rainfall characteristic over the basin is highly variable from month to month, season to season and annual to annual. To show this variability, the average value of estimated rainfall and gauge records were calculated for each period in the year of 2008, 2009 and 2010. The variability of rainfall in each HRR of the basin has also tested by using statistical parameters (Table 4.2)

Table 4.2: Annual mean rainfall distribution and variability over the basin for the year of 2008, 2009, 2010 and long year mean

Region	Long year mean (1990 – 2010)			2008			2009			2010		
	Mean	SD	CV	Mean	SD	CV	Mean	SD	CV	Mean	SD	CV
HRR_1	969.2	222.1	22.9	985.1	168.1	16.4	931.9	332.1	35.6	1348.0	484.5	35.9
HRR_2	1027.3	137.5	13.4	1031.6	140.1	16.0	877.6	347.4	33.7	1316.0	500.1	38.0
HRR_3	413.1	288.8	69.9	119.5	45.2	37.8	175.1	117.6	67.2	589.3	267.2	45.3
HRR_4	650.5	200.2	30.8	605.4	171.9	28.4	411.0	226.9	55.2	860.7	239.6	27.8

The table illustrate that the rainfall variations as well as the spatial differences within the river basin. The mean annual rainfall amount of the basin is about 765mm with mean coefficient of variation 34.25 percent. The coefficient of variation with smaller values indicated that the rainfall is less variable and more consistent. In regard to spatial distribution, the highest mean annual values are occurred in the HRR2 and HRR1, both in western and northwestern highlands of the basin which are experiencing better rainfall distribution. The lowest mean annual rainfall values are occurred in HRR3. In general, the rainfall profile shown in (Table 4.2) can give us an understanding that the inte-annual variability is one of the most important indicators of the reliability of the rainfall as the base for the interpretation of RFE data in the next section. The high variability in the rainfall was also confirmed by analysis of the mean and the standard deviation of these rainfall values over the region. It was observed that the standard deviation of the rainfall tracks or compares to the mean of the rainfall which can be used to infer strong spread hence variability. Similarly, the analysis of the coefficient of variability showed that areas with high variability coincide with regions of relatively low mean rainfall similar to suggestions in similar studies, e.g. (Maidment et al., 2012).

4.4.1 Dekadal Pattern Analysis of RFE and Gauge Value

The Dekadal time serious analysis can provide great opportunity for detecting, describing and to identify the onward and backward tendency of the variability of the estimated rainfall over the study area. By using this method, the Dekadal RFE and gauge value from all 50 stations for the selected three years were processed and used

to characterize the pattern of Dekadal estimated rainfall and gauge rainfall data (Figure 4.9).

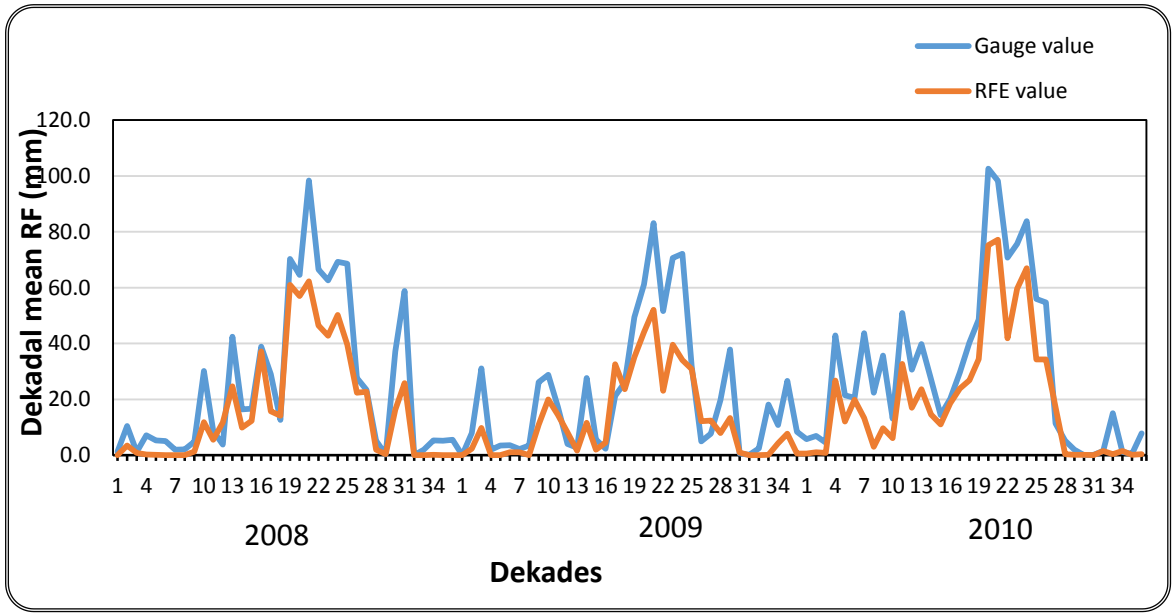

Figure 4.19: Plots of Rainfall Pattern and Characterization for RFE value (Using Pattern analysis, Dekadal in2008, 2009 and 2010)

The plot on (Figure 4.19) shows that the RFE value is nearly follow the shape of the dekadal cycle of the gauge and represented well in all three years. The RFE value is underestimated in all dekade of the three consecutive years. The bimodal regime type B is propagated throughout the three years, in which, estimated dekadal rainfall followed the gauge rainfall pattern and the occurrence of the peak rainfall time over the study area.

In general, the graph is a good indicator of the pattern agreements between the estimated and gauge values in order to determine their performance. The peak dekadal rainfall values were observed in kiremt season for both RFE and gauge rainfall values. The gap shown between the two lines are the errors that show the error between the estimated and the gauge value.

4.4.2 Monthly Pattern Analysis of Gauge and RFE value

The result obtained from this analysis confirms that satellite estimated rainfall Value is subsequent to inter-annual variability within the basin. Even though the values of RFE for most of the months are underestimated it can be seen that the pattern and

distribution is in agreement with the corresponding gauge record and the climate system over the basin.

For the whole basin, the estimated rainfall is also closely represented the rainfall regime characterized by type B with similar peaks During February to May and June to September.

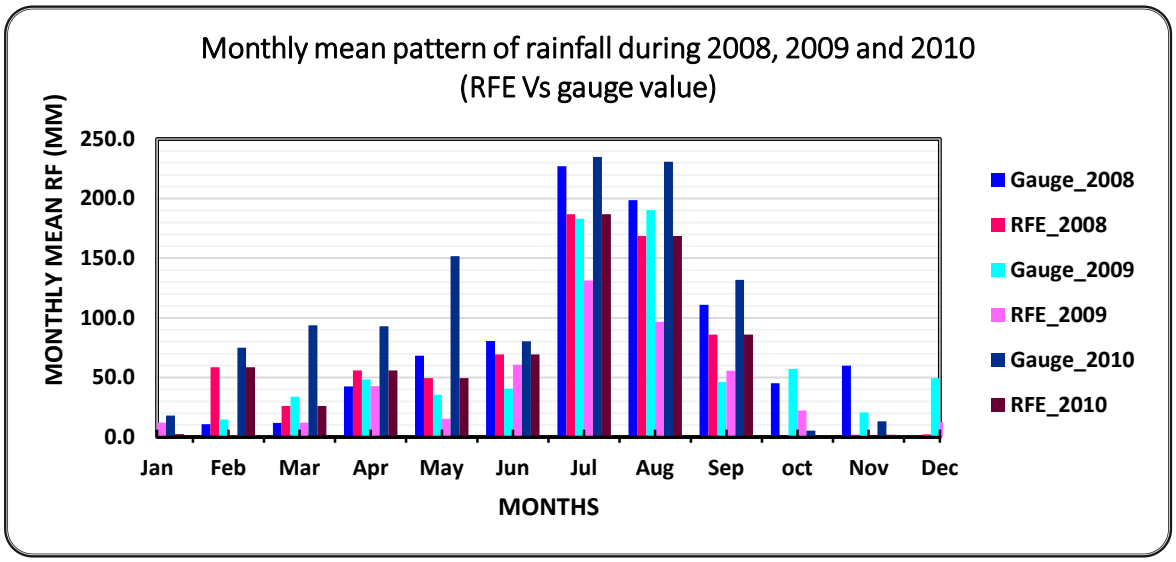

Figure 4.20: Average Monthly Rainfall Profile

As it is shown in the graph, the performance of rainfall during each month is clearly indicated. Mean monthly rainfall of RFE and gauge value show a better rainfall during the year of 2010. On both rainfall data the maximum average amount of rainfall were observed during normal year of 2008 and wet year of 2010. The pattern of monthly RFE value is in agreement with gauge value during all months. The maximum rainfall recorded by gauge is exceed 200 mm during July and August month of 2008 and 2010 but the mean monthly RFE value is not exceeds 150 mm except for July 2008 (Figure 4.20).

4.4.3. Monthly Maximum Rainfall Profile of Gauge and RFE value

The other significant feature that can be compared and characterized the RFE and the gauge recorded value were the maximum rainfall existed in each dataset and commonly applied to characterize extreme condition like flood occurrence and studying rainfall depth and pattern between the maximum rainfall and physical basin. Summery statistics of the monthly maximum rainfall are presented in (Table 4.3).

Table 4.3 Monthly Maximum Rainfall Profile for RFE and Gauge Value

year	Gauge Recorded(mm)			Location		Estimated Rainfall(mm)			Location	
	Month	Max.	Station	Long	Lat	Month	Max	Station	Lon	Lat
2008	July	441.2	Wejhed	39.8	10.5	August	306.0	Kimoye	38.3	9
2009	August	436.1	Ataye	37.7	10	August	239.0	Ambo	37.9	8.9
2010	August	900.0	Akaki	38.3	7.3	July	300.0	Werebabo	39.3	11.3

The table reveals that most of maximum monthly estimated rainfall exhibited, during August and July at which the seasonal rainfall peak is apparent for most of HRR within the basin. The maximum rainfall for both RFE and gauge values are occurred in upstream of HRR-1and northwestern areas of the basin (HRR-2) where the highest topography is observed. Most of the big tributaries also originate from this upstream region of the basin.

4.4.4. Seasonal Analysis of Gauge and RFE value

Mean seasonal rainfall for the RFE and gauge values are calculated, at HRRs level for all three selected years. This situation will help to evaluate the performance of RFE value at each HRRs in different season.

(a) Based on RFE Value

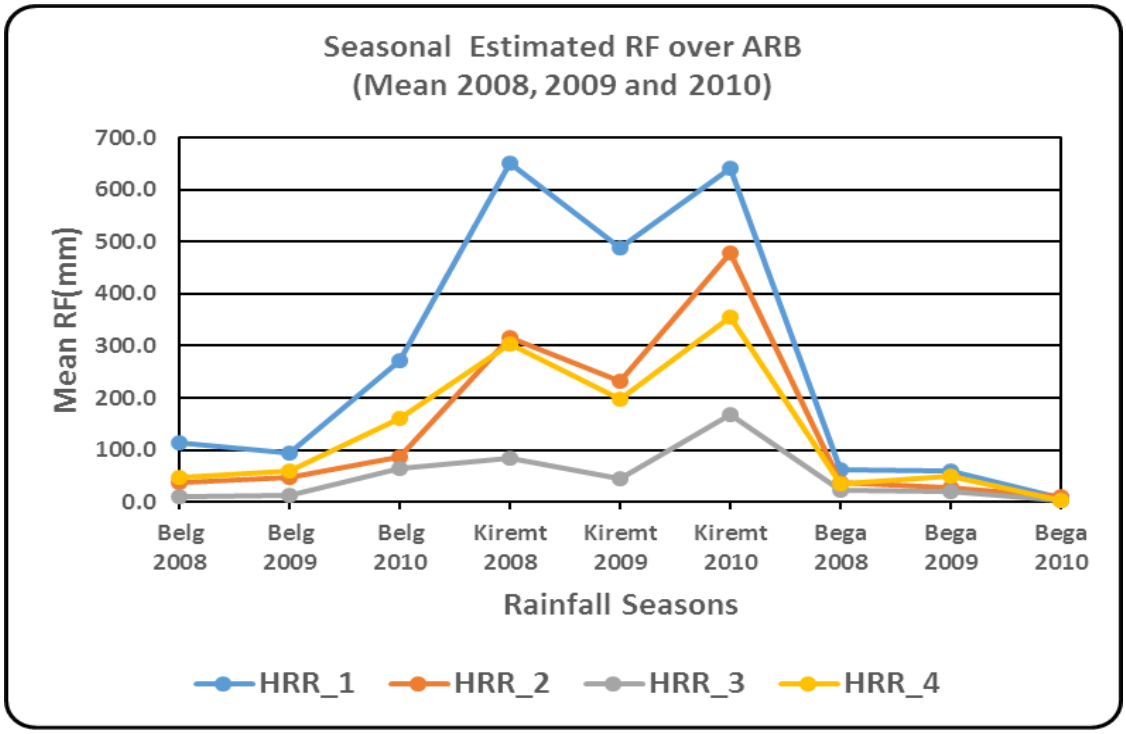

Figure 4.21: Plot of Spatial Pattern of RFE Value on Seasonal Basis

The seasonal RFE value plot (Figure 4.21) shown that, seasonality of the rainfall at each HRRs in the basin is the same with a variation of rainfall amount. The dry, normal and wet condition of the year of 2008, 2009 and 2010 respectively are also indicated in better way. Western catchment of the basin in HRR-1 receives better rainfall in all seasons of the three selected years. The northeastern lowland in HRR-3 receives the least amount of seasonal rainfall when it compared with the rest of the HRRs in the basin. During Bega seasons all the HRRs in the basin are not benefitted much rainfall amount. During kiremt 2010, rainfall amount was better in all HRRs.

Interestingly, the average rainfall estimated for kiremt 2008 and 2010 was high for HRR-1 and it is decreasing to the northeastern lowland in HRR-3 to below200mm rainfall. In Kiremet 2010, most parts of the western catchment of the basin in HRR-1 and northwestern areas of the catchment in HRR-2 of Awash River were attained much rain amounting above 600 mm (Figure 4.21). In this case, we can suggest that the satellite based rainfall estimation is an essential for getting rainfall information.

b) Based on Gauge Value

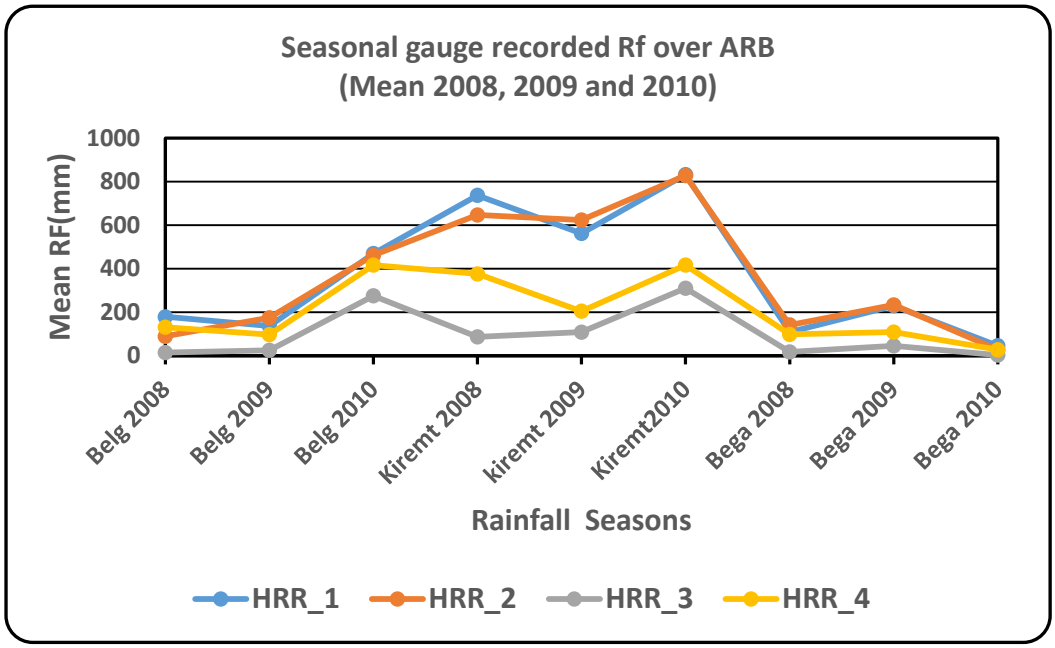

Figure 4.22: Plots of Spatial Pattern of gauge Value on Seasonal Basis

The plots of spatial pattern of gauge value (Figure 4.22) show the occurrence of better rainfall conditions during kiremt 2010. During kiremt 2010 HRR-1 and HRR-2 receives the same amount of rainfall by about 800 mm. The northeastern lowland in HRR-3 receives the least amount of rainfall in all season when it compared with HRR-1, HRR-2 and HRR - 4 this condition is also observed in plot of spatial pattern of RFE value in (Figure 4.22). Therefore, the temporal and spatial pattern of RFE and gauge value show a similar pattern in all areas of HRRs in the basin.

4.4.5. Annual Rainfall amount distribution of Gauge and RFE value at each HRR in the basin

Both RFE and gauge values for the selected years were averaged and the mean annual values are presented based on annual basis (Table 4.4). The main purposes of these table is to compare the average estimated rainfall and gauge values in each of the relatively dry, normal and wet years, and to understand the spatial structure of the background rainfall climatology within the basin.

Table 4.4 : Annual rainfall of Estimated and Gauge Values

Rainfall	Year	Regions				Basin Average Rainfall(mm)
		HRR_1	HRR_2	HRR_3	HRR_4	
Gauge	2008	985.1	1031.6	119.5	605.4	685.4
	2009	931.9	877.6	175.1	411.0	598.9
	2010	1348.0	1316.0	589.3	860.7	1028.5
Estimated	2008	825.90	391.6	118.5	387.0	430.7
	2009	644.5	306.6	79.7	308.0	334.7
	2010	920.8	574.9	235.7	519.9	562.8

The estimated annual mean rainfall forHRR-3 has been clearly indicated on the Table 4.4 with very low rainfall in all three years. But as we discussed it earlier, this region is getting rain during Belg and Kiremt season. On the contrary, the regions in western and northwestern highlands of the basin in HRR-1 and HRR-2 are received much rain during those periods. The year of 2008 mean annual estimated and gauge value rainfall conditions over HRR-3 are nearly the same. Similarly, the correlation within the basin for annual average gauge and estimated rainfall value in year of 2008 is higher than the year of 2009 and 2010.

5. CONCLUSION AND RECOMMENDATIONS

5.1. Conclusion

High resolution satellite-based rainfall estimates provide an alternative source of rainfall data for different applications especially in developing countries, where conventional rain gauges are sparse. The near-real-time availability of the satellite based rainfall estimates makes them suitable for water resource management, drought assessment and early warning applications, however, an over or underestimation in the satellite based rainfall estimate could lead to analysis results that give a false sense of interpretation. Given that satellite rainfall estimates are contaminated by sources such as temporal sampling, instrument and algorithm error, it is important to assess the accuracy of these estimates.

The ability of rainfall estimation technique TAMSAT, to give a real time rainfall estimates over the study area was investigated using continuous verification statistics and visual analysis techniques that compares map of satellite rainfall estimates and observation with climatologically characterization of the estimated value with the gauge recorded value at temporal and spatial perspective for each delineated HRRs with in the basin. In this regard, all the input data for satellite estimates and gauge recorded value were processed and converted to the spatial extent of each HRR rather than to the whole Awash River basin which is too coarse to represent the rainfall estimations.

To delineate Homogeneous Rainfall Regions for Awash River basin, the long year seasonal rainfalls mean (1990 to 2010) was used and Principal Component Analysis (PCA) technique was applied. The delineation result showed that Awash River basin has 4(four) HRRs because of its slight different character of receiving rainfall. The analysis result reveal that all HRRs in the basin receive a bi-modal rainfall cycle but the rainfall cycle at HRR1 is slightly near to mono-modal type rainfall. The two rainy seasons with in the basin at each HRRs are Kiremt (June to September) and Belg (February to May). The result showed that all of HRRs of the basin receive high amount of rainfall during Kiremt season with a peak rainfall amount in August and July month. The monthly mean rainfall amount is peak at HRR2, HRR3 and HRR4 during August month with a value of 261.3mm, 99.0 mm and 125.0 mm respectively. But the monthly mean peak rainfall amount at HHR1 is during July with a rainfall amount of 229.8 mm. The contribution of Belg season rainfall over each HRRs of the basin is not as high as kiremt season rainfall.

The peak rainfall amount months of Belg season at each HRRs are variable. The Belg season monthly mean rainfall amount peak at HRR2 and HRR4 is during April month with a rainfall amount of 93.6mm and 84.4mm respectively. Whereas, the Belg season monthly mean rainfall amount peak at HRR1 and HRR3 is during May and March with a rainfall amount of 66.3 and 52.3mm respectively. According to the result from this study, HRR2 receives over two-fold of monthly mean rainfall during Kiremt season of August. Among all HRRs in the basin, HRR2 receives better rainfall amount during both seasons but HRR3 is one of the region that receives the lowest amount of rainfall less than 413mm/yr. Therefore, the rainfall patterns with in Awash River basin is dissimilar homogeneous rainfall regions.

Validation and comparison of satellite rainfall estimate with rain gauge data was made to analyze the ability of rainfall estimation technique TAMSAT, to give a real time estimates over the four HRRs of Awash River basin for some selected dekades, months, seasons and years. The result showed that the mean error of estimated rainfall during the dekades of kiremt season is higher than the dekades of belg season. Geographically the mean error between satellite rain estimates and rain gauge value are higher (>-10mm dekade^{-1}) at HRR1 and HRR2during second dekade of August where the distribution and amount of rainfall amount is high. However, the mean errors were generally minimal over the arid and generally low latitude areas of the region (HRR3). The same situations were observed for monthly mean error calculations of April month of belg season but the mean error does not exceeded -8mm month^{-1}. The mean error value observed during kiremt season over HRR1 and HRR2is as high as -120mm season^{-1} but the mean error value is different for each HRRs and years. This shows the limitation of TAMSAT methodology with topography, calibration with historical data, station network distribution, weather systems and together with systematic bias of the different rainfall measurement techniques. For the year 2008 which is considered as relatively normal rainfall year, the correlation coefficient result against the gauge record was found to be higher (r=0.73) compared to the selected years. The correlation coefficient result for the year considered as wet year (2010) is 0.52. In relatively low rainfall year (2009) the correlation coefficient result is 0.46. A number of factors can be thought of to contribute to the low r value; hence low correlation coefficient. These include high rainfall variability indicated by existence of large extreme rainfall values that are not detected by TAMSAT algorithm (systematic error) with other factors.

The satellite estimated rainfall totally explained in better way the spatial and temporal pattern relationship of the rainfall climatology characteristics of each HRRs for dekadal, seasonal and annual cases considering the observed differences in the rainfall magnitude between the satellite rainfall estimates and gauge rainfall value. However, there was a tendency of underestimation in all HRRs of the basins in most of the situations. The maximum rainfall values and the occurrence of peak month for both satellite estimated rainfall and gauge value within the basin is during kiremt season of July and August but the maximum rainfall value recorded by rain gauge and estimated by satellite is at different location of the basin within a given month. The result from spatial distribution rainfall map show that the estimated rainfall was well characterized and represents the climatology of the area in monthly seasonal and annual variability in most places of the basin.

As discussed above, it becomes apparent that the TAMSAT rainfall estimates are generally lower in representation of magnitude of rainfall amounts, but generally in agreement in terms of structure or pattern to gauge recorded rainfall value in estimating and representing the mean rainfall over much of Awash River basin. Variations in errors highlight the deficiencies of satellite rainfall algorithms for estimating spatially and temporally variable rainfall with topography and rainfall amount. Considering the observed differences in the rainfall magnitude amongst the rainfall estimates, it would be desirable to understand the effect of these differences in other climate related studies.

5.2 Recommendations

To improve on the effect of the systematic errors in satellite rainfall estimates, near real time gauges or a direct combination of near real time rainfall observations should be included in the TAMSAT methodology, as those proposed by (Grimes et al., 1999). It is however worth noting that this suggestion will not be without challenges especially in regions where the gauge network is sparse. Augmentation of availability of gauge data can be possible through participation of local meteorological and hydrological services in regular validation e.g. (multiannual time scale) exercises which also assist improving understanding, applicability and visibility of satellite derived rainfall estimates. Understanding the operational accuracy requirements for satellite rainfall estimates would offer an additional incentive to the local national meteorological and hydrological services to invest on improving the local rain gauge networks and exchange available gauge data with the global centers for calibration purpose.

Basically, reliability of rainfall forecasts or associated events depends on the availability of rainfall information. For instance, in the case of floods and drought, rainfall forecast is indispensable. Their accuracy is not sufficient yet. Further refinements are required. Although the accuracy of satellite-based rainfall product is not fully clarified and need to be further study, but such a source of rainfall data could be still of some help for un gauged and inaccessible areas since they show a rainfall climatology of a given area.

LIMITATION OF THE WORK

Comparison of TAMSAT methodology and gauge recorded with other satellite rainfall estimation methods and techniques like: PERSIANN, NRLB, TRMM-3B42, TRMM-3B42RT, CMORPH, and other have not been carried out. Additionally, rain/no rain contingency table statistics (hits, misses, false alarms, probability of detection and other statistics) are not carried out in this study due to limitation of time**.**

FUTURE WORK

Noting the results of the study, further studies are desirable to consider improving or optimizing the accuracy of TAMSAT rainfall estimates by correcting for bias error using localized rain gauge measurements. From the consistency in the bias errors over time, it is likely to fit a model for bias correction or optimization of the TAMSAT rainfall estimates. Also noting that the satellite rainfall estimates represent climatology of rainfall over the region with good skill, future work should consider also investigating characterization of inter and intra seasonal rainfall variability utilizing satellite derived rainfall estimates such as onset, cessation of rainfall and variability over the region.

The satellite rainfall estimate found to be good performance to explain the climatology of the study area. Hence, this work should be extended to other drought and flood prone area and to all over the country at large. It is also recommended that the work is very useful in providing information of the rainfall in time and space. Efficient, appropriate and effective communication system among the major stakeholders and collaborators should be also necessary with respect to agricultural planning, flood and drought early warning system.

REFERENCES

Abraha Adugna, (2006). Flood Modeling and Forecasting for Awash River Basin in Ethiopia, unpublished MSc. Thesis, UNESCO-IHE Institute for Water Education, Delft, the Netherlands, 85 pp.

ADF (2003) proposal: Flood control and watershed management study-constructing dikes along a river in Awash (http://www.afdb.org/pls/portal/docs)[Accessed on: 8 February, 2013]

Adler, R.F., Negri, A.J., 1988. A Satellite Infrared Technique to Estimate Tropical Convective and Stratiform Rainfall. J. Appl. Meteorol. 27, 30–51.

Adler, RF; Chang, GJ; Ferraro, R; Xie, P; Janowiak, J; Rudolf, B; Schneider, U; Curtis, S; Bolvin, D; Gruber, A; Susskind, J; Arkin, P; Nelkin, E (2003) 'The version-2.

Admasu Gebeyehu, 1989. Regional flood frequency Analysis. Technical Report. Royal Institute of Technology, Stockholm, Sweden.

AMS Glossary (2012). Glossary of Meteorology, American Meteorological society, USA. http://glossary.ametsoc.org/index.php?title=Special:AllPages/R

Arkin, P. A., and B. N. Meisner, 1987: The relationship between large-scale convective rainfall and cold cloud over the Western Hemisphere during 1982-84. Monthly weather review.ams, 115, 51-74.

Artan, GA; Gadain, H; Smith, JL; Asante, K; Bandaragoda, CJ; Verdin, JP (2007) 'Adequacy of satellite derived rainfall data for stream flow modeling.' Nat. Hazards 43: 167-185.

Basistha, A; Arya, DS; Goel. NK (2007) 'Spatial distribution of rainfall in Indian Himalayas. A case study of Uttarakhand region.' Water Resources Management 22: 1325–1346. DOI 10.1007/s11269-007-9228-2.

Bekel,F 1993: Probability of Drought Occurrence under Different Events ,Addis Ababa, Ethiopia: NMA

Chadwick, R., Grimes, D., 2012. An Artificial Neural Network Approach to Multispectral Rainfall Estimation over Africa. J. Hydrometeorol. 13, 913–931.

Conway, D., 2002. Extreme Rainfall Events and Lake Level Changes in East Africa: Recent Events and Historical Precedents. In E.O. Odada and D. O. Olago (eds.) the East African Great Lakes: Limnology, palaeolimnology and biodiversity. Advances in global change research.V. 12. Kluwer, Dordrecht. pp. 63-92.

Dereje Mekonnen, (2012). Satellite-Based Rainfall Estimation, Evaluation and Characterization Using GIS and Remote Sensing Techniques. LAP LAMBERT Academic Publishing, Saarbrucken, Germany.

Dinku, T., Ceccato, P., Grover-Kopec, E., Lemma, M., Connor, S., Ropelewski, C., 2007. Validation of satellite rainfall products over East Africa's complex topography. Int. J. Remote Sens. 28, 1503–1526.

Dinku, T; Chidzambwa, S; Ceccato, P; Connor, SJ; Ropelewski, CF (2008) 'Validation of high-resolution satellite rainfall products over complex terrain.' Int. J. Remote Sens. 29(14): 4097-4110.

Diro, G. T., E. Black, and D. I. F. Grimes, 2008: Seasonal forecasting of Ethiopian spring rains. Meteor. Appl., 15, 73–83.

Dugudal G, 1994. Satellite-derived Rainfall estimates over Africa: their validation and use in monitoring climate change. In global precipitation and climate change, proceeding of Global Environmental metering, Amsterdam, November 1994.

Dutarter, P.Coudert., J.M and Delponi.G.1993.Evolution in the use of satellite data for the location and development of Ground water. Article in advanced space research.102, 300-567.

Ebert, EE (1996) Result of the 3rd Algorithm Inter comparison Project (AIP-3) of the Global Precipitation Climatology Project (GPCP), Bureau of Meteorology Centre, Report No 55. Melbourne, Australia: Bureau of Meteorology Centre.

Ebert, EE; Janowiak, JE; Kidd, C (2007) 'Comparison of near-real-time precipitation estimates from satellite observations and numerical models'.Bull. Amer. Meteorol. Soc. 88(1): 47-64.

Engman E.T and Gurney.1991. Remote sensing in hydrology. Current operational application of remote sensing in hydrology, WMO no.884, 1999.

EUMETSAT (1997a), satellite-derived Rainfall estimates over Africa: their validation and use in monitoring climate change. Proceeding of meteorological data user conference. Brussels, Belgium 29th September 1997.

EVDSA, 1989. Master Plan for the development of surface water resources in the Awash Basin. Halcrow, Final report Vol.I, Addis Ababa, Ethiopia.

Field A. (2009) 'Discovering Statistics using SPSS for Windows.' Third Edition. Sage Publications, London.

Funk, C., Senay, G., Asfaw, A., Verdin, J., Rowland, J., Michaelsen, J., et al.(2005). Recent Drought Tendencies in Ethiopia and equatorial-subtropical eastern Africa. FEWSNET Special Report.

Gebremichael, M., Krajewski, W. F., Morrissey, M., Huffman, G., and Adler, R.: A detailed evaluation of GPCP one-degree daily rainfall estimates over the Mississippi River Basin, J. Appl. Meteorol.,44(5), 665–681, 2005.

Gissila, T., Black, E., Grimes, D., and Slingo, J. (2004). Seasonal forecasting of the Ethiopian summer rains. International Journal of Climatology, 24, 1345-1358.

Global Precipitation Climatology Project (GPCP) monthly precipitation analysis (1979-present).' J. Hydrometeorol. 4: 1147–1167.

Griffiths C.G, 1971. The variation with height of the top brightness of precipitating convective cloud. Report of WMO technical report, N0 .237/2000, Switzerland, zananghug. April 2000.

Grimes, D.I.., Pardo-Iguzquiza, E., Bonifacio, R., 1999. Optimal areal rainfall estimation using rain gauges and satellite data. J. Hydrol. 222, 93–108.

Grimes, D.I.F., DIOP, M., 2003. Satellite-based rainfall estimation for river flow forecasting in Africa. I: Rainfall estimates and hydrological forecasts. Hydrol. Sci. J. 48, 567–584.

Habtemichael,A., Pedgley,DE., 1974. Synoptic case study of spring rains in Eritrea. Arch Meteor Geoph Biokl Ser A, 23: 285–295

Hallikainen.M., 1984:Satellite microwave radiometry of snow cover: Proceeding of the 18th international symposium on remote sensing of environment,1-5 October, Paris.

Herman S.B., Hallikainen.M., and Tayor.B.N.,1997:A comparison of two satellite rainfall estimates technique over tropics. Journal of applied Meteorology, 20 .120-178.

Hong, Y; Adler, RF; Negri, A; Huffman, GJ (2007) 'Flood and landslide applications of near real-time satellite rainfall estimation.' Nat. Hazards 43: 285–294.

Houghton and Taylor, 1973/1975/1988.The accuracy of estimates of areal mean rainfall .In proceeding results of research representative and experimental basins Wellington, international association of hydrology science publication No.93. p 203-218.

Huffman, GJ; Adler, RF; Bolven, DT; Gu, G; Nelkin, EJ; Bowman, KP; Hong, Y; Stocker, EF; Wolfe, DB (2007) 'The TRMM Multisatellite Precipitation Analysis (TMPA): Quasi-global, multiyear, combined-sensor precipitation estimates at fine scales.' J.Hydrometeorol. 8: 38–55.

Hulme. M., (1992.) A 1951-80 Global land precipitation climatology for the evaluation General Circulation Models. Climate Dynamics, 7, 57-72.

International Centre for Integrated Mountain Development (ICIMOD), 2013. Validation of NOAA CPC_RFE Satellite-based Rainfall Estimates in the Central Himalayas. ICIMD Working paper 2013/5. ICMOD, Kathmandu, Nepal.

Joyce, JJ; Janowiak, JE; Arkin, PA; Xie, P (2004) 'CMORPH: A method that produces global precipitation estimates from passive microwave and infrared data at high spatial and temporal resolution.' J. Hydrometeorol. 5: 487–503

Kaiser H.F. (1959) Computer program for varimax rotation in factor analysis, Psychological Measurement, 19, 413-420.

Kassahun, B., 1986: Local weather systems over the Red Sea area.Local Weather Systems Prediction for the Red Sea Countries,Tropical Meteorology Research Programme Rep. Series, No. 29,WMO, 1–18.

Kazmin, V., Seifemichael Berhe, Nicoletti, M. and Petrucciani, C., 1980. Evolution of the Northern Part of the Ethiopian Rift. In Geodynamic Evolution of the Afro-Arabian Rift System, Academia Nazionale dei Lincei, Roma, Atti dei Convegni Lincei, 47, p. 275-292.

Kidd, C (2005) 'Validation of satellite rainfall estimates over the mid-latitudes.' In Proceedings of the 2nd IPWG working group workshop, Monterey, CA, 25-28 October 2004, pp 205-215. Monterey CA, USA: Naval Research Laboratory, Marine Meteorology Division, and Darmstadt, Germany: EUMETSAT.

Kidder S.Q .and T.H Vonder Haar 1997. Tropical oceanic precipitation frequency from microwave data. Atmospheric Science paper No.248, Department of atmospheric science Colorado state university.

Kronberg, P., Schonfeld, M., Gunther, R. and Tsombos, P., 1975. ERTS 1-Data on the Geology and Tectonics of Afar/Ethiopia and Adjacent Regions. In Pilger, A. and Rosler, A. (Editors), Afar Depression of Ethiopia, Inter-Union Commission on Geodynamics Scientific Report, n.14, p.19-27.

Kubota, T; Ushio, T; Shige, S; Kachi, M; Okamoto, K (2009) 'Verification of high resolution satellite-based rainfall estimates around Japan using a gauge-calibrated ground-radar dataset.' J. Meteorol. Soc. Japan 87A: 203–222.

Laurent, H; Jobard, I; Toma, A (1998) 'Validation of satellite and ground based estimates of precipitation over the Sahel.' Atmospheric Research 47-48: 651-670.

Maheras P. (1985) A factorial analysis of Mediterranean precipitation, Archives of Meteorological and Geophysical Bioclimatology Series B, 36, 1-14.

Maidment, R.I., Grimes, D.I.F., Allan, R.P., Greatrex, H., Rojas, O., Leo, O., 2012. Evaluation of satellite-based and model re-analysis rainfall estimates for Uganda. Meteorol. Appl..

Ministry of Water Resource (MoWR), 1996. Master plan study. Executive Summary Report: Omo-Gibe river basin integrated development master plan study, Addis Ababa, Ethiopia.

MOWR, (2010). Ministry of Water Resources. Addis Ababa, Ethiopia. http://www.mowr.gov.et, accessed on: 24.05.2013.

Milford J.R. and Dugdale G., 1989: Estimation of rainfall using geostationary satellite data. In Application of remote sensing in agriculture. Proc. 48th Easter School in Agri. Sci. Univ. Nottingham. April, 1989. Butterworth, London.

Milford, J.R., McDougall, V.D., Dugdale, G., 1994. Rainfall estimation from cold cloud duration, experience of the TAMSAT group in West Africa, in: Validation Problems of Rainfall Estimation by Satellite in Intertropical Africa, Guillot B., Edt., Proc. Niamey Workshop. pp. 1–3.

National Meteorological Agency (NMA), 1996. Climate and agro-climatic resource of Ethiopia. NMA, Ethiopia. Meteorological research. Report serious Vol.1,1-137.

Organization for economic co-operation and Development (OECDE), 1988. Satellite Remote Sensing and the Sahel, Western Africa Regional research groups, Annual report, May 1988.Abuja, Nigeria.

Segele, Z. T., and P. J. Lamb, 2005: Characterization and variabilityof Kiremt rainy season over Ethiopia. Meteor. Atmos.Phys., 89, 153–180.

Segele, Z. T., P. J. Lamb, et al. (2009). Large-scale atmospheric circulation and global sea surface temperatureassociations with Horn of Africa June-September rainfall. International Journal of Climatology 29(8): 1075–1100.

Shrestha, MS; Artan, GA; Bajracharya, SR; Sharma, RR (2008a) 'Applying satellite-based rainfall estimates for streamflow modelling in the Bagmati Basin, Nepal.' J. Flood Risk Management 1: 89–99.

Shrestha, MS; Bajracharya, SR; Mool, P (2008b). Satellite rainfall estimation in the Hindu Kush-Himalayan Region. : ICIMOD, Kathmandu, Nepal

Sogreah, 1965. Survey of the Awash River Basin, Volume II (Soils and Agronomy). Edited subsequently by: FAO of the UN (FAO/SF: 10/ETH). Imperial Ethiopian Government, United Nations Special Fund Project.

Stevens J.P. (1992) 'Applied Multivariate Statistics for the Social Sciences.' 2nd Edition. Erlbaum, Hillside, USA.

TAMSAT Research Group, Department of Meteorology, University of Reading.

http://www.met.reading.ac.uk/~tamsat/data/RFE.html

Tadiwos Chernet, 1995. Petrological, Geochemical and Geochronological Investigation of Volcanism in the Northern Main Ethiopian Rift-southern Afar Transition Region. Ph.D. Dissertation, Miami University, Oxford, Ohio.

Tadiwos Chernet, Hart, W.H., Aronson, J.L. and Walter, R.C., 1998. New Age Constraints on the Timing of Volcanism and Tectonism in the Northern Main Ethiopian Rift-Southern Afar Transition Zone (Ethiopia). Journal of Volcanology and Geothermal Research, 80, p.267-280.

Tadiwos Chernet and Hart, W.H., 1999. Petrology and Geochemistry of Volcanism in the Northern Main Ethiopian Rift-southern Afar transition region. Acta Vulcanologica, v.11 (1), p.21-41.

Thorne, V., Coakeley, P., Grimes, D., Dugdale, G., 2001. Comparison of TAMSAT and CPC rainfall estimates with raingauges, for southern Africa. Int. J. Remote Sensing. 22, 1951–1974.

Tufa Dinku, 1994. The use of smaller calibration zones for better rainfall estimation over Ethiopia. Paper presented at a workshop on Evaluation of Precipitation by Satellite, 1- December 1994, Niamey, Niger

Tuker M.R .1997.satelite Derived rain storm distributions an aid to forecasting African armyworm out breaks .Weather report. American meteorological association. April /August. No. 23-27, 1997.

Turk, F. J., G. D. Rohaly, and P. Arkin, 1997. Utilization of satellite-derived tropical rainfall for analysis and assimilation into a numerical weather prediction model. Presented on 9th Conference Hurricanes and Tropical Meteorology. AMS.

Vila, D; Scofield, R; Kuligowski, R; Davenport, J (2003). Satellite rainfall estimation over South America: Evaluation of two major events, NOAA Technical Report NESDIS 114.Washington DC, USA: U.S. Department of Commerce, National Oceanic and Atmospheric Administration.

Ushio, T; Sasashige, K; Kubota, T; Shige, S; Okamota, K; Aonashi, K; Inoue, N; Takahashi, T; Iguchi, T; Kachi, M; Oki, R; Morimoto, T; Kawasaki, ZI (2009) 'A Kalman filter approach to the global satellite mapping of precipitation (GS_Map) from combined passive microwave and infrared radiometric data.' J. Meteorol. Soc. Japan 87A: 137–151.

Vila, D; Lima, A (2006) 'Satellite rainfall estimation over South America: The hydroestimator technique.' In WW Grabowski (ed) 14th International Conference on Clouds and Precipitation, Bologna, Italy, 18–23 July 2004. Amsterdam, Netherlands: Elsevier

Workineh Degefu, 1987. Some aspects of meteorological drought in Ethiopia. pp 23- In, Drought and Hunger in Africa: denying famine a future, M.H. Glantz (Ed.). Cambridge University Press.457 pp.

World meteorological organization (WMO), 1988a: Application of satellite data for estimation of precipitation. Technical report to the commission for hydrology No.26, WMO/TD- No.300, Geneva.

World meteorological organization (WMO), 1994. In remote sensing for hydrology Progress and prospect, operational report.No.36.WMO No.7.

Xie, P; Yarosh, Y; Love, T; Janowiak, J; Arkin, PA (2002) 'A real-time daily precipitation analysis over South Asia.' Preprints of the 16th Conference on Hydrology, Orlando, Florida. Washington DC, USA: American Meteorological Society.

APPENDIX- I

Monthly long year mean rainfall (mm) (1990-2010) for the stations within Awash River

No	Stations	Long.	Lat.	Elev.	Jan	Feb	Mar	Apr	May	Jun	Jul	Aug	Sep	Oct	Nov	Dec	Bega	Belg	Kiremt	Annual
1	Ambo	37.9	9.0	2130.0	22.0	36.6	58.4	68.2	78.3	155.6	226.3	203.2	110.8	41.5	5.3	12.7	81.6	241.6	695.9	1019.1
2	Welliso	38.0	8.6	2000.0	18.0	29.9	54.4	75.1	93.5	178.0	262.2	278.7	144.6	39.4	6.5	7.3	71.1	252.9	863.6	1187.6
3	Ginchi	38.1	9.0	2132.0	25.3	46.9	69.6	85.6	88.6	138.3	238.1	230.1	145.6	42.0	13.6	11.2	92.2	290.8	752.0	1135.0
4	Busa	38.1	8.8	2200.0	21.9	44.2	53.7	82.3	83.6	175.7	331.7	366.8	161.8	39.4	11.7	9.0	82.0	263.9	1035.9	1381.8
5	Teji	38.4	8.8	2091.5	16.4	33.4	53.5	74.8	67.1	114.1	214.9	212.5	94.4	24.8	6.6	5.0	52.7	228.9	636.0	917.6
6	Addis Alem	38.4	9.0	2372.0	0.2	1.4	8.9	18.2	96.1	144.5	239.7	200.1	131.3	123.3	15.9	3.1	142.4	124.6	715.6	98
7	A/Melka	38.6	8.7	2030.0	11.2	27.6	59.8	73.9	61.7	108.4	228.9	219.1	83.8	17.2	3.4	5.5	37.4	222.9	640.3	900.6
8	Sebeta	38.6	8.9	2175.9	12.9	45.6	69.3	84.1	77.9	137.5	264.0	293.1	129.5	28.1	7.4	5.2	53.6	277.0	824.1	1154.6
9	Ejersa Lele	38.7	8.2	1797.0	15.3	36.5	58.0	71.2	53.5	74.6	165.7	146.1	81.5	23.3	6.8	3.7	49.2	219.2	467.9	736.3
10	Addis Obs	38.7	9.0	2364.0	17.5	36.2	69.1	91.0	75.2	125.6	439.6	277.1	175.2	219.4	7.8	10.6	255.3	271.5	1017.5	1544.3
11	Akaki	38.8	8.9	2057.0	13.0	37.5	64.7	90.0	69.1	119.6	258.4	280.6	130.9	24.6	4.3	3.7	45.6	261.4	789.6	1096.5
12	G/Met	38.8	9.0	2245.0	10.0	33.2	50.6	64.1	65.6	95.9	219.6	238.5	132.9	29.5	3.2	3.1	45.9	213.5	686.9	946.2
13	Hombole	38.8	8.4	1743.0	12.5	34.9	54.5	58.0	46.7	90.5	231.5	222.5	95.2	27.9	6.1	2.7	49.3	194.1	639.7	883.1
14	Debre Zeit	39.0	8.7	1900.0	9.8	25.3	45.8	57.7	51.6	92.7	219.1	219.0	104.0	21.5	5.1	3.3	39.7	180.5	634.9	855.1
15	Chefedonsa	39.1	9.0	2392.0	9.2	20.9	40.1	44.0	33.7	82.3	182.5	205.3	79.1	15.8	2.4	6.9	34.3	138.8	549.2	722.3
16	Aleltu	39.1	9.2	2550.0	15.7	18.1	65.6	63.2	52.8	97.2	306.0	320.2	118.8	22.4	3.6	1.8	43.6	199.6	842.2	1085.4
17	Mojo	39.1	8.6	1763.0	11.9	26.1	45.8	52.2	50.5	93.1	227.3	222.8	115.1	26.9	9.5	1.9	50.2	174.5	658.2	883.0
18	Koka	39.3	8.4	1618.0	10.9	20.6	40.4	51.1	42.5	57.4	180.8	182.2	81.6	24.1	7.3	6.9	49.2	154.6	502.0	705.9
19	Nazreth	39.3	8.6	1763.0	11.1	27.2	48.0	49.8	56.7	65.6	218.4	214.2	102.0	31.8	7.8	6.0	56.6	181.6	600.2	838.5
20	Etheya	39.3	8.1	2129.0	20.5	24.1	63.8	82.8	77.8	88.9	183.5	183.4	137.3	45.4	10.3	5.6	81.8	248.5	593.1	923.4
21	Ginchi	39.3	8.1	2129.0	26.6	44.9	70.8	93.7	87.5	138.2	237.6	249.1	14	38.3	12.4	9.5	86.8	296.9	767.5	1151.3

22	Huruta	39.3	8.1	2044.0	16.0	20.3	50.5	62.3	75.3	79.2	119.4	119.9	95.8	32.4	9.3	4.8	6	208.4	414.4	685.4
23	Ejere	39.3	8.8	2254.0	14.0	26.9	55.6	56.8	45.4	67.1	184.4	207.7	99.9	32.0	7.1	10.8	63.9	184.6	559.0	807.5
24	SODERE	39.4	8.4	1351.0	7.1	4.8	55.6	36.4	27.6	43.7	136.5	169.4	62.1	33.4	7.4	9.3	57.2	124.3	411.6	593.2
25	Bologiorgis	39.4	8.8	1963.0	16.5	45.1	52.0	58.7	50.6	62.5	212.9	221.6	86.5	31.0	10.6	6.6	64.8	206.4	583.5	854.7
26	Guder	39.8	9.0	2002.0	19.2	35.0	76.3	75.3	114.8	213.6	245.1	224.3	136.7	39.5	16.7	10.9	86.3	301.4	819.7	1207.4
27	Mersa	39.2	12.0	2100.0	49.4	62.1	103.8	110.4	68.3	29.9	230.5	245.5	87.5	46.8	28.3	40.5	165.0	344.7	593.5	1103.2
28	Sh/ Gebeya	39.3	9.1	2500.0	9.8	24.4	47.0	62.3	48.8	6	271.5	297.1	93.1	28.9	7.3	3.4	49.4	182.5	724.2	956.1
29	Sirinka	39.6	11.6	2000.0	47.1	60.9	97.7	102.9	70.4	29.3	210.2	247.3	90.6	59.2	26.8	35.5	168.6	331.9	577.4	1077.9
30	Desse	39.6	11.1	2500.0	25.9	36.1	79.0	91.6	73.2	39.1	289.2	297.6	152.8	53.0	22.8	20.5	122.3	279.9	778.7	1180.9
31	Haik	39.7	11.3	2660.0	34.0	68.5	99.6	111.2	82.3	33.0	278.1	284.5	125.7	45.5	22.2	24.5	126.3	361.5	721.3	1209.1
32	Tita	39.7	11.2	2464.5	28.1	18.5	56.0	96.2	29.8	34.0	28	328.8	6	25.4	10.2	15.7	79.4	200.5	708.0	987.8
33	Kombolcha	39.7	11.1	1857.4	27.8	37.4	75.6	94.9	58.8	32.2	265.1	256.3	121.2	36.4	19.8	18.9	102.9	266.7	674.8	1044.5
34	Chefa	39.8	10.8	1466.1	23.1	22.3	47.6	68.5	38.1	21.8	183.9	20	99.5	23.8	21.6	14.2	82.7	176.5	507.7	767.0
35	Rick	39.9	10.8	1749.0	32.0	44.7	89.6	103.6	66.7	37.1	254.6	282.9	109.3	58.0	32.1	46.8	168.9	304.7	683.9	1157.5
36	Bokeksa	39.9	11.4	1711.5	44.2	36.4	8	117.1	58.7	22.2	194.4	232.5	87.2	35.7	22.2	20.1	122.3	294.8	536.3	953.3
37	Bati	40.2	11.2	1600.0	16.1	33.6	57.3	71.3	60.5	86.8	193.1	199.5	98.3	28.9	9.6	7.8	62.4	22	577.7	862.7
38	Gewane	40.6	10.2	568.0	11.0	37.4	65.3	41.6	36.0	11.4	89.2	100.3	34.0	16.1	6.1	6.6	39.8	180.4	234.9	455.1
39	Asayita	41.5	11.6	430.0	3.8	9.2	19.5	17.5	9.9	3.3	34.1	36.3	12.8	6.3	3.5	0.6	14.3	56.1	86.5	156.9
40	Dubti	42.0	12.0	376.0	4.1	17.0	24.7	20.9	13.5		43.4	48.0	16.2	8.3	2.4	4.8	19.6	76.2	110.2	206.0
41	A/Sheleko	40.2	9.2	745.0	5.4	18.2	36.1	36.8	13.6	1	80.6	82.7	33.8	13.6	20.2	10.5	49.7	104.7	209.8	364.2
42	Abayater	40.1	9.7		23.6	17.0	115.7	66.7	30.9	22.1	189.6	227.5	77.2	44.9	35.7	32.3	136.6	230.2	516.4	883.2
43	Abomsa	39.8	8.5	1800.0	34.5	52.0	104.9	91.8	71.4	56.5	161.6	161.5	113.7	76.7	21.0	15.5	147.7	320.2	493.3	961.2

44	Metehara	39.9	8.9	944.0	8.4	30.5	49.4	46.8	35.4	24.1	120.0	125.0	46.3	21.7	3.9	5.5	39.6	162.1	315.4	517.1
45	Meiso	40.8	9.2	1332.0	20.3	39.9	77.7	104.0	58.6	48.1	129.5	166.2	78.8	52.4	20.6	12.3	122.7	280.2	42	787.0
46	Asebe	40.9	9.1	1792.0	43.2	99.3	109.5	73.7	76.5	111.6	163.8	125.6	45.2	22.1	6.2	0.0	71.5	359.0	446.1	876.6
47	Dire Dawa	41.9	9.6	1260.0	21.7	3	71.1	102.8	46.8	22.8	9	126.6	68.2	25.5	15.6	9.6	72.4	253.3	310.2	636.0
48	Lefasa	43.0	9.6	1733.0	9.7	13.9	37.0	75.9	42.2	26.1	49.1	72.9	59.3	25.3	7.4	4.9	47.2	168.9	207.3	423.4
49	Teferi Ber	43.2	9.8	1611.0	1.9	0.9	21.6	131.7	57.3	21.5	77.8	111.5	24.3	20.2	22.7	0.0	44.7	211.4	235.0	491.2
50	Awramelka	40.0	9.2	816.0	13.6	47.9	55.3	47.9	31.4	16.6	97.5	110.7	40.5	21.2	15.3	13.9	64.1	18	265.2	511.9

APPENDIX – II

Monthly long year mean temperature (^{o}c) (1990-2010) for stations in Awash River basin

Stations	Long.	Lat.	Elev.	Jan	Feb	Mar	Apr	May	Jun	Jul	Aug	Sep	Oct	Nov	Dec	Belg	Bega	Kirre.	Ann
A.A.Obs	38.750	9.033	2354	16.1	17.3	18.1	18.1	18.5	17.1	15.8	15.8	16.1	16.2	15.7	15.4	18.0	16.8	16.2	16.7
Abomsa	39.817	8.467	1800	20.0	21.1	22.1	22.8	23.4	24.1	22.4	21.8	22.0	21.4	20.5	20.1	22.4	18.9	2	21.8
Alemtena	38.933	8.300	1200	19.0	21.1	21.5	22.5	22.5	21.1	20.5	20.4	21.0	20.8	19.5	18.9	21.9	20.8	20.8	20.7
Ambo	37.867	8.967	2130	19.0	19.8	20.4	20.3	19.6	17.9	17.1	17.0	17.2	17.8	18.0	18.3	20.0	18.5	17.3	18.5
Asebetefri	40.867	9.067	1900	19.0	19.4	20.4	20.6	21.2	21.4	20.7	20.5	20.4	20.3	19.5	18.8	20.4	21.0	20.8	20.2
Asaita	41.450	11.567	430	25.6	26.4	28.4	30.4	31.9	33.3	32.8	31.9	31.7	29.4	27.3	25.8	29.3	24.2	32.4	29.6
Diredawa	41.850	9.600	1260	21.8	23.1	25.3	26.3	27.7	28.7	27.1	26.5	26.7	25.6	23.1	21.7	25.6	21.6	27.3	25.3
Debrezeit	38.950	8.733	1900	17.9	19.2	20.5	20.7	20.7	19.8	18.6	18.4	18.6	18.3	17.5	17.2	20.3	19.2	18.8	18.9
Dubti	41.100	11.750	376	25.4	26.9	29.1	30.8	33.0	35.0	33.8	32.5	32.5	29.5	26.6	25.5	29.9	27.1	33.4	30.0
Gewane	40.633	10.150	605	25.1	26.4	28.2	29.3	30.6	32.4	30.4	29.2	29.6	27.6	25.9	25.0	28.6	24.8	30.4	28.3
Metehara	39.900	8.867	930	23.0	24.4	26.4	26.9	27.8	29.2	26.7	26.0	26.7	25.2	23.0	22.4	26.4	2	27.1	25.6
Miesso	40.750	9.233	1400	19.9	21.2	22.8	23.9	25.0	25.3	24.2	23.6	23.3	22.1	20.2	19.8	23.2	20.3	24.1	2
Nathret	39.283	8.350	1622	19.8	21.5	22.3	2	23.4	23.5	20.7	20.6	21.0	20.1	19.3	19.1	22.4	17.7	21.4	21.2

Sirinka	39.617	11.550	2000	17.4	18.3	19.6	20.7	21.8	23.5	22.2	21.3	20.8	19.2	18.0	17.2	20.1	17.2	21.9	20.0
Weliso	37.983	8.550	2000	19.1	20.0	20.2	20.2	19.6	17.7	16.7	16.5	17.3	18.2	18.5	18.9	20.0	18.5	17.1	18.6

APPENDIX-III

Principal Component Analysis (PCA) loadings

		Location			PCA									
No	Stations	Lon.	Lat.	Elev.	1	2	3	4	5	6	7	8	9	10
1	ADDIS ABABA	38.8	9.0	2330.0	0.111	0.184	-0.145	-0.043	0.145	-0.189	-0.126	-0.063	0.142	0.223
2	ABOMSA	39.8	8.5	1630.0	0.273	0.511	0.143	0.411	-0.095	-0.34	-0.129	0.576	0.033	0.032
3	ADAIYTU	40.8	11.1	507.0	0.066	0.323	0.406	-0.293	-0.036	0.039	0.083	0.13	0.174	0.764
4	ARBGEBEYA	39.4	8.1	2471.0	-0.249	-0.015	-0.489	-0.445	0.486	0.014	-0.061	0.283	-0.238	-0.351
5	ASEBETEFERI	40.9	9.1	1792.0	0.44	0.062	0.1	-0.017	0.245	-0.094	0.202	0.907	0.045	-0.003
6	ASSAITA	41.5	11.5	430.0	-0.022	-0.302	0.006	0.548	0.493	0.353	0.258	0.343	0.111	-0.211
7	A/MELKA	40.0	9.2	816.0	0.413	0.084	0.301	0.151	0.249	-0.145	0.075	-0.006	0.174	0.153
8	A/SHELEKO	40.2	9.2	745.0	0.415	-0.262	0.074	0.284	0.086	0.603	-0.142	-0.028	0.148	0.508
9	BANTULIBEN	38.4	8.6	2167.0	0.123	0.198	-0.622	0.172	0.151	-0.043	0.198	-0.131	0.11	0.288
10	BATI	40.2	11.2	1600.0	-0.114	-0.143	0.113	0.23	0.133	0.934	-0.03	0.073	0.055	0.053
11	BOLOGIORGIS	39.4	8.8	1963.0	0.112	-0.09	0.32	0.589	0.564	0.027	0.344	0.207	0.026	-0.029
12	BONEYA	38.6	8.8	2251.0	0.11	0.018	0.308	0.479	0.154	0.055	0.192	-0.041	0.154	-0.1
13	BUSA	38.1	8.8	2166.0	0.012	0.123	-0.176	-0.131	0.027	-0.516	0.368	0.15	-0.017	-0.176
14	CHEFEDONSA	39.1	9.0	2392.0	0.012	-0.716	0.212	0.066	0.236	0.155	0.057	0.025	0.565	0.186
15	COMBOLCHA	39.7	11.1	1857.4	0.123	-0.296	0.72	0.296	0.002	0.209	0.195	0.216	0.255	0.143
16	DEBRESINA	39.8	9.9	2800.0	-0.37	0.54	0.407	0.025	-0.185	0.002	-0.489	-0.059	0.055	0.352

17	DERTULIBEN	38.1	9.0	1991.0	0.093	0.974	0.124	-0.021	0.048	-0.099	-0.005	-0.034	0.054	0.105
18	DIREDAWA	41.9	9.6	1180.0	0.908	-0.187	0.03	0.219	0.075	0.085	0.043	0.072	0.26	-0.063
19	DUBITMET	41.0	11.7	376.0	0.055	-0.292	-0.134	0.202	0.241	0.032	-0.098	-0.122	0.413	-0.128
20	EFESON	40.0	10.4	1500.0	-0.529	0.575	0.209	-0.038	0.02	0.04	-0.293	0.038	-0.324	0.388
21	EJERE	39.3	8.8	2254.0	0.014	-0.061	0.124	-0.041	0.958	-0.108	-0.006	0.139	0.037	0.171
22	EJERSALELE	38.7	8.2	1797.0	0.0123	0.136	0.248	0.456	0.122	0.185	0.018	0.605	0.203	0.294
23	ENSELALE	38.4	8.9	2123.0	0.043	0.134	-0.147	0.488	0.258	-0.086	0.299	-0.174	0.156	0.132
24	ETHEYA	39.3	8.1	2129.0	0.123	0.496	-0.304	-0.656	0.277	0.209	0.119	0.168	-0.003	-0.03
25	GEWANE	40.6	10.2	568.0	0.08	-0.747	0.186	0.218	-0.108	0.027	-0.168	0.055	0.279	-0.024
26	GINAGER	39.6	9.3	3100.0	-0.639	0.69	0.082	-0.089	0.053	-0.04	0.053	0.123	-0.079	0.271
27	GINCHI	38.1	9.0	2132.0	0.012	-0.347	0.061	0.264	0.11	0.035	0.188	0.179	0.237	0.251
28	GURANDA	38.6	8.9	2187.0	0.043	0.176	-0.201	-0.032	0.839	0.221	0.213	0.093	0.125	0.14
29	HAIK	39.7	11.3	1984.8	0.001	0.003	0.174	0.112	-0.136	-0.15	0.057	0.173	-0.215	-0.216
30	HOMBOLE	38.8	8.4	1743.0	0.121	0.1234	-0.045	0.238	0.628	-0.115	0.07	-0.003	-0.05	0.321
31	HURUTA	39.3	8.1	2044.0	0.417	0.032	-0.234	0.454	-0.308	0.107	0.241	0.09	-0.27	-0.565
32	KIMOYE	38.3	9.0	2150.0	-0.074	0.102	-0.115	0.014	0.296	0.217	-0.306	-0.064	-0.384	0.768
33	KORA	40.5	9.1	1239.0	0.441	-0.121	0.287	0.853	-0.011	0.178	-0.031	-0.013	0.109	-0.004
34	KOREMASH	39.3	9.2	2665.0	-0.346	0.54	0.184	-0.252	0.084	-0.288	0.19	-0.026	-0.548	0.251
35	LEFASA	43.0	9.6	1733.0	0.467	-0.083	0.228	-0.126	-0.051	-0.334	-0.146	-0.035	0.73	0.196
36	MAJETE	39.9	10.5	2000.0	0.161	0.139	0.793	0.13	0.259	-0.174	-0.337	-0.043	0.081	0.041
37	MEISOMISSION	40.8	9.2	1332.0	0.452	0.311	-0.299	0.138	0.442	0.126	0.106	0.6	0.091	-0.023
38	MERSSA	39.7	11.7	1577.9	-0.08	0.196	0.905	0.243	-0.056	0.215	-0.023	-0.035	0.06	0.145
39	METEHARA	39.9	8.9	944.0	0.121	-0.063	0.052	0.824	0.218	0.113	0.138	0.259	0.309	0.111
40	MOJO	39.1	8.6	1763.0	0.092	-0.036	0.24	0.161	0.262	-0.734	-0.076	0.199	0.496	0.09
41	NAZERET	39.3	8.6	1622.0	0.123	-0.232	0.23	0.404	0.055	0.203	0.047	0.047	0.796	-0.018
42	SEBETA	38.6	8.9	2175.9	0.123	0.092	-0.389	0.726	0.093	0.222	-0.042	-0.267	0.021	-0.078
43	SENBETE	40.0	10.3	1554.0	-0.059	-0.032	0.182	-0.174	-0.224	0.028	-0.912	-0.209	-0.006	0.073

44	SENDAFA	39.0	9.2	2569.0	0.477	-0.178	0.225	0.04	0.183	-0.359	0.17	0.152	0.685	-0.065
45	SHOLAGEBEYA	39.6	9.2	2500.0	0.153	0.393	0.47	0.14	0.405	-0.423	-0.042	0.122	0.323	0.041
46	SIRINKA	39.6	11.8	1860.7	-0.067	-0.02	0.958	-0.09	-0.004	-0.157	-0.013	0.094	0.162	0.096
47	SODERE	39.4	8.4	1351.0	0.041	0.834	0.037	-0.025	0.093	0.031	-0.106	0.482	-0.214	-0.052
48	TEFERIBIRHANE	39.8	8.4	2196.0	0.654	-0.089	0.257	0.713	-0.128	-0.174	0.088	0.319	-0.16	-0.132
49	TEJI	38.4	8.8	2091.5	0.064	0.032	0.174	0.192	0.501	-0.145	0.41	0.103	0.138	0.677
50	WEREBABOSCH	39.8	11.3	2378.4	0.116	-0.038	0.389	-0.566	-0.041	-0.047	0.554	-0.33	-0.103	0.287
51	YEKATITSCHOOL	38.7	9.0	2456.0	0.123	0.137	-0.231	0.54	-0.199	0.361	-0.015	0.016	0.1	-0.087

APPENDIX – IV

Monthly Satellite Rainfall Estimated value (mm) over Awash River basin HRRs

Months	Years											
	2008				2009				2010			
	HRR-1	HRR-2	HRR-3	HRR-4	HRR-1	HRR-2	HRR-3	HRR-4	HRR-1	HRR-2	HRR-3	HRR-4
Jan	2.4	8.2	8.0	3.0	13.6	8.9	10.2	1	3.7	1.1	3.0	0.0
Feb	0.7	0.1	0.0	0.0	1.0	2.7	0.7	0.0	78.3	22.8	37.4	63.1
Mar	2.2	0.0	0.0	0.4	15.2	10.6	1.0	11.4	38.5	10.5	6.7	21.7
Apr	40.3	14.6	8.2	23.1	54.7	29.1	11.0	42.3	76.8	33.2	18.0	46.9
May	71.0	22.1	2.7	24.6	24.3	5.6	0.7	7.0	77.1	21.1		29.9
Jun	99.3	32.0	9.7	38.1	89.3	33.5	12.2	32.5	106.2	34.8	11.3	34.6
Jul	241.1	163.1	24.3	87.6	172.7	136.4	6.0	61.1	224.4	225.8	41.0	100.4
Aug	200.5	39.3	33.0	133.5	143.1	34.0	25.0	74.6	195.4	150.5	97.7	158.1
Sep	109.0	82.1	18.3	43.5	84.1	27.2	2.2	30.4	115.2	67.2	18.0	62.9
Oct	24.2	10.5	7.2	19.4	26.2	14.3	10.3	27.6	1.4	0.0	0.0	0.3
Nov	35.0	19.7	7.2	13.6	0.1	0.0	0.0	0.4	2.8	0.7	0.0	2.0

Dec	**0.2**	**0.1**	**0.0**	**0.1**	**20.0**	**4.4**	**0.5**	**8.1**	**0.9**	**7.5**	**0.0**	**0.0**
Bega	**61.8**	**38.4**	**22.3**	**36.1**	**59.9**	**27.6**	**21.0**	**48.8**	**8.8**	**9.2**	**3.0**	**2.3**
Belg	**114.2**	**36.8**	**10.8**	**48.1**	**95.2**	**47.9**	**13.3**	**60.6**	**270.7**	**87.5**	**64.7**	**161.6**
Kiremt	**649.9**	**316.4**	**85.3**	**302.8**	**489.3**	**231.1**	**45.3**	**198.6**	**641.3**	**478.2**	**168.0**	**356.0**
Annual	**825.9**	**391.6**	**118.5**	**387.0**	**644.5**	**306.6**	**79.7**	**308.0**	**920.8**	**574.9**	**235.7**	**519.9**

DECLARATION

I hereby declare that the dissertation entitled "**Satellite Based Rainfall Estimation: Evaluation and Characterization with Homogeneous Rainfall Region Classification Using GIS and Remote sensing, (Case study of Awash River Basin)"** has been carried out by me under the supervision of Dr. K. V. Suryabhagavan, School of Earth Sciences, Addis Ababa University, Addis Ababa during the academic year of 2011/12-2014 as a part of Master of Science program in GIS and Remote Sensing. I further declare that this work has not been submitted to any other University or Institution for the award of any degree or diploma.

Zerihun Bikila

Signature _____

Place: Addis Ababa, Ethiopia

Date: June, 2014

CERTIFICATE

This is certified that the dissertation entitled "**Satellite Based Rainfall Estimation: Evaluation and Characterization with Homogeneous Rainfall Region Classification Using GIS and Remote sensing, (Case study of Awash River Basin)**" is a work carried out by Zerihun Bikila under my guidance and supervision. This is the actual work done by Zerihun Bikila for the partial fulfillment of the award of the Degree of Master of Science in GIS and Remote Sensing from Addis Ababa University, Addis Ababa, Ethiopia.

Dr. K. V. Suryabhagavan

Signature _____

School of Earth Sciences

Addis Ababa University

Addis Ababa, Ethiopia

Date: June, 2014